Hydroxyl Radical-Mediated Modification of Proteins as Probes for Structural Proteomics

Guozhong Xu† and Mark R. Chance*

Center for Proteomics, Case Western Reserve University School of Medicine, 10900 Euclid Avenue, Cleveland, Ohio 44106

Received February 15, 2007

Contents

* Address correspondence to this author. Mail stop: BRB 930. Telephone: 216-368-4406. Fax: 216-368-6846. E-mail: mark.chance@case.edu.
† Current address: Stryker Biotech, Analytical Development, 35 South Street, Hopkinton, MA 01748. E-mail: Guozhong.Xu@stryker.com, Guozhong.Xu@gmail.com.

1. Introduction

"Footprinting" refers to assays that examine ligand binding and conformational changes by determining the solvent accessibility of the backbone, bases, or side chain structures of macromolecules through their sensitivity to chemical or enzymatic cleavage or modification reactions. Protein footprinting methods have been developed to examine protein structure and conformational changes by monitoring solvent accessibility using either modification or cleavage reactions. Examples of such methods include acetylation, nonspecific limited proteolysis, or probing the accessibility of a range of sites that can be specifically or nonspecifically cleaved or modified. The basis of these diverse chemical approaches is to monitor the change in accessibility of susceptible residues as a function of relevant conformational fluctuations. Protein footprinting methods based on protease cleavage have been used to map protein structure, nucleic acid−protein interactions, and protein folding intermediates. However, cleavage techniques using proteases suffer from limited structural resolution due to the large size of the probe. Hydroxyl radical methods of cleavage and modification have been pursued to overcome this drawback. In this article, we introduce the methods of footprinting, including hydroxyl radical methods (section 1), review the various approaches to generate hydroxyl radicals (section 2), and review the chemistry of hydroxyl radical mediated oxidation of the protein backbone and side chains (section 3). Although some examples of the use of the method are provided, this is not emphasized, as previous reviews have provided a number of relevant examples.[1−3] Thus, this review provides a comprehensive reference work for understanding the chemistry of radical generation and oxidative reactions appropriate for application to structural mass spectrometry experiments.

1.1. Background and History of Protein Footprinting

Understanding the details of protein structure and their interactions in macromolecular assemblies is one of the most important problems in biology. The interactions of proteins and their assembly into large complexes control processes as fundamental as replication, transcription, translation, metastasis, apoptosis, and many other signal transduction pathways relevant to development and cell−cell communication. Protein footprinting approaches, paralleling the successful development of nucleic acid footprinting approaches (see other papers in this Thematic Issue), have been developed and refined over the last 20 years in order to provide the molecular details of these interactions and their dynamics.[4,5]

"Footprinting" refers to assays that examine ligand binding and conformational changes by determining the solvent

10.1021/cr0682047 CCC: $65.00
Published on Web 08/08/2007

Dr. Guozhong Xu received his bachelor's degree in Chemistry from Peking University in Beijing, China, in 1989, his master's degree from the Chinese Academy of Science in 1992, and his Ph.D. degree from the University of Georgia in 2001. Upon completing his graduate studies, he worked as a postdoctoral fellow with Professor Mark R. Chance at Albert Einstein College of Medicine, where he worked in structural proteomics and developed methods for investigating protein–ligand interactions using chemical probes and mass spectrometry. In 2005, Dr. Xu became a faculty member at Case School of Medicine. After one year, he joined CuraGen Corporation, where he was a senior scientist and manager of mass spectrometry facility for biopharmaceutical research and development. In 2007, he moved to Stryker Biotech, where he is furthering his mass spectrometric research in biopharmaceutical development.

Dr. Mark R. Chance received his bachelor's degree in Biology from Wesleyan University and his Ph.D. degree in Biophysics from the University of Pennsylvania. Dr. Chance furthered his training as a Postdoctoral Research Associate at AT&T Bell Laboratories. He went on to become Assistant Professor in the Department of Chemistry at Georgetown University. He then served as Assistant Professor at Albert Einstein College of Medicine in Bronx, New York, and was soon promoted to Associate Professor of the Departments of Physiology & Biophysics and Biochemistry. He was Professor at AECOM when he moved to Case School of Medicine in 2005, where he is currently the Director of both the Case Center for Proteomics and the Case Center for Synchrotron Biosciences and Professor of Physiology and Biophysics.

accessibility of macromolecules through their sensitivity to chemical or enzymatic modification and cleavage reactions. A fundamental feature distinguishing footprinting from other techniques is the covalent modifications of the macromolecule that are essential to probing the solvent accessible sites. These irreversible changes to the macromolecule can negatively influence the experimental results unless sufficient care is taken in experimental design and analysis. Fortunately, during the 25 years of successful development of macromolecular footprinting approaches, a number of basic principles and control experiments have been established that have allowed the successful examination of structure and dynamics for a wide range of protein and nucleic acid systems, as illustrated in the thousands of footprinting publications that have appeared in the literature.[6]

The initial approaches to examining the specific interactions of macromolecules from the standpoint of either proteins or the nucleic acids were of two types: the first involved cleavage of the macromolecule followed by readout of the cleaved fragments, and the second involved the covalent modification of the macromolecule and analysis of the modified products. In each case, the footprint represents the differential reactivity of accessible sites compared to those that are buried within the structure. For nucleic acids, the first cleavage based methods that were developed were enzymatic and involved isolation of a fragment of DNA that was "protected" from nuclease digestion due to its binding to a specific protein.[7] Footprinting using chemical modification was developed shortly thereafter;[8−10] the ligand induced protection of a nucleic acid from methylation was used to map protein−DNA interactions. These approaches evolved into the explicit implementation of (nucleic acid) cleavage based footprinting that closely resembles the approaches in use today.[11,12] These footprinting experiments rely on limited cleavage of the backbone (where each position along the backbone is sampled with equal probability) and the ability to uniquely identify the distinct cleavage products so multiple sites could be individually measured.

Paralleling the approaches pioneered for nucleic acids, the introduction of protein end labeling and proteolytic mapping was outlined by Jay.[13] This led to the first explicit implementation of protein footprinting, which used enzymatic cleavage of the macromolecular backbone to probe the contact interface between a protein and its ligand, in this case the interaction of an antigen−antibody complex.[14] Monoclonal antibodies interact with specific epitopes, and the antibody−antigen interactions were shown to protect these specific binding sites from protease cleavage. Different proteases were used to probe different sites within the antigen depending on the sequence specificity. In addition, the authors detected antibody binding induced conformational changes in the antigen, demonstrating the power of footprinting techniques to, in principle, probe sites throughput the macromolecule. A drawback of this particular experiment was that [35-S] methionine labeling was used to label the antigen; this labeled methionines throughout the sequence, and the cleavage products generated fragments that could not be uniquely identified by size. Refinements of this method were made by Heyduk and co-workers and Kallenbach and co-workers.[15,16] In these cases, end-labeling was used to uniquely identify the fragments. Footprinting of proteins by chemical modification was refined by Hanai and Wang in 1994.[17] This method mapped the solvent accessibility of lysine residues by determining their reactivity to modification by acetylation. Although these two approaches incorporated fundamental features of footprinting as introduced by Galas and Schmitz,[11] it should be noted that the methods to modify proteins and probe their structure (originally using diazonium salts) are nearly 100 years old (Pauly, 1904). In addition, specific methods to use modification reagents to map "buried" versus "free" histidine side chains go back over 40 years.[18,19] However, these modification methods primarily evolved into approaches to generate specific sites within proteins that were optically active so as to probe conformational changes using the covalent adducts.

Nevertheless, the modification and cleavage approaches outlined above fit the definition of "footprinting" for the purposes of this review, and they illustrate the two distinct approaches that are commonly used. Although the methods outlined above are valuable, additional footprinting assays have been developed using a number of additional approaches. In particular, some of the drawbacks of a number of chemical and enzymatic footprinting reagents include preference of a footprinting reagent for specific positions within proteins, limiting the number of sites that can be probed. For example, proteases are often quite specific and cut only at a subset of the positions along the protein sequence. Also, the size of proteases, which often can be of the same size as the ligand, can result in an overestimation of the size of the protected region, as well as be blind to any variations in reactivity within the binding site. Modification methods where lysine is acetylated are suitable for probing accessible lysine side chains but cannot probe at other sites. Chemical proteases, if they are small, can provide enhanced structural information compared to enzymatic proteases. For example, CNBr can cleave at methionine sites, and thus its cleavage products are sensitive to burial of methionine residues.[17] However, the most effective chemical protease and the one in widespread use is the hydroxyl radical ($HO^{\bullet}$), which is commonly generated by the venerable Fenton−Haber−Weiss reaction using Fe(II)-EDTA. Heyduk and co-workers showed that hydroxyl radicals could provide a relatively nonspecific probe of protein structure[16] and map the sites of protein−DNA binding. The use of hydroxyl radical based cleavage has advantages of not only a small size of the probe but also a relatively nonspecific cleavage activity, maximizing the number of potential sites along the backbone that can be probed. However, the use of tethered sources of hydroxyl radicals, which generate the radicals at defined sites, has also proven to be a powerful approach in defining protein−protein interfaces and specific sites of interaction.[20,21] Hydroxyl radicals have also been developed as side chain modification reagents, and this approach has been coupled to proteolysis and mass spectrometry techniques to precisely map the modification sites.[1−3]

1.2. Cleavage Based Protein Footprinting

The key publication that has critically influenced the field of footprinting was published in *Nucleic Acids Research*[11] by Galas and Schmitz and was entitled "DNase footprinting: a simple method for the detection of protein−DNA binding specificity". Aside from popularizing the term footprinting, the paper carefully laid out many of the basic principles of the method that are common to all successful footprinting approaches today.

The demonstration of cleavage based footprinting methods for nucleic acids inspired similar methods to be developed for the analysis of proteins. Initial approaches to examining protein structure and interactions utilized proteases or other cleavage based reagents (like hydroxyl radicals) in order to assay the solvent accessible sites.[15,16] The experimental steps are as follows. Proteins are labeled at one end (see below) and then are subjected to the cleavage agent. The cleavage products are assayed for size by SDS-PAGE (Figure 1). For nonspecific cleavage, solvent accessible sites throughout the macromolecule would be sensitive to cleavage, would, in principle, be probed, and would provide a wide range of fragments. One fundamental difference between footprinting studies of DNA and proteins is that for DNA, since the backbone is on the outside of the canonical helical structure, almost every site is potentially accessible. For proteins, the backbone may be buried on the inside of the molecule for much of the structure; thus, the number of potential cleavage sites is lessened. Thus, the resultant data will not cleave at each and every monomer position. However, sites on the "inside" are not likely candidates for the binding of a ligand, such that the impact of this "disadvantage" is lessened. In addition, the variation in cleavage across the macromolecular sites interrogates the protein's tertiary structure. When a ligand binds to the protein, accessible cleavage sites on the macromolecule may experience reduced reactivity at the interface. Many sites should remain unchanged, but allosteric interactions could increase or decrease the solvent accessibility at other sites throughout the macromolecule as well.[14]

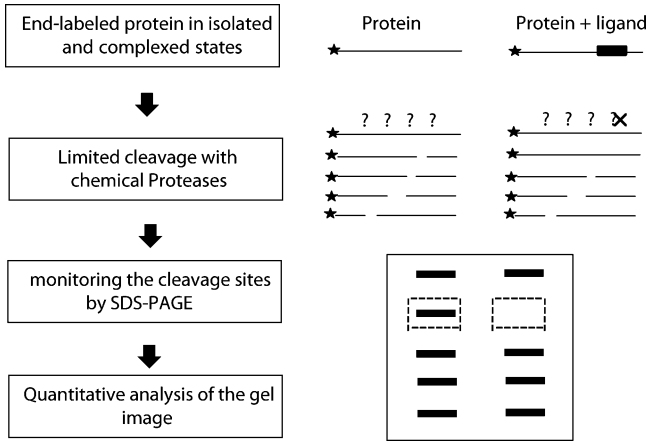

Figure 1. Schematic representation of cleavage-based protein footprinting. A protein is specifically end-labeled and then subjected to limited cleavage under single-hit conditions in the presence and absence of the ligand. The cleavage products are then separated by size using high-resolution SDS-PAGE, followed by quantitative analysis of a digitized gel image. After correction for protein loading or cleavage-efficiency differences, the intensities of the corresponding bands in the lanes with and without the ligand are compared to get information about the changes in susceptibility to cleavage as a result of ligand binding. Reprinted with permission from ref 4. Copyright 2004 Wiley-VCH.

Protein Cleavage. Protein cleavage is accomplished by either enzymatic or chemical means. Enzymes to cleave proteins have widespread and variable specificity. To achieve cleavage at a wide range of sites using proteases a "cocktail" of several proteases is useful.[15] However, the protease method has the ultimate drawback that the enzyme is large and may not be sufficiently sensitive to accessibility of the structural backbone to accurately probe the structure. As in the case of nucleic acids, the advent of the use of hydroxyl radicals enhanced the structural resolution of the technique considerably. Hydroxyl radicals have been used free in solution, where they probe the entire molecular surface, tethered to specific probe sites, or tethered to sites throughout the macromolecule. A tethered source of hydroxyl radicals provides a cleavage agent with a defined radius of action, generally 10−15 Å. In the case of tethering to a wide distribution of sites, Meares and co-workers have found that if the tethers are linked to one molecule in a pair of an interacting molecules, the target cleavage sites are localized close to the interacting surface of the binary partner.[20,21] Thus, the modulation of reactivity "observed" in the hydroxyl radical assay can be dissected into the allosteric effects (which are observed in addition to the effects of burial of the interface when "free" radicals are used) and the formation

of an interface (which are observed in the experiment with tethered sources of radicals).

1.3. Modification Based Protein Footprinting

As outlined above, Hanai and co-workers[17]demonstrated that modification reagents could be used to provide "footprints". The lysines of a viral topoisomerase that were involved in intermolecular contacts with DNA were specifically mapped. The modified lysines provide sites that, with the proper chemical workup, could ultimately be cleaved. As above, gel electrophoresis methods were used to map the susceptible sites. Hanai has also pointed out that many reagents available for the modification of proteins that were developed in the 1960s and 1970s could be "revived" to be used in footprinting assays. In fact, a number of novel approaches to modifying the backbone and specifically incorporated side chain groups have been developed and successfully applied (see refs 2, 3, and 22).

Another approach that has been recently developed is to use chemical modification reagents that are less specific to provide footprinting approaches. It has been well-known for some time that hydroxyl radicals, besides generating backbone cleavage events, modify the side chains of proteins quite efficiently.[23] Sulfur containing, aromatic and aliphatic side chains provide targets that are more sensitive to attack than the protein backbone. Thus, these events are more frequent than the abstraction of hydrogen from the α-carbons at main chains that is the first step in hydroxyl radical based protein cleavage. Chance and co-workers combined the ability of side chains to be modified with mass spectrometric detection to develop a protein footprinting technique.[24−27] Hydroxyl radicals as a reagent for footprinting can be derived from Fenton reagents or from radiolysis sources.[28] In the former case, the Fenton reagent induces a metal catalyzed reaction of hydrogen peroxide to produce hydroxyl radicals. In the latter case, ionization of water produces hydroxyl radicals directly.

The development of the hydroxyl radical as a modification reagent for footprinting and its application in conjunction with mass spectrometry were directly inspired by the development of deuterium exchange mass spectrometry methods. The protein of interest is subjected to a pulse of deuterium intended to label structural regions that are solvent accessible and to monitor changes in accessibility in response to the binding of a ligand.[29,30] After solvent labeling, the reaction is quenched, the protein is fragmented by proteolysis, the peptide fragments are separated by high-pressure liquid chromatography (HPLC), and mass spectrometry analysis is performed. Peptide fragments with increased mass relative to control experiments without addition of deuterium indicate *specific segments* that were solvent accessible and exchange competent during the deuterium pulse. The method used to minimize back-exchange during the analytical steps is lowering the pH to ∼2.5; thus, only proteases with activity at acid pH (e.g., pepsin) can be used to fragment the protein.

Hydroxyl radical mediated protein footprinting is similar. The overall method is outlined in Figure 2. In this case, the protein solution is exposed to ionizing radiation and the hydroxyl radicals covalently react with surface accessible residues, primarily side chain groups.[25] As in the deuterium exchange methods, the protein is subjected to proteolysis. However, in contrast to deuterium exchange, the production of stable modifications through hydroxyl radical exposure allows a wide range of samples as well as proteases to be used to fragment the protein under a wide range of solution conditions and pH values. Also, the stable modification of side chains allows a specific probe site to be identified using tandem mass spectrometry methods, while, for deuterium exchange, typically the conformational change can only be localized to the specific peptide fragment. The drawback is that if a reactive side chain is not present in a particular peptide segment, there are no probes. However, the examination of side chains is complementary to the deuterium exchange method that examines backbone structure.

To generate the limited dose required for footprinting and to quantitatively examine the reactivity of the specific peptides in question, a series of samples are exposed to variable doses, the samples are digested, and the individual peptides are analyzed by HPLC and mass spectrometry. Thus, a dose response curve is generated for each peptide of interest; this generates a quantitative biophysical measure (based on the observed rate of modification) of the relative reactivity of the sites in the different peptides. Consistent and reliable quantitation, which is essential to footprinting, is provided by measuring the relative amounts of the modified and unmodified peptide products in the same experiment. Since the modifications are stable, it is relatively straightforward to use tandem mass spectrometric methods to specifically identify the amino acid positions of the protein that have been modified (bottom right of Figure 2); these represent the probe sites for the analysis.[26,31]

On the right-hand side of Figure 2, where the reaction is carried out in the presence of a protein−protein complex, modification is suppressed at the site corresponding to the interacting surface, and unchanged at sites distal to the contact. The decrease of reactivity of peptides in the interface is quantitatively measured using the dose−response curves; a sample dose−response for a peptide whose reactivity is suppressed in the presence of the ligand is shown at the bottom left of the figure. It is critical for the method that the dose response curves indicate a linear regime extrapolated to zero fraction modified; this assures that the reactivities of particular sites are not changing due to the oxidation process itself. Also, the method of examining loss of the unmodified fraction emphasizes the interrogation of intact material. Although these particular refinements are unique to the hydroxyl radical mediated protein footprinting approach, they are derived from a detailed knowledge and respect for safeguards that have evolved throughout the long history of development of "footprinting" research;[5,32] such safeguards ensure that the structural and biochemical information provided by footprinting methods is reliable. It must be emphasized, however, that footprinting provides only "local" information about the reactivity of the side chain probes. Allosteric changes in conformation induced by ligand binding can also give rise to either protections (decreases in side chain reactivity) or enhancements (increases in reactivity) depending on the induced conformational changes. This must be carefully borne in mind when interpreting data from these experiments, and various examples are mentioned in this review.

2. Generation of Hydroxyl Radicals in Solution

2.1. Introduction

The generation of hydroxyl radicals for footprinting and other chemical purposes has a long history. In this section, we provide a review of many of the methods used for generating hydroxyl radicals, organized by method of

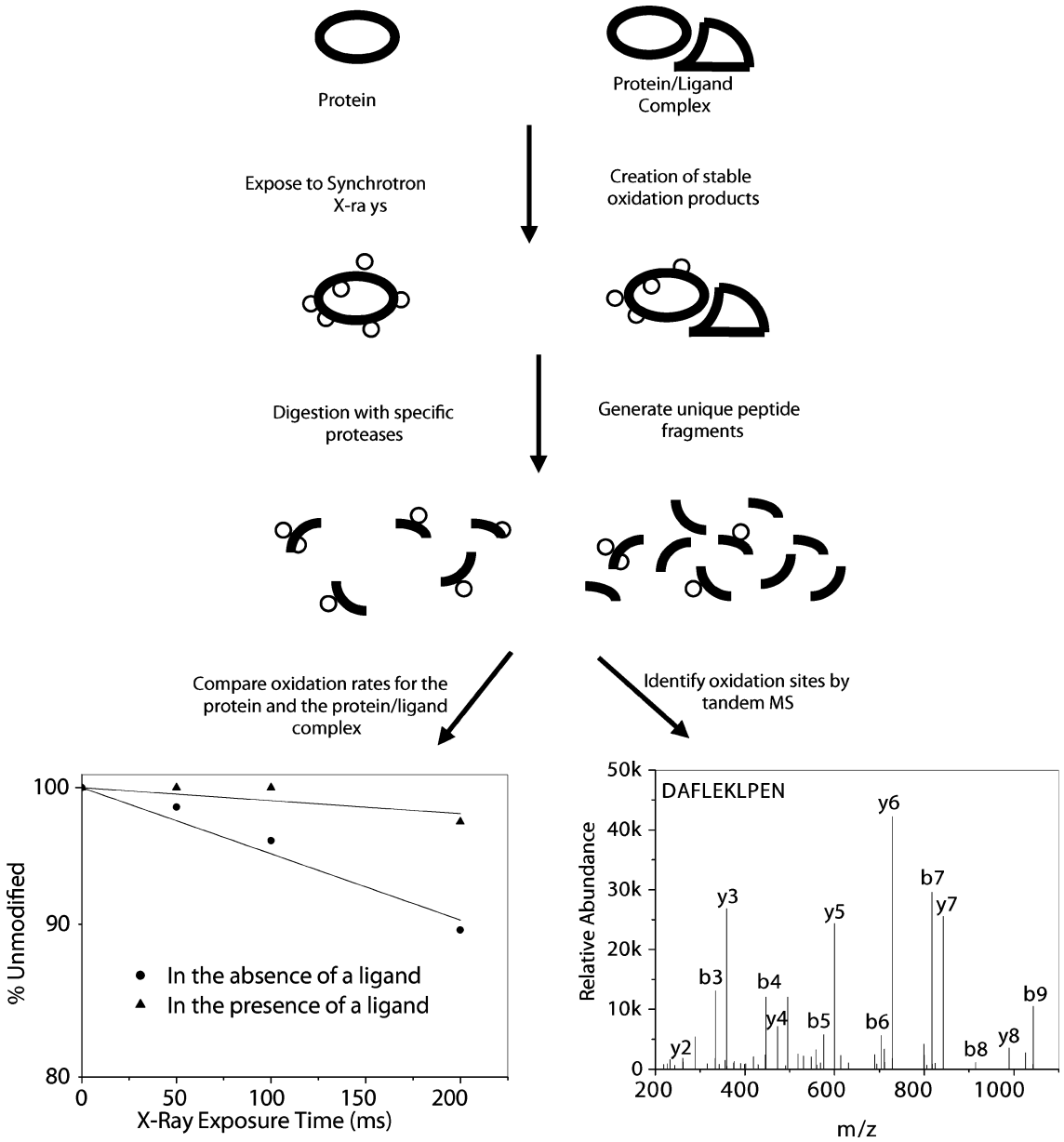

Figure 2. Schematic representation of hydroxyl radical footprinting. A protein and its complex with a ligand are exposed to radiolysis or Fenton reagents, which produce hydroxyl radicals that modify the side chains of the protein. Subsequent to this X-ray exposure, the protein samples are digested with proteases, and MS is applied to quantitate the extent of modification. This quantitation provides information about the solvent accessibility of each peptide in both the isolated and complexed states. The particular modification sites are determined by tandem MS (MS/MS). In the dose−response example, a slower rate of modification is seen for the peptide when isolated from the complex compared to the case for the free protein. Thus, it is indicated that this peptide contains reactive side chain residues influenced by the binding process.

generation. Although this does not provide the most compelling historical narrative, it does permit the presentation of the methods in a way that readers can jump between sections to learn the different approaches and to find appropriate primary and secondary references. This review overall emphasizes the chemistry of hydroxyl radical production and reaction mechanism in the service of protein footprinting technologies. To a first approximation, the method of generation is less important, since each of the methods below can be used to generate surface oxidation data. However, each method of generation has its advantages and disadvantages, and this section highlights these points. In addition, the section reveals the historical context in which these chemistries have been developed; this provides an opportunity to mention many of the other important chemical applications for hydroxyl radical oxidation methods.

2.2. Electron Pulse Radiolysis

Electron pulse radiolysis is a technique to deliver reproducible pulses (typically ranging from 1 to 100 ns duration) of electrons, which are accelerated to megaelectronvolt scale energies by a linear accelerator (LINAC).[33−36] The technique is primarily used to investigate reactions in dilute aqueous solutions, although it has also been successfully applied to gaseous and solid-phase systems. The megaelectronvolt energy of the electrons is almost a million-fold higher than necessary for rupture of covalent bonds or molecular ionization. The primary method by which the electrons lose energy is Columbic interaction with electrons in the absorber; molecules close to the particle tracks may be ionized, and those further away may be excited. Most of the ejected electrons will be sufficiently energetic to ionize and excite

further molecules and form spherically symmetrical "spurs" or clusters of ionization and excitation events along the tracks of the electrons, giving rise to secondary electron tracks in a chain ionization process.[36] An individual high-energy electron loses its energy through a consecutive series of about 10^4 individual interactions and generates spurs within 10^{-14} s.

In dilute aqueous solutions at micromolar concentrations, the ionizing chemistry involves interactions only with water (at ~55 M concentration) whereas the radiation effects on the solute are entirely indirect. The initial products are a positive water radical $H_2O^{\bullet+}$ and a dry electron e_{dry}^-, or excited water H_2O^*[35] (eq 1).

$$H_2O \xrightarrow{h\nu} H_2O^{\bullet+} + e_{dry}^-, \text{ or } H_2O^* \quad (1)$$

These are then converted within 10^{-12} s into highly reactive primary radical species, namely hydroxyl radical $HO^\bullet$, hydrated electron e_{aq}^-, and hydrogen atom $H^\bullet$ via the following reactions.

$$H_2O^{\bullet+} \xrightarrow{H_2O} HO^\bullet + H^+ \quad (2)$$

$$e_{dry}^- \xrightarrow{H_2O} e_{aq}^- \quad (3)$$

$$H_2O^* \longrightarrow HO^\bullet + H^\bullet \quad (4)$$

The excited water molecules may also deactivate through collision. The overall ionization generates freely diffusing species with the following yields.[37]

$$4.14H_2O \xrightarrow{100\ eV} 2.87HO^\bullet + 2.7e_{aq}^- + 0.61H^\bullet + 0.03HO_2^\bullet + 0.61H_2O_2 + 0.43H_2 + 2.7H^+ \quad (5)$$

The stoichiometric coefficients are called *G* values, which can be converted to standard units by multiplying by 0.104.[38] For every 100 eV of energy absorbed, $2.87HO^\bullet$, $2.7e_{aq}^-$, $0.61H^\bullet$, and $0.03HO_2^\bullet$ are generated. When a single electron with 3 MeV of energy (penetration depth in water, 1 cm) has lost its energy, it can give rise to as many as 2×10^5 radicals after completion of the spur reactions.[34] Detection of the solute-derived intermediates is usually carried out using UV/vis spectroscopy or conductometry.

In pure water, the primary radicals can quench via recombination at diffusion-controlled rates.[35]

$$HO^\bullet + e_{aq}^- \rightarrow HO^- \quad (6)$$

$$2HO^\bullet \rightarrow H_2O_2 \quad (7)$$

In air equilibrated aqueous solutions (~0.3 mM O_2), e_{aq}^- and $H^\bullet$ will react with O_2 and quickly convert into $HO_2^\bullet$ or $O_2^\bullet$ via the following reactions, with rate constants of 1.9×10^{10} and 2.1×10^{10} M^{-1} s^{-1}, respectively.[39]

$$e_{aq}^- + O_2 \rightarrow O_2^{\bullet-} \quad (8)$$

$$H^\bullet + O_2 \rightarrow HO_2^\bullet \quad (9)$$

The relative yield is determined by the following acid−base equilibrium with a pK_a of 4.9.[40]

$$O_2^{\bullet-} + H^+ \rightleftharpoons HO_2^\bullet \quad (10)$$

Table 1. Rate Constants for Reaction of Amino Acids with Hydroxyl Radical and Hydrated Electrons[a]

	HO^-		e_{aq}^{-1}	
substrate	rate (M^{-1} s^{-1})	pH	rate (M^{-1} s^{-1})[b]	pH
Cys	3.5×10^{10}	7.0	1.0×10^{10}	−7
Trp	1.3×10^{10}	6.5−8.5	3.0×10^8	7.8
Tyr	1.3×10^{10}	7.0	2.8×10^8	6.6
Met	8.5×10^9	6−7	4.5×10^7	7.3
Phe	6.9×10^9	7−8	1.6×10^7	6.9
His	4.8×10^9	7.5	6.0×10^7	−7
Arg	3.5×10^9	6.5−7.5	1.5×10^8	6.1
cystine	2.1×10^9	6.5	1.5×10^{10}	6.2
Ile	1.8×10^9	6.6	N/A	N/A
Leu	1.7×10^9	~6	$<1 \times 10^7$	6.5
Val	8.5×10^8	6.9	$<5 \times 10^6$	6.4
Pro	6.5×10^8	6.8	2.0×10^7	6.7
Gln	5.4×10^8	6.0	N/A	N/A
Thr	5.1×10^8	6.6	2.0×10^7	7.0
Lys	3.5×10^8	6.6	2.0×10^7	7.4
Ser	3.2×10^8	~6	$<3 \times 10^7$	6.1
Glu	2.3×10^8	6.5	$1\text{--}2 \times 10^7$	5.7−7
Ala	7.7×10^7	5.8	1.2×10^7	7.4
Asp	7.5×10^7	6.9	1.8×10^7	7.0
Asn	4.9×10^7	6.6	1.5×10^8	7.3
Gly	1.7×10^7	5.9	8.0×10^8	6.4

[a] http://allen.rad.nd.edu/browse compil.html. [b] Davies, M. J.; Dean, R. T. *Radical-mediated protein oxidation: from chemistry to medicine*; Oxford University Press: 1997; pp 44−45.

Most amino acid residues except Cys react with solvated electron e_{aq}^{-1} at a much lower rate than that of O_2 (see Table 1). It seems that only Cys and disulfide can compete with O_2 for reacting with e_{aq}^{-1} under aerobic conditions. Overall, in the air saturated aqueous solutions with micromolar protein concentrations, the primary oxidizing species is hydroxyl radical, which can react with target molecules at rates up to 10^{10} M^{-1} s^{-1}(depending on the target).

The hydrated electron can be converted into hydroxyl radical in N_2O saturated solution (24 mM N_2O, 1 atm, room temperature) to effectively double the yield of $HO^\bullet$, via the following reaction at a rate of 9×10^9 M^{-1} s^{-1}. It results in a chemical system with $HO^\bullet$ as the dominant reactive species (90% plus 10% $H^\bullet$).

$$e_{aq}^- + N_2O \rightarrow HO^\bullet + N_2 + HO^- \quad (11)$$

2.3. Synchrotron Radiolysis of Water

The radiolysis of water with photons in the kilovolt X-ray range primarily involves the photoelectric effect,[41] in which the energy of an incoming photon is transferred to an electron, which is then ejected from water molecules or other targets. The electrons are thermalized (dry electrons) and deposit their energy in discrete ionizations of other water molecules. The ionized water molecule reacts with another water molecule to produce $HO^\bullet$ radical according to the reactions outlined above.[37]

Beamline X-28C at the National Synchrotron Light Source at Brookhaven National Laboratory is a national resource dedicated to radiolytic biological footprinting and is an excellent source of X-rays to conduct radiolysis experiments.[42] The beamline provides white light synchrotron X-rays over an energy range of 3−30 keV with beam currents ranging from 300 to 150 mA over a 12 h injection cycle.[43] At a ring energy of 2.8 GeV and a beam current of 250 mA, 5.5×10^{14} photons are absorbed per second by a 10 μL sample of 7 mm^2 cross-sectional area. The photon

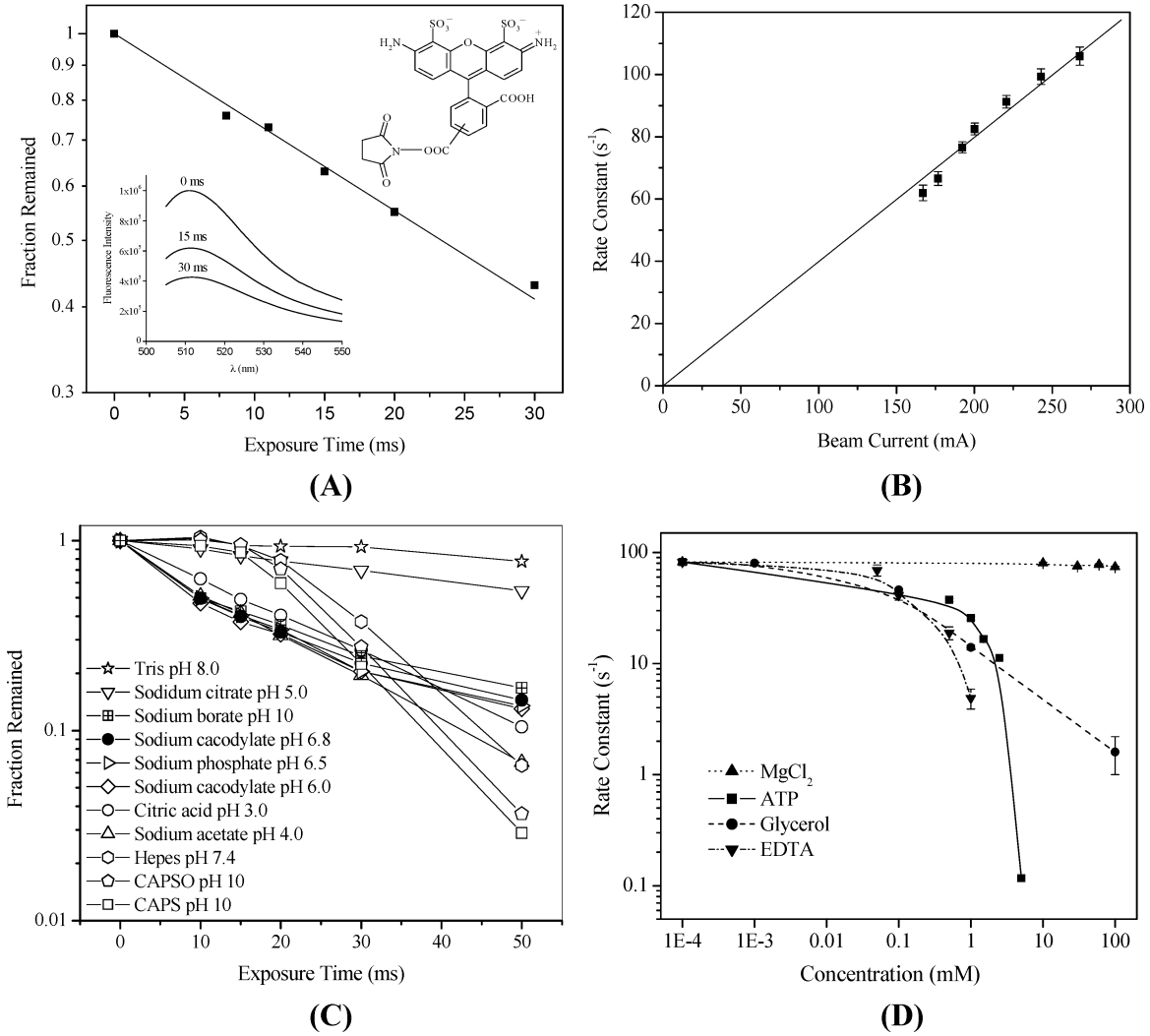

Figure 3. Alexa radiolysis and determination of X-ray dose. **(**A**)** Dose response plot of 1.0 μM Alexa Fluor 488 in 10 mM sodium cacodylate pH 7.0 buffer containing 0.1 mM EDTA irradiated with synchrotron X-rays at 190−220 mA beam current. After exposure, the Alexa is diluted (1:500) prior to fluorescence analysis. The Turner Biosystems TBS-380 Fluorometer is used to determine the emission intensity at 516 nm with an excitation wavelength of 496 nm. The solid line represents the fitting of data to a first-order reaction kinetics. The insets in the top-right and the bottom-left corners show the dye structure and the decrease in fluorescent emission caused by irradiation at different times, respectively. **(B)** Rate constant of 1.0 μM Alexa 488 in 10 mM sodium cacodylate pH 7.0 buffer without EDTA as a function of the beam current. The solid line represents the linear fit with a slope of 0.41 $\pm$ 0.03 s^{-1} mA^{-1}. (C) Dose response plots of 1.0 μM Alexa 488 in 10 mM of different buffers. (D) Rate constants of radiolytic degradation of 1.0 μM Alexa 488 in 10 mM sodium cacodylate pH 7.0 buffer with addition of $MgCl_2$, ATP, glycerol, and EDTA at different concentrations. The connections between the points are represented by respective spline-lines. Reprinted with permission from ref 42. Copyright 2007 International Union of Crystallography (http://journals.iucr.org/).

flux yields a steady-state concentration of $HO^{\bullet}$ of approximately 1 μM.[44] The radiolytic oxidation reactions are complicated, involving many different reactive oxygen species (ROS), including $HO^{\bullet}$, $HO_2^{\bullet}$, $O_2^{\bullet -}$, etc., similar to those observed in electron pulse radiolysis above. The typical dose of the unfocused beam permits radiolysis experiments to be completed with milliseconds of dose, which is controlled by a precise X-ray shutter.[42]

Dosimetry. A particular problem in radiolysis experiments is comparing different sources of radical generators or providing a measure of the dose delivered to biological samples under various conditions. The effects of experimental and sample conditions on the generation of hydroxyl radicals by synchrotron radiolysis have been evaluated using a fluorescent dye, Alexa (Fluor) 488, as a target "dosimeter" molecule. The known factors that influence radiolysis dose include synchrotron beam current, the energy characteristics and geometry of the beam, buffer composition and concentration, and the presence of small molecular additives such as salts, metal ion chelators (e.g., EDTA, EGTA, etc.), cofactors (e.g., ATP, ADP, etc.), reducing agents (e.g., dithiothreitol, β-mercaptoethanol, etc.), or stabilizing agents (e.g., glycerol, polyethylene glycol, sucrose, etc.), all of which are often present, or even required, in biological samples. The assay method using the Alexa 488 dosimeter can be used to find the optimum conditions for radiolytic footprinting studies or to compare radiolysis under different conditions to normalize experiments. Essentially, the intensity of Alexa fluorescence is decreased by radiolysis dose in an apparent first order process (Figure 3A). The rate at which Alexa is oxidized is measured in water; this rate is then compared to the rate of oxidation in the presence of the sample to be oxidized or in the presence of ligands or other molecules desirable to poise the biochemical system.[42] This approach has become an important procedure to guide the

synchrotron footprinting experiments for a wide range of studies.

Effect of Beam Current. The amount of $HO^{\bullet}$ generated in a sample solution is directly proportional to the absorbed photon energy, which is in turn proportional to the beam current of the synchrotron light source. The beam current falls exponentially as a function of elapsed time starting from the point when the beam is refilled in the electron storage ring. Thus, for a prolonged experiment or an experiment with the same system at different beam currents, it is necessary to understand and ultimately calibrate the observed dose at each exposure time during the experimental period. A linear relationship exists between the degradation rate of 1.0 μM Alexa 488 in 10 mM sodium cacodylate pH 7.0 buffer vs beam current (Figure 3B). The plot of Alexa radiolysis at the various beam currents can be directly correlated to the amount of the hydroxyl radical inside the solution at any available beam current, which in turn will allow the experimenter to pre-estimate the required exposure time to optimize the synchrotron dose for a sample of interest before starting any experiment. Moreover, the slope of radiolytic rate vs beam current can be used to calibrate the dose. For example, an experiment carried out at or around 200 mA beam current would have a dose that is 20% less than that of the one carried out at 250 mA. Thus, the oxidation rate constants observed for the former experiment need to be adjusted up by 20% for a direct comparison to data taken at 250 mA.

Effect of Buffers. Selection of buffer is a critical step in the planning of radiolysis experiments due to the need to optimize the stability and activity of the biological system and to optimize the dose of radicals for the footprinting experiment. Figure 3C shows the dose response of 1.0 μM Alexa 488 in various buffers at 10 mM concentration; radiolysis in the presence of these buffers was carried out near their p*K* values, which range from 3 to 10. Most of the commonly used biochemical buffers such as Tris, HEPES, MOPS, CAPS, citrate, and CAPSO buffers hinder the degradation of the fluorophore due to the quenching of hydroxyl radicals. This effect is seen to be complex and will result in suppression of modifications/cleavages during the initial time points of the experiment; the likely oxidation of susceptible buffer molecules in this process may reduce the buffering capacity of the solution. After this initial lag phase, the fluorescence decreases rapidly. This complex kinetics of reaction makes these buffer systems likely unsuitable for footprinting experiments using hydroxyl radicals.

Radiolysis in sodium cacodylate or phosphate buffers follows apparent first-order kinetics with an observed rate constant of 80 s^{-1} at 200 mA beam current using the unfocused white beam at the X28-C beamline (Figure 3C) These buffers are the typical choice for footprinting experiments because of their minimum quenching of $HO^{\bullet}$. Alexa radiolysis also indicates that sodium citrate and acetate are appropriate buffers for footprinting experiments at low pH while sodium borate is suitable for studies at higher pH. Increases in buffer concentration are correlated with an increased need for radiation dose, especially in the case of scavenging buffers; thus, the buffer concentration is normally limited to 20 mM for synchrotron footprinting studies. In general, radiolysis of Alexa 488 provides a fast and convenient tool for determining the optimal conditions for efficient sample exposure suitable for use with many hydroxyl radical mediated footprinting methods.

Effect of Additives. Different additives such as glycerol, ATP, ADP, EDTA, and $MgCl_2$ are frequently included in biological samples as cofactors, as stabilizers, or for other purposes, and they may significantly impact radiolytic footprinting because of their quenching effects. Figure 3D shows the effect of glycerol on the degradation rate of Alexa 488, indicating that even 1.0 mM of glycerol can diminish the rate of radiolysis by a factor of 5. Thus, thorough removal of such stabilizing agents or substantial focusing of the X-ray beam is essential to maintaining exposure times in the millisecond range. In the cases where the presence of a certain amount of glycerol is mandatory for the stabilization of macromolecular complexes, an Alexa radiolysis assay would help the experimenters to adjust the exposure time through pilot experiments under different beam focusing conditions. Significant quenching of $HO^{\bullet}$ is also observed with ATP, ADP, and EDTA. EDTA at concentrations of 0.1 and 0.5 mM leads to 50% and 75% decreases in the rate constant of Alexa 488, respectively. $MgCl_2$ does not exhibit any appreciable impact on the radiolytic oxidation rate of Alexa. No effects are observed with chlorides, sulfates, and phosphates of sodium, potassium, and magnesium, indicating that these inorganic ionic species have no effect on radiolytic dose.

High flux radiation sources, like synchrotrons, can generate $HO^{\bullet}$ radicals with sufficient flux density to provide cleavage of nucleic acids or modification of proteins on the microsecond to millisecond time scales.[1,32] These sources have high repetition rates (in the Megahertz range) and thus function as pseudocontinuous sources. Combined with millisecond rapid mixing devices, this allows for time-resolved studies of dynamic biological processes. The most valuable aspects of a synchrotron X-ray source to carrying out footprinting experiments include speed and the reproducibility that is achieved in sample dosing and the ease of varying the dose using timing shutters. Radiolysis sources in general have the advantage that no reagents need to be added to the solutions, thus simplifying the experimental methods. As outlined below, methods that require direct addition of peroxide can have undesirable secondary oxidations. However, the limitation of a synchrotron radiation source lies in its lack of accessibility to everyday users and its high cost of operation. However, these sources have proven to be reliable sources for both nucleic acids and protein footprinting experiments over a 10 year period for dozens of user groups. These experiments have been extensively documented in the primary literature and in a number of recent review articles;[1,42] thus, they are not repeated here.

2.4. Laser Photolysis of H_2O_2

UV-light induced homolysis of hydrogen peroxide in aqueous solution leads to the generation of two hydroxyl radicals.[45−47] In contrast to radiolytic methods, where energy is deposited in the solvent water, photolysis results from the absorption of photons by H_2O_2 directly; the subsequent excitation and cleavage are represented in eq 12

$$H_2O_2 \xrightarrow{h\nu} 2HO^{\bullet} \tag{12}$$

The primary quantum yield of H_2O_2 decomposition is 0.4−0.5.[46,47] The hydroxyl radicals undergo subsequent Haber−Weiss chain reactions,

$$HO^{\bullet} + H_2O_2 \rightarrow H_2O + HO_2^{\bullet} \tag{13}$$

$$HO_2^{\bullet} + H_2O_2 \rightarrow H_2O + O_2 + HO^{\bullet} \quad (14)$$

that proceed at rate constants of 2.7×10^7 and 7×10^9 M^{-1} s^{-1}, respectively.[48] The former reaction competes with the diffusion-controlled self-quenching reaction

$$2HO^{\bullet} \rightarrow H_2O_2 \quad (15)$$

that proceeds with a rate constant of 4.7×10^9 M^{-1} s^{-1} at 25 °C.[48]

The UV photolysis of H_2O_2 has been widely used in industrial processes such as water treatment, medical equipment sterilization, and bleaching applications. More recently, it has been employed for nucleic acids footprinting studies[49] and in protein surface oxidation (footprinting) studies. In 2004, Sharp et al. applied this method to analyze the solvent accessible surface of two model proteins, specifically lysozyme and β-lactoglobulin.[50] Protein samples containing 15% H_2O_2 were irradiated using a UV lamp, and irradiated samples were then subjected to tryptic digestion and mass spectrometric analysis. The oxidation of amino acid side chains was found to be consistent with solvent accessibility.

To reduce the exposure time and concentration of H_2O_2 needed for protein surface modification, Aye and co-workers developed a nanosecond laser-induced photochemical oxidation method for protein surface mapping with mass spectrometry.[51] In this method, two model proteins, ubiquitin and apomyoglobin, were prepared at concentrations ranging from 20 to 80 μM in 10 mM phosphate buffer (pH 7.0) with H_2O_2 added to the sample at a final concentration from 0.3 to 1% just before laser irradiation. The sample was oxidized by hydroxyl radicals generated by exposure to a Nd:YAG pulse laser operating with a 3−5 ns pulse duration and a 2 mJ/pulse energy output at 266 nm for 1 to 100 laser shots. Immediately after irradiation, the samples were quenched by freezing in liquid nitrogen and subsequently lyophilizing in a vacuum to remove the residual H_2O_2. The protein samples were then reconstituted, digested by enzyme, and analyzed by mass spectrometry to map the oxidized amino acid residues. The result indicated that a single laser shot can generate extensive protein surface oxidations, and LC/FT-MS was capable of detecting more oxidized peptides than LC/ion-trap MS/MS. It was also found that the mono-oxidized ubiquitins were more susceptible to further oxidation than nonoxidized ones, indicating that oxidation may induce some conformational change of proteins. This result indicated that it was important to perform the experiment with a single laser pulse to avoid oxidizing proteins after conformation change had occurred.

At the same time, Hambly and Gross also developed laser flash photolysis of H_2O_2 to oxidize protein solvent accessible residues on the microsecond time scale.[52] A 17-ns KrF excimer laser with a 50 mJ/pulse output (compared to a 2 mJ/pulse used by Aye) and operated at 248 nm was developed to minimize laser absorption of protein species. Apomyoglobin was prepared at a 10 μM concentration in 10 mM phosphate pH 7.8 buffer with 15 mM H_2O_2 (~0.04%) added just before irradiation. The sample (50 μL) solution was loaded into a 100 μL gastight syringe and introduced via a syringe pump coupled to 100 μm i.d. fused silica tubing with a 2.5 cm length of polyimide coating removed as a UV transparent window. The exposed sample solution was incubated with agarose-immobilized catalase to remove residual H_2O_2. The reaction duration and protein exposure to radical were tuned by adding glutamine as a free radical scavenger. The time required to remove 99% of the generated hydroxyl radicals in the absence of a radical scavenger was calculated as 20 μs based on the $HO^{\bullet}$ self-quenching reaction, while the oxidation interval was calculated to decrease to 0.5 μs in the presence of 20 mM glutamine as radical scavenger.

2.5. Fenton and Fenton-like Reactions

Fenton's reaction was invented in the 1890s by H. J. H. Fenton, who discovered that ferrous iron(II) catalytically promoted the oxidation of tartaric acid by hydrogen peroxide (H_2O_2).[53] Later, many transition metal ions in their lower oxidation states (e.g., Fe(II), Cu(I), Ti(III), Cr(II), and Co(II)) and their complexes were found to display similar oxidative features to those of the Fenton reagents, and the metal-catalyzed oxidations were called "Fenton-like" reactions. These reactions play an important role in a variety of catalytic and biological processes, and they are believed to be the main source of reactive oxygen species (ROS) in the cells related to a variety of diseases;[54−57] the oxidation products in fact are diagnostic biomarkers for disease progression and/or severity.[58] In the past century, the Fenton and Fenton-like reactions have been subjected to extensive investigation; however, the detailed reaction mechanism is not entirely understood. The Fenton and Fenton-like reactions have been repeatedly discussed in many publications and review articles.[59−74]

It is a common belief that the freely diffusible hydroxyl radical ($HO^{\bullet}$) is a key product generated in Fenton's reaction. In 1934, Haber and Weiss[75] proposed a chain reaction mechanism involving $HO^{\bullet}$ production as a key step to explain the Fenton reaction, which is now known as the "Haber−Weiss Cycle". The mechanism was later expanded and revised by Barb and co-workers to provide what is now referred to as the "classical Fenton pathway" or the "free radical" Fenton chain reaction. The decomposition of H_2O_2 in simple acidic solutions in the dark may include reactions described by eqs 16−22 in the absence of strongly coordinating ligands and other redox species.[59,60,76] Reaction 16 is free radical initiation reaction, reactions 17−21 are radical propagation, and reaction 22 is radical termination.

$$Fe^{2+} + H_2O_2 \rightarrow Fe^{3+} + HO^{\bullet} + OH^- \quad (16)$$

$$Fe^{3+} + H_2O_2 \rightarrow Fe^{2+} + HO_2^{\bullet} + H^+ \quad (17)$$

$$H_2O_2 + HO^{\bullet} \rightarrow HO_2^{\bullet} + H_2O \quad (18)$$

$$HO_2^{\bullet} \leftrightarrow O_2^{\bullet -} + H^+ \quad (19)$$

$$Fe^{3+} + HO_2^{\bullet} \rightarrow Fe^{2+} + O_2 + H^+ \quad (20)$$

$$Fe^{3+} + O_2^{\bullet -} \rightarrow Fe^{2+} + O_2 \quad (21)$$

$$Fe^{2+} + HO^{\bullet} + H^+ \rightarrow Fe^{3+} + H_2O \quad (22)$$

Hydroxyl radical is generated via reaction 16 through the oxidation of Fe(II) to Fe(III) by H_2O_2. Meanwhile, Fe(III) can be reduced back to Fe(II) via reaction 17. The interconversion of ferrous and ferric ions may catalyze the continuous generation of $HO^{\bullet}$. In the presence of excess Fe(II) over H_2O_2, two Fe(II) are oxidized per H_2O_2 via reactions 16 and 22. In contrast, when H_2O_2 is present in excess, oxygen (O_2)

evolution via reactions 16−21 dominates. The presence of reducible organic species (e.g., RH) will impact the above reactions by inhibiting the reactions of HO• with Fe(II) (reaction 22) and H_2O_2 (reaction 18).

The hydroxyl radical may be generated stoichiometrically simply by combining an Fe(II) salt with H_2O_2. The reaction is optimal at pH 3−4.[59,77] However, the oxidation product Fe(III) can readily hydrolyze and precipitate out as amorphous ferric oxyhydroxides $Fe_2O_3 \cdot nH_2O$ as the pH is increased from strongly acidic to neutral. The colloids even begin to form slowly at about pH 3. Soluble Fe(III) species can be obtained by complexation with strong chelators.

An elegant Fenton system was developed by Tullius and Dombroski[78,79] to generate hydroxyl radical for biological footprinting to map the protein binding sites on DNA. The Fenton system includes three essential components, Fe(II)-EDTA, H_2O_2, and ascorbate. A typical hydroxyl radical mediated reaction is initiated by the addition of 1 μL of a solution containing 1 mM $(NH_4)_2Fe(SO_4)_2$/2 mM EDTA, 1 μL of 10 mM ascorbate, and 1 μL of 0.3% H_2O_2 to 7 μL of nucleic acid in 10 mM Tris·EDTA buffer (pH 8.0). The reaction is run at 25 °C for a controlled time of a few minutes and then quenched by the addition of 7 μL of 100 mM thiourea.[80]

The Fe(II)-EDTA/H_2O_2/ascorbate Fenton system has become a standard method for studying nucleic acid−ligand interaction and nucleic acid dynamic processes.[81,82] In the process, EDTA increases the solubility of the metal ions, thus allowing the reaction to be carried out at neutral pH, and prevents the transition metal ion from binding to the macromolecules.[63] EDTA also increases the efficiency of Fe(III)/Fe(II) to catalyze the generation of HO• from H_2O_2,[83] since EDTA sequesters Fe(III) much more strongly than Fe(II), as demonstrated by the stability constants of the complexes: $\log K_1 = 25.7$ for Fe(III)-EDTA compared to 14.3 for Fe(II)-EDTA. The ascorbate reduces the Fe(III)-EDTA back to Fe(II)-EDTA.

Similar to iron, other transition metals combined with appropriate ligands are also able to undergo Fenton-like reactions under the appropriate reaction conditions.[65,84−89] These transition metals include Cu(II), Mn(II), Co(II), Ni(II), Cd(II), Cr(III), etc., which are in some cases essential biological elements bound to proteins. Typically, an oxidizing agent like O_2, H_2O_2, or a peracid is combined with the transition metal complex. There are also examples where metals in high oxidation states were used in the presence of a reductant. Cu(II)/Cu(I) complexes with bis(1,10-phenanthroline) or other ligands in the presence of H_2O_2 have been demonstrated as very efficient footprinting reagents for proteins, nucleic acids, and DNA−protein interactions.[88,90−94] The Mn(II)/Mn(III) redox couple generates ROS when incubated with H_2O_2.[61,95,96] Co(II) can catalyze the production of ROS when bound to small organic molecules and proteins.[97−99] Ni(II)[100] is also able to generate ROS under the right conditions when bound to nucleotide derivatives, peptides, and proteins.[101−105]

2.6. Tethered Metal Chelates

Tethered metal chelates were first developed by Rana and Meares in 1990.[106,107] This approach localizes the metal−chelate complex by linking it to proteins or nucleic acids through a spacer arm and a coupling reagent group. In contrast to the typical Fe-EDTA Fenton reagents, which freely diffuse in solution and generate freely diffusible oxidizing species, the tethered metal chelate becomes attached on the specific sites of the macromolecules to generate a local site-directed concentration of oxidizing species. Scheme 1 illustrates the structure of a typical tethered metal chelate, iron (S)-1-(*p*-bromoacetimidobenzyl)-EDTA (abbreviated as Fe-BABE, also called Meares' reagent). The reagent (Scheme 1) consists of three essential structural components: a metal chelate for generating oxidizing species, a sulfhydryl-reactive moiety (Br-acetyl) for conjugating to protein cysteines, and a spacer arm connecting them together. The Fe-BABE can be conjugated with a native cysteine residue of a protein, or a cysteine residue can be introduced at a site of interest by genetic manipulations. The Fe-BABE−protein conjugate is allowed to form a macromolecular complex with its interacting partner, the target or prey protein, or a nucleic acid. When incubated with H_2O_2 and ascorbate, the conjugated Fe-BABE will produce oxidative oxygen species, such as hydroxyl radicals, which will cut a peptide chain or a nucleotide chain located within the reach of its spacer arm near the binding site (12 Å for this specific BABE). The modification of macromolecules by Fe-BABE possibly goes through both hydroxyl radical and peroxide-Fe intermediate oxidation mechanisms.[108] The Fe-BABE reaction has the advantages of a mild conjugation reaction with a peptide or a protein, mild cleavage reaction conditions, rapid reaction and high yield, and a directed chain cleavage reaction of nucleic acids or proteins with minimal sequence specificity. In these initial experiments, it was applied for cleavage of the protein backbone, a Fenton technique for probing protein structure that is inefficient. However, the method has been a useful tool for the analyses of spatial relationships for protein−nucleic acid and protein complexes in many biological reactions,[109−114] and even to monitor structural changes during the course of a multistep reaction.[115] Information on the 3D structure of a protein can be analyzed by the sequential analysis of intramolecular cleavage sites by Fe-BABE conjugated at various positions along the protein. Analysis of the resulting nucleotide or peptide fragments aids in mapping the contact area between the two interacting partners. To facilitate the analysis of fragments, the proteins or nucleic acids can be end-labeled using radioactive isotopes or fluorescent dye (see also section 1). It can also be detected by Western blot analysis using an antibody directed to an expression tag (His-tags, GST-tags, or peptide sequences that are biotinylated during expression) or to an endogenous N or C terminal epitope.[116] The interaction site between two proteins can be further defined using other tethered reagents that have longer or shorter spacer arms or that are reactive with other amino acid residues or conjugating to different selective sites through cysteine mutagenesis.[112,114] Reactive groups have been fashioned that will react and covalently conjugate with a

Scheme 1. Structure of FE-BABE

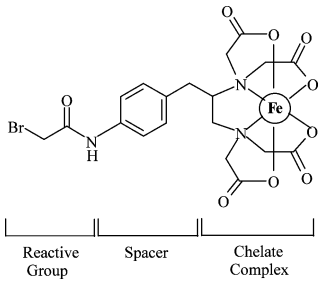

specific amino acid side chain such as cysteine thiol[106] or lysine amine (by using 2-iminothiolane as a linker to randomly modify lysine to introduce free sulfhydryl groups) in proteins[117] or the nucleophilic sulfur-modified phosphodiester backbone of nucleic acids.[109,116] Other approaches have been developed to prepare protein−EDTA[110,117−119] or nucleic acid−EDTA conjugates.[109] (see also refs 108 and 116). Other tethered metal complexes have also been used for study of protein structure. For instance, copper-5-(α-bromoacetamido)-1,10-phenanthroline was used to probe the higher order structure of G-protein-coupled receptors.[120] Modified proteins have also been analyzed using mass spectrometry;[121] in fact, Vachet and co-workers have used the intrinsic metal atom within a protein to provide a site-specific source of radicals for structural analysis.[100,122−124]

2.7. Disproportionation of Peroxynitrous Acid

Peroxynitrite is a powerful oxidant whose reactions and decomposition products are involved in multiple biological reactions.[125] The endogenous synthesis of peroxynitrite ($ONOO^-$) occurs by the diffusion-controlled reaction between cell-derived nitric oxide ($^{\bullet}NO$) and superoxide radicals ($O_2^{\bullet-}$)[126]

$$^{\bullet}NO + O_2^{\bullet-} \rightarrow ONOO^{\bullet} \quad (23)$$

The peroxynitrite anion ($ONOO^-$) is relatively stable in alkaline solution; however, its conjugated acid, peroxynitrous acid with a pK_a of 6.8, undergoes homolytic fission to form $HO^{\bullet}$ and nitrogen dioxide ($NO_2^{\bullet}$) with a half-life of 1 s at pH 7.0[125,127,128]

$$ONOOH \rightarrow NO_2^{\bullet} + HO^{\bullet} \quad (24)$$

The two radicals (the "geminate" pair) can either diffuse apart, giving free radicals that can perform oxidations, or react together, either to form nitrate or to reform ONOOH.[129] In a neutral aqueous solution, $NO_2^{\bullet}$ disproportionates to yield nitrite and nitrate via following two-step reactions with rate constants of 9×10^8 and 1×10^3 M^{-1} s^{-1}, respectively.[130]

$$2NO_2^{\bullet} \rightarrow N_2O_4 \quad (25)$$

$$N_2O_4 + H_2O \rightarrow NO_3^- + NO_2^- + 2H^+ \quad (26)$$

In order to generate $HO^{\bullet}$ for *in vitro* biological study, one needs to prepare a stable aqueous solution of $ONOO^-$ stabilized in alkaline solution. Addition of the $ONOO^-$ solution to a biological sample buffered at pH 7 results in instant protonation of a significant fraction of peroxynitrous acid (ONOOH), which decomposes in situ to give rise to $HO^{\bullet}$.

There are several approaches available for synthesis of peroxynitrite in aqueous solution,[131] such as reaction of hydrogen peroxide with nitrite at low pH followed by alkali quenching,[131−134] reaction of superoxide O_2^- with nitric oxide NO in deaerated aqueous solutions at pH 12−13,[135−137] photolysis of aqueous solutions of azide and nitrate,[138,139] interaction of nitric oxide and hydrogen peroxide,[140] pulse radiolysis of nitrate and nitrite solutions,[141] reaction of ozone (~5% in oxygen) with sodium azide (0.02−0.2 M in water) at pH 12 and 0−4 °C,[126,142] autoxidation of hydroxylamine in alkaline solutions,[143] reaction of hydrogen peroxide with alkyl nitrites in alkaline solutions,[144,145] and reaction of $^{\bullet}NO$ with tetramethylammonium superoxide in liquid ammonia[146] or with solid potassium superoxide.[147] A convenient method to synthesize peroxynitrite is to rapidly mix the precooled acidified H_2O_2 with nitrite, followed by instantaneous quenching of the reaction mixture with an excess of alkali.

The use of peroxynitrous acid as a source of hydroxyl radicals has been successfully applied to probe the higher order structure of RNA and to the study of protein−nucleic acid interactions. King et al.[148] successfully applied peroxonitrite anion for hydroxyl radical footprinting of the binding the *c*I-repressor of phage λ with the right operator. It was also found that the individual-site binding isotherms determined by quantitative DNase I, Fe(II)-EDTA, and ONOOK footprinting are identical within experimental error. The identical isotherms obtained with the three different reagents with greatly differing sampling times indicate that the sampling time of the footprinting probe need not be short relative to the kinetic dissociation constants that govern protein−DNA interactions. Gotte and co-workers used the peroxynitrous acid to footprint the higher order structure of RNA through cleavage of the sugar backbone of the nucleic acid strand and compared this approach to treatment using $[Fe(II)\text{-}EDTA]^{2-}$.[149] Although ONOOH is neutral and significantly smaller than the metal complex, both reagents generate the same protection pattern on tRNAs, suggesting that access of the commonly formed hydroxyl radical, rather than access for its source, is the determining factor when probing the higher order structure of RNA. A strong difference in reactivity is only seen at the modified 2-thiouridine S34 of tRNA(Lys3), which shows hyperreactivity toward ONOOK treatment. This particular reaction may require interaction between the peroxynitrite anion and the thiocarbonyl group of the base, since hyperreactivity is not observed when probing the dethiolated tRNA(Lys3).

Since the decomposition of peroxynitrite generates multiple reactive species, the reaction of peroxynitrite with proteins may involve ONOOH and $[HO^{\bullet}...NO_2^{\bullet}]$ in addition to $HO^{\bullet}$, possibly through three possible pathways.[150,151] First, peroxynitrite reacts directly with cysteine, methionine, and tryptophan residues. Second, peroxynitrite reacts fast with transition metal centers and selenium-containing amino acids. Third, secondary free radicals arising from peroxynitrite homolysis such as hydroxyl and nitrogen dioxide, and the carbonate radical formed in the presence of carbon dioxide, may react with protein moieties as well. Therefore, the modification of proteins by this radical source is expected to be more complicated than that with pure hydroxyl radicals, as both oxidation and nitration will occur. The detailed chemistry of peroxynitrite, reaction mechanisms, and kinetics can be found in several reviews.[129,139,152−154]

2.8. High Voltage Electrical Discharge

A source of hydroxyl radicals was developed by Maleknia and co-workers to probe the protein surface.[155−159] The technique takes advantage of the atmospheric pressure electrospray ion source in mass spectrometry.[160] Technically, a protein solution in micromolar concentration is infused at a few microliters per minute into a conventional electrospray source of mass spectrometry, a high electrical voltage of about 8000 V (maximum allowed) is applied to the electrospray needle to produce a discharge that results in the production of solution-based radicals around the needle tip, and oxygen is used as a nebulizer sheath gas at an approximately 10 L/min flow rate. A visible discharge is

formed at the needle tip. When a dilute protein solution is sprayed out of the needle, the protein molecules become oxidized on the surface with the bulk solution at the needle tip and within the sprayed droplets. The electrosprayed sample is collected by condensation of droplets into a ground aluminum-capped sample tube. The collected sample is then subjected to enzymatic digestion and mass spectrometric analysis. This technique provides a snapshot of the structures of proteins or protein complexes in solution.

The oxidation of the protein molecules under such electrospray conditions results from the oxygen-containing reactive species generated by the corona discharge around the high-voltage spray tip. A corona is a process developing from an electrode with a high potential in a neutral fluid (usually air) by ionizing that fluid so as to create a plasma around the electrode. Corona discharge usually involves two asymmetric electrodes: one highly curved (such as the tip of an electrospray needle) and one of low curvature (such as a plate or the ground). The high curvature ensures a high potential gradient around the electrode (spay tip) for the generation of a plasma. The discharge of electricity causes a faint glow adjacent to the surface of the active electrode, a well-known phenomenon due to the generation of ozone in atmosphere corona discharge.

Thomas and co-workers used the similar in-source corona discharge electrospray to identify phospholipid double bond positions.[161] The corona discharge generated was achieved by using O_2 as the electrospray nebulizing gas in combination with high electrospray voltages (−6 kV) to initiate the formation of an ozone producing plasma. A corona discharge was observed around the electrospray capillary tip as shown in Figure 4. The double bond(s) present in unsaturated phospholipids are cleaved by ozonolysis within the ion source to give two chemically induced fragment ions that may be used to unambiguously assign the position of the double bond.

The in-source corona discharge is similar to the gas phase and steamer corona discharges, which have been widely used for air cleaning and water treatment.[162−169] Various oxygen-containing active species, including O_3, $HO^•$, H_2O_2, $HO_2^•$, $O_2^{•−}$, and $^1O_2$, can be produced in the electrosprayed liquid droplets. The use of O_2 as nebulizing gas greatly enhances the generation of oxygen-containing reactive species. The corona discharge can be performed in either positive or negative polarity, even though the negative polarity gives rise to more stable corona discharge and produces significantly more ozone than using a positive potential.[161]

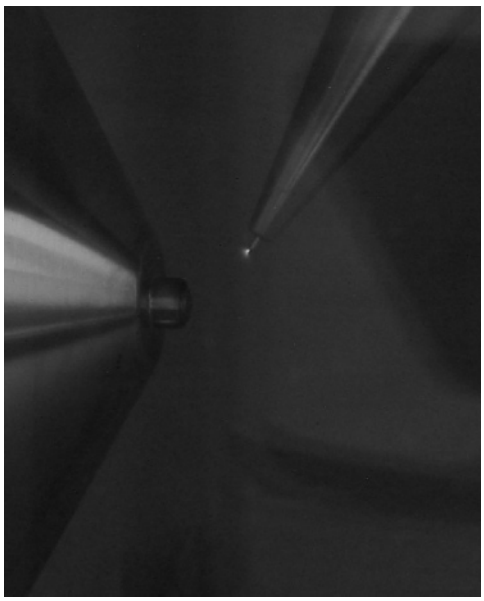

Figure 4. A photograph taken of the corona discharge observed at the electrospray ionization needle of the Thermo LTQ ion trap mass spectrometer when O_2 is used as the electrospray nebulizing gas and an electrospray voltage of −6 kV is applied. Reprinted with permission from ref 161. Copyright 2006 American Chemical Society.

In-source O_2-assisted high voltage discharge has been employed in the studies of protein structure[155] and protein−protein interfaces.[157,159] Wong et al. demonstrated the use of radicals generated by an electrical discharge combined with mass spectrometric analysis to study the interaction between ribonuclease (RNase) S-protein and S-peptide. They found that the S-peptide was preferentially protected from reactions with radicals under conditions in which it was bound to S-protein, while a region of S-protein comprising residues 96−100 constituted the S-peptide binding domain based on its decreased reactivity with radicals within the RNase-S complex over the free S-protein. Wong et al. also use the method to study the calcium-dependent interaction of calmodulin and melittin.[159] The residues in both proteins involved in the interaction and/or shielded from solvent within the protein complex were identified.

2.9. Other Hydroxyl Radical Generation Techniques

Other methods of hydroxyl radical generation have been developed; these include the following: production of $HO^•$ radicals by photosensitization[170−175] and photolysis of *N*-hydroxypyridine-2(1H)-thione;[63,176,177] X-ray radiolysis using a rotating anode source;[178] γ-ray radiolysis;[179−181] electron radiolysis;[179,180,182] use of fast neutrons;[183−186] and sonolysis of water.[187−194]

3. Hydroxyl Radical Mediated Cleavage of the Main Chain and Modification of Side Chains

3.1. Selectivity of Hydroxyl Radical Oxidation

The reactions of organic molecules with hydroxyl radicals normally occur via hydrogen abstraction from saturated carbon sites or hydroxyl addition to the unsaturated carbon−carbon double bonds or aromatic rings; this gives rise to a transient radical species that undergo further reactions depending on structure and radical environment. The controlling factors governing both types of reactions include the following:[74] (a) the strength of the C−H bond; (b) the electronegativity of the substituents on the target sites; (c) the stability of the nascent organoradical; (d) steric effects, and (f) statistical factors related to the number of sites available for attack, that is, the number of equivalent H atoms or positions of attack.

$HO^•$ appears to be weakly electrophilic and shows some selectivity in the types of bonds with which it will react, although this is in the context of a highly reactive and indiscriminate species overall.[195] The H-abstraction by hydroxyl radical is primarily dependent upon the single bond strength of the target atom with a hydrogen atom. For example, the average single bond energies for C−H, N−H, O−H, and S−H are 411, 386, 459, and 363 kJ/mol at 25

Scheme 2. Backbone Cleavage by H-Abstraction at the α-Carbon Site

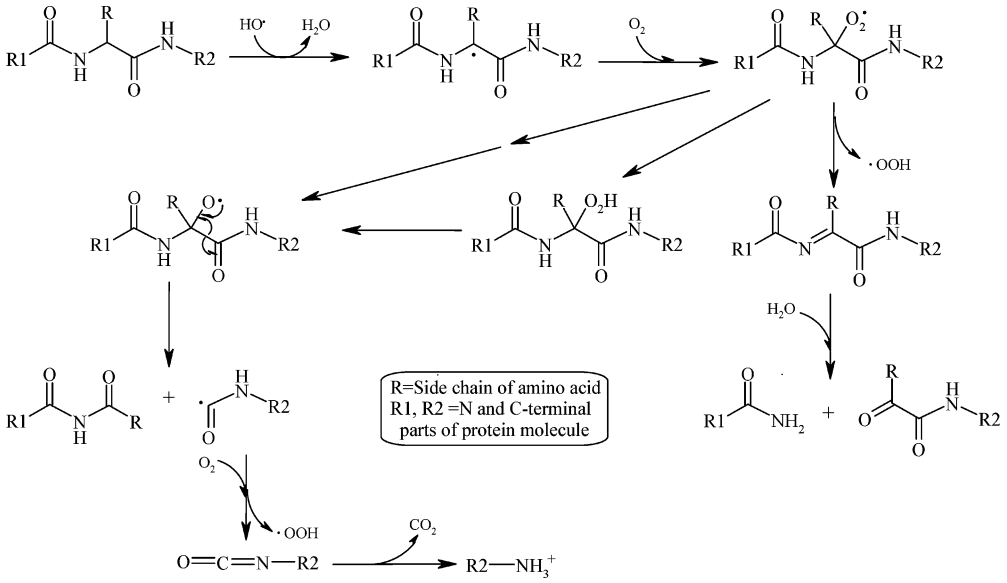

°C, respectively (see http://wulfenite.fandm.edu). S−H has the lowest single bond energy, and thus, Cys is the most reactive side chain toward hydroxyl radical via H-abstraction, while amine is normally positively charged at neutral pH (and thus electron-deficient) and not subject to direct attack by hydroxyl radical. Therefore, the various C−H bonds at saturated carbon atoms become the second most reactive type of site for direct H-abstraction. Meanwhile, an electron-donating substituent will increase the electron density of the target sites and thus the reactivity with hydroxyl radical, while an electron-withdrawing substituent (e.g., carbonyl group located in the α-position) will decrease the reactivity. The oxidation is also preferred at sites where the nascent radical can be stabilized by neighboring functional groups such as unsaturated bonds or electron-rich heteroatoms through electron delocalization to these neighboring atoms. The overlap of the unpaired electron's orbital with p or π orbitals and, to a lesser degree, stabilization by electron-releasing alkyl groups through electron donation via the σ bond to the electron deficient radical centers will all enhance reactivity.[196−200] For alkane functional groups, the order of C−H reactivity is typically *tertiary* > *secondary* > *primary*. This is the same order as the electron density on the carbon atom as well as the same order as the stability of the nascent organoradical and the inverse order in C−H bond strength. However, the degree of selectivity between different types of C−H bonds will be attenuated within proteins due to variations in solvent accessibility.

3.2. Cleavage of Protein Main Chains

Hydroxyl radicals attack preferentially at the side chains of amino acids residues due to the steric hindrance of main chain α-carbon under typical reaction conditions.[196−198] In typical protein footprinting experiments, the experimental conditions are controlled to minimize protein backbone cleavage with, in fact, only limited oxidative modification of protein side chains; this low oxidation regime is experimentally observed when the loss of unmodified species exhibits pseudo-first-order reaction kinetics.[1,26] However, hydroxyl radical oxidation does lead to the cleavage of protein backbones to some extent either via direct attack on the protein main chain α-carbon or by radical transfer from side chains. Understanding the pathways of backbone cleavage will help in the design of footprinting experiments and can take advantage of the main chain cleavage reactions to provide useful structural information.

3.2.1. Main Chain Cleavage via Direct Attack at the α-Carbon

Hydroxyl radical may abstract a hydrogen atom from the α-carbon positions of the protein backbone, particularly at Gly, due to its lowered steric hindrance. The rate constant for hydrogen abstraction from N-Ac-Gly ($CH_3C(O)$-$NHCH_2COO^-$) is about 4×10^8 M^{-1} s^{-1} at neutral pH.[201] Since an α-carbon radical is a secondary radical species at Gly compared to the tertiary radical formed at other amino acid α-carbon sites, the increased reactivity at Gly compared to other amino acid residues is due to the absence of steric interaction between the side chain and the carbonyl main chain.[202,203] Such interactions hinder the formation of α-carbon radical, precluding a planar conformation; this reduces the ability to delocalize the unpaired electron onto the neighboring nitrogen and carbonyl groups.[202] Thus, the secondary Gly α-carbon radical appears to be more stable than the tertiary α-carbon radical formed at other amino acid residues. Racemization can occur at the radical center. Subsequent reactions of the α-carbon-centered radicals with oxygen in air-saturated solutions will result in the fragmentation of the protein backbone. The direct H-abstraction from α-carbon sites is limited in proteins in the case of highly reactive radicals such as $HO^\bullet$ due to competing reactions and steric shielding from side chains.[197] Less reactive radical species can give rise to a relatively higher reactivity toward Gly and other α-carbon sites.[203]

At least two major pathways have been proposed for backbone cleavage after initiation of radicals on the backbone, as shown in Scheme 2. Both mechanisms involve the formation of peroxyl radicals on the α-carbon as intermediates, which is consistent with the observed requirement of oxygen in order to obtain significant yields of peptide fragments; low yields may arise in the absence of oxygen via the solvated electron reactions, even though this does

Scheme 3. Backbone Cleavage and Side Chain Modification of Pro

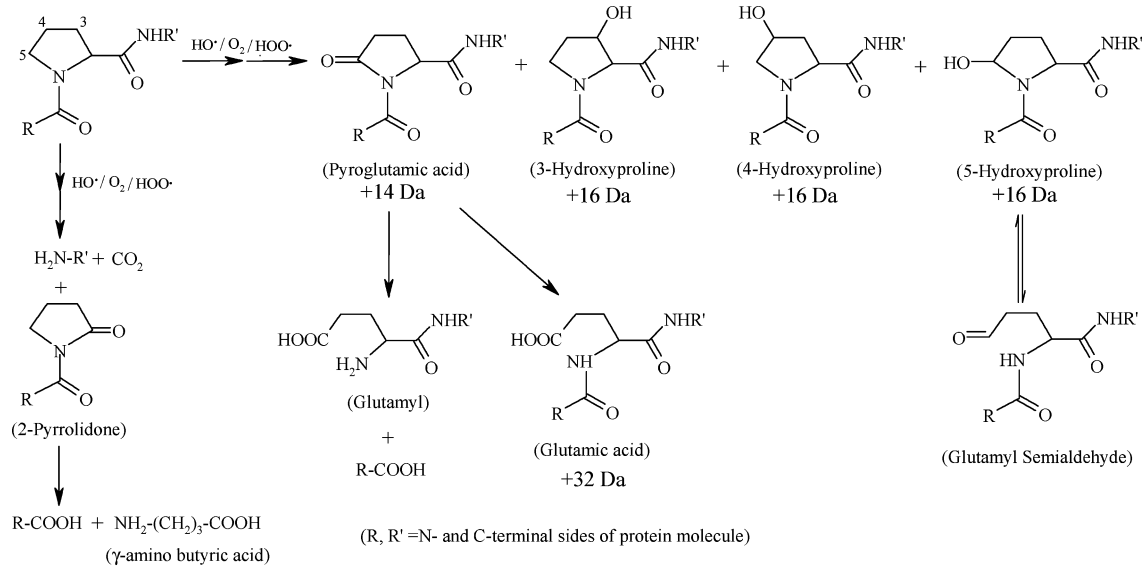

not play a significant role in air-saturated solution chemistry.[196] One fragmentation process involves the loss of $HO_2^•$ from peroxyl radical and subsequent hydrolysis of the newly generated imine species. The other pathway involves the formation of alkoxyl radical at the α-carbon, followed by further fragmentation to cleave the backbone.

3.2.2. Main Chain Cleavage via Attack at the Pro Side Chain

Oxidation of the Pro side chain may also give rise to backbone fragmentation.[204] Schuessler and Schilling found that the number of peptide fragments formed in the radiolysis of proteins is approximately equal to the number of proline residues.[205] Later Uchida et al. confirmed the cleavage pathway by a mechanism that involved the oxidation of Pro to the 2-pyrrolidone derivative (Scheme 3), which hydrolyzed to cleave the backbone.[206] Moreover, γ-aminobutyric acid, derived from hydrolysis of 2-pyrrolidone, has also been identified as a major derivative of proline oxidation in acid hydrolysis of proline-rich proteins[207] and may be used as a presumptive measure of peptide bond cleavage by this pathway. Oxidation at the C-5 site of Pro generates a pyroglutamyl residue with a mass addition of +14 Da, which may be acid hydrolyzed to glutamyl and results in peptide backbone cleavage.

3.2.3. Main Chain Cleavage via Radical Transfer from γ-Carbon at Side Chains

Free radical transfer from side chains to the backbone can result in the cleavage of the protein's main chain.[208,209] H-abstraction from γ-(C-4) or β-carbon (C-3) sites on the side chains (in the presence of oxygen) generates radicals that can transfer from side chains to the protein backbone.[208] Abstraction of hydrogen from the γ-(C-4) carbon of aliphatic side chains in the presence of oxygen can yield C-2−C-3 dehydropeptides, via the formation of peroxyl radicals from the γ-carbon-centered radical.[208,210] For example, in the oxidation of the Glu side chain, the γ-carbon peroxyl radical may undergo subsequent reactions leading to the formation of side chain modification products with a mass shift of −30 Da due to decarboxylation;[209,211] +14 and +16 Da products; or an unsaturated product, a C-2−C-3 dehydropeptide (Scheme 4). The dehydropeptide behaves like an oxygenated enol species, which readily undergoes tautomerism to the keto form. This species is easily hydrolyzed to yield two protein fragments: a new amide and a keto acid.[210] Oxidation of aspartic acid seems similar to the case of Glu and may also result in the cleavage of the protein backbone[212] or decarboxylation of a side chain carboxyl group,[211] except at a lower rate than that for Glu.[211]

3.2.4. Main Chain Cleavage via Radical Transfer from the β-Carbon at Side Chains

Initial hydroxyl radical attack at the β-carbon (C-3) position can lead to the formation of α-carbon radicals and subsequent main chain rupture.[213,214] In this case, alkoxyl radicals are generated after initial H-abstraction to produce carbon-centered radicals and subsequent reaction with O_2 to give peroxyl radicals (Scheme 5). A number of different pathways may generate alkoxyl radical from different precursors, including termination reactions of the peroxyl species with other radicals and decomposition of the intermediate hydroperoxides.[215,216] The alkoxyl radicals can undergo β-scission at a rate $>10^7$ s^{-1}, leading to the loss of a side chain and/or generation of α-carbon radicals and subsequent backbone cleavage.[213,214]

The β-scission reaction of alkoxyl radicals appears to be common for aliphatic side chains such as Val, Leu, and Asp,[214] resulting in the release of a family of carbonyls including formaldehyde, acetone, isobutyraldehyde, and glyoxylic acids. The rate of such β-scission reactions is affected by the nature of the substituents, R and R′, with the rate of fragmentation increased by the presence of electron releasing alkyl groups and substituents that can stabilize the incipient radical center. The α-carbon radicals generated by the β-scission reaction of alkoxyl radicals are stable due to the delocalization of unpaired electrons onto the neighboring carbonyl and amide functions and relief of steric strain in the alkoxyl radical.[217]

Scheme 4. Backbone Cleavage by Radical Transfer from the γ-Carbon at Side Chains: Oxidation of Glu

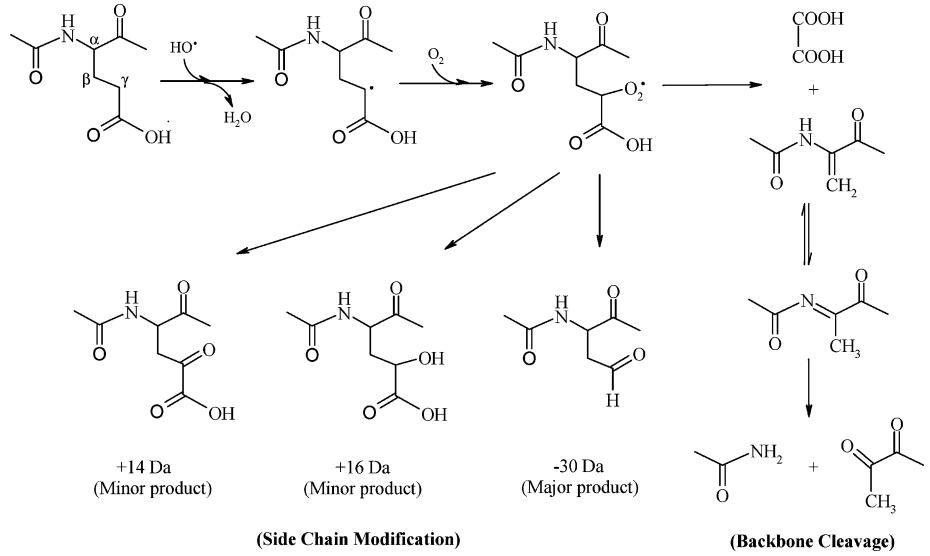

Scheme 5. Backbone Cleavage by Radical Transfer from the β-Carbon at Side Chains

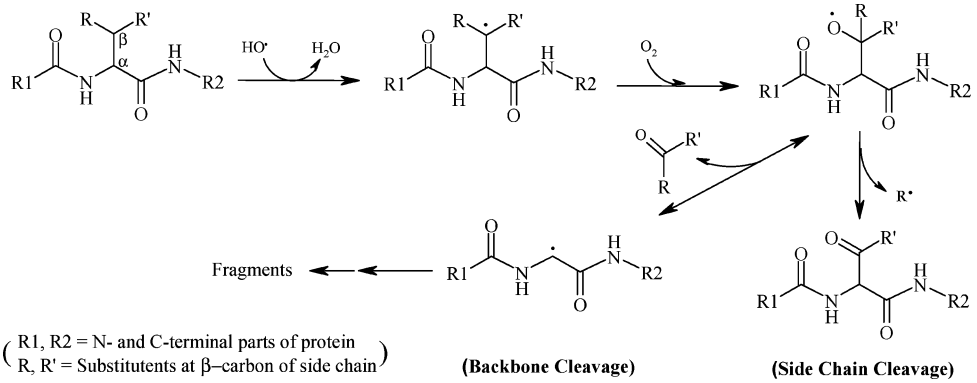

3.3. Oxidation of Amino Acid Residue Side Chains

3.3.1. Oxidation of Aliphatic Side Chains

Radiolysis of aqueous solutions produces a hydroxyl group at aliphatic hydrocarbon side chains, i.e., Leu, Ile, Val, and Ala, resulting in +16 Da mass shifts, as major products along with carbonyl (aldehyde/ketone) groups, resulting in a +14 Da mass shift, as minor products. Products with multiple oxygen additions can also be generated dependent on the extent of modification. Mass spectrometry analysis of the radiolytic oxidation of Leu-NH_2 is presented in Figure 5 as an example. The peak at *m*/*z* 131.0 corresponds to the unmodified Leu-NH_2, while the peaks at *m*/*z* 147.0 and 163.0 correspond to the +16 and +32 Da oxidation products, respectively. The carbonyl product with a +14 Da mass shift is observed at *m*/*z* 145.0 as a minor product.

The hydrocarbon side chains are generally attacked with little selectivity by $HO^{\bullet}$, and the reactivity of the hydrocarbon side chains increases with the number of C−H bonds and the length of the hydrocarbon side chains.[197,218] The pathway of hydroxyl radical oxidation of aliphatic side chains is shown in Scheme 6. The first step is hydrogen abstraction by $HO^{\bullet}$ to give a carbon-centered radical, which reacts rapidly (diffusion-controlled) with O_2 under aerobic conditions to form a peroxyl radical. The peroxyl radical can undergo a series of radical reactions, giving rise to hydroperoxide (+32 Da), hydroxide (+16 Da), or carbonyl (+14 Da, aldehydes or ketones) products or alternatively alkoxyl radicals and O_2.[218] Peroxyl radicals undergo dimer formation with other peroxyl radicals or related species such as $O_2^{\bullet-}$/$HOO^{\bullet}$ and rearrange through a Russell six-membered transition state to yield carbonyl products.[219] Alkoxyl radicals once formed can undergo rapid hydrogen abstraction reactions to give alcohols or rearrangement/fragmentation reactions which produce carbonyl products.[196] Normally, hydroperoxides are

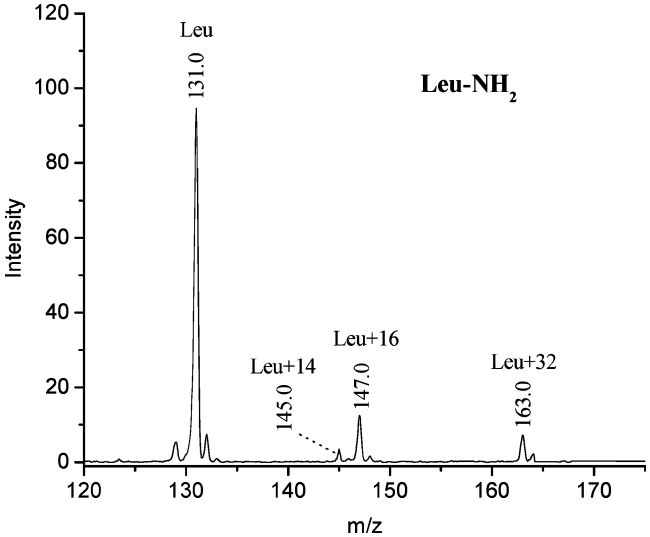

Figure 5. Mass spectrometry analysis of leucine oxidation. MS spectrum of 30 μM Leu-NH_2 exposed to γ-rays for 8 min.

Scheme 6. Oxidation of Hydrocarbon Side Chains

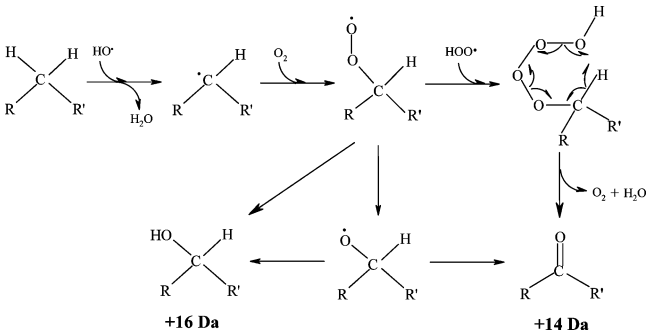

not stable and can decompose to give rise to further radicals as well as further alcohol and carbonyl products.

Proline. Proline has an aliphatic side chain but differs in that the side chain is bonded to both nitrogen and the α-carbon atom. The cyclic structure results in it being often found in the bends of folded protein chains, and it is not averse to being exposed to water. The peculiar structure gives rise to oxidative behavior different from that of other aliphatic side chains. The oxidation of proline side chains and the transfer of its oxidation products to the protein backbone have been summarized above (Scheme 3). Hydroxyl radical may abstract a hydrogen atom from the C-3, C-4, or C-5 carbons of the Pro side chain, with preference at C-5.[195] H-abstraction from the C-5 site of Pro generates a secondary carbon-centered radical, which reacts with O_2, resulting in a peroxyl radical. The subsequent reaction of this peroxyl radical gives rise to 5-hydroxyproline with +16 Da mass change or pyroglutamic acid with a +14 Da mass shift. The latter species (β-diketo compound) can hydrolyze via two pathways: one by ring-opening, giving rise to glutamic acid with a mass increase of +32 Da, and another pathway leading to the cleavage of the protein backbone and formation of two protein fragments.[195,204,208] The 5-hydroxyproline is in equilibrium with glutamic semialdehyde, which is the same product formed by oxidation of arginine via deguanidination.[200,212,220,221]

3.3.2. Oxidation of Basic Side Chains

Arginine. Arg is potentially one of the most valuable probes for studying protein interactions, given the fact that it is often a key residue for stabilizing protein interfaces due to its capacity for multiple types of favorable interaction.[222] It is able to form up to five H-bonds and a salt-bridge through the positively charged guanidino group, and it can participate in hydrophobic interactions because of the pseudoaromatic character of the electron-delocalized guanidino π-system and the three hydrophobic methylene carbon atoms. Arginine and lysine also play a key role in protein−nucleic acid recognition and interactions.[223−225]

Arg is subject to hydroxyl radical-mediated modification and gives rise to characteristic oxidation products. Shown in Figure 6A is the positive ESI-MS spectrum of peptide ARRA exposed to cesium-137 γ-rays for 4 min.[226] The primary oxidation product has the second most intense signal at *m*/*z* of 430.3 Da, with a characteristic −43 Da mass shift from the original peptide at *m*/*z* 473.3. Other oxidation products include +14 and +16 Da oxygen-addition products at *m*/*z* 487.2 and 489.2. The characteristic −43 Da oxidation product has been found in metal-catalyzed oxidation[220,227] as well as in radiolytic oxidation[228] of proteins. An oxidation pathway has been proposed and shown in Scheme 7.[220,227,228]

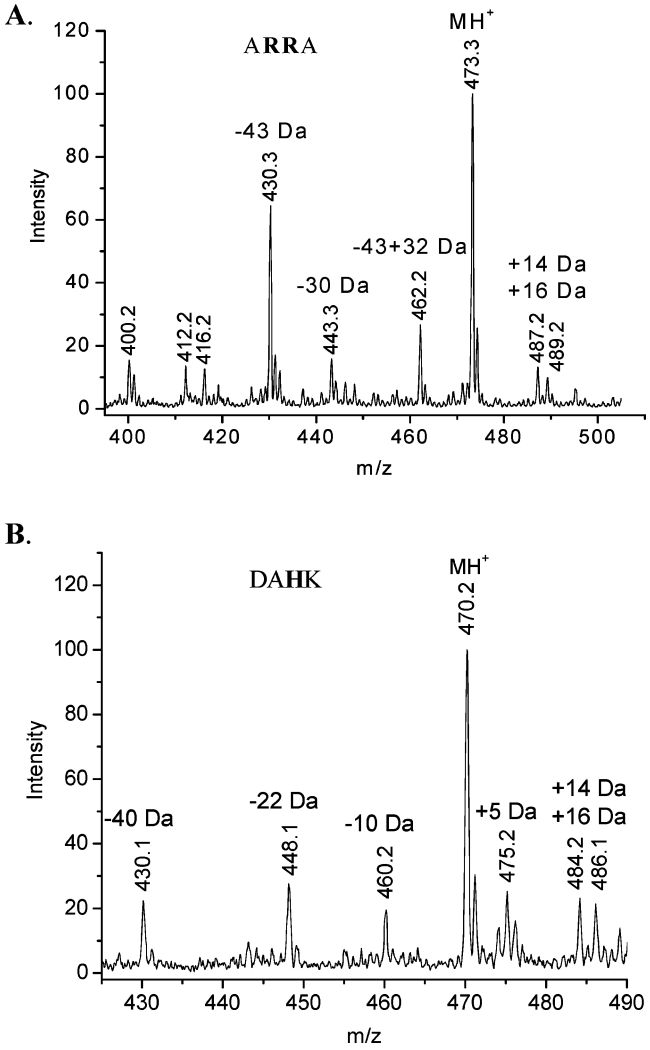

Figure 6. (A) ESI-MS spectrum of peptide ARRA exposed to ^{137}-Cs-source γ-rays for 4 min. (B) ESI-MS spectrum of peptide DAHK irradiated by synchrotron X-rays for 25 ms.

A hydroxyl radical abstracts a hydrogen from the δ-carbon of the side chain and adds a O_2 to form an intermediate peroxyl radical. The subsequent reactions lead to the loss of the guanidino group and generation of a γ-glutamyl semialdehyde. The initial radical attacks at other sites of the Arg side chain are likely to give rise to +14 and +16 Da oxygen-addition products, such as other aliphatic side chains, as discussed above. This preferred initial attack at the δ-carbon has been confirmed by deuterium exchange NMR studies[229] and by EPR spin trapping studies.[229,230]

EPR has been used to investigate the reaction of hydroxyl radicals generated by UV photolysis of H_2O_2 with 14 aliphatic amines and polyamines and compounds containing one and two guanidino groups.[230] For the amines and polyamines below pH 7, the predominant reaction of hydroxyl radical was the abstraction of a hydrogen atom from the carbons not adjacent to the protonated amino group. In contrast, for the two compounds containing one and two guanidino groups, the hydrogen abstraction occurred at the carbon adjacent to the guanidino groups. This indicates that the C−H bonds vicinal to the guanidino group are particularly susceptible to hydrogen atom abstraction by hydroxyl radicals.

Histidine. His is a very important amino acid residue critical for the function of many enzymes. His is susceptible

Scheme 7. Oxidation of Arginine

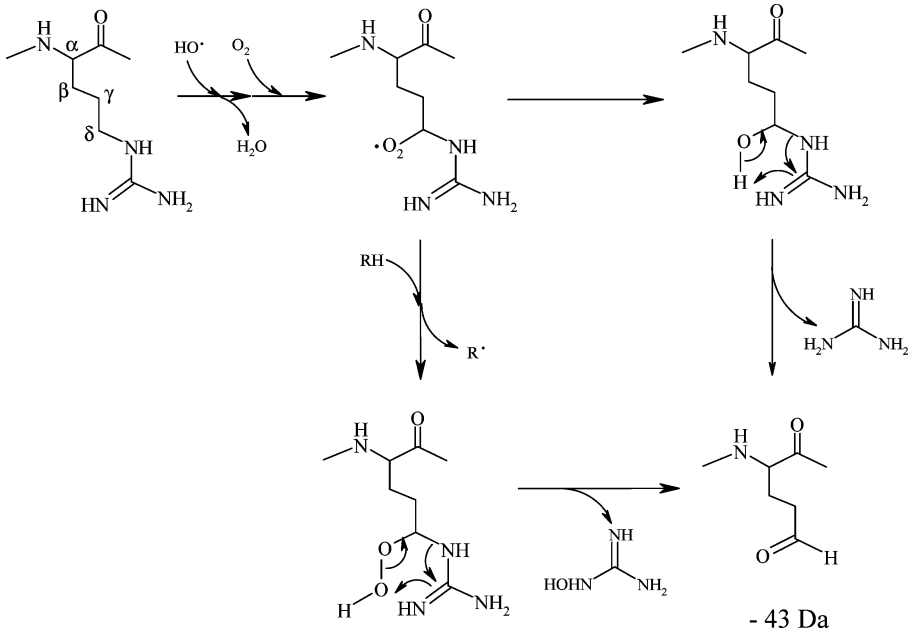

Scheme 8. Oxidation of Histidine

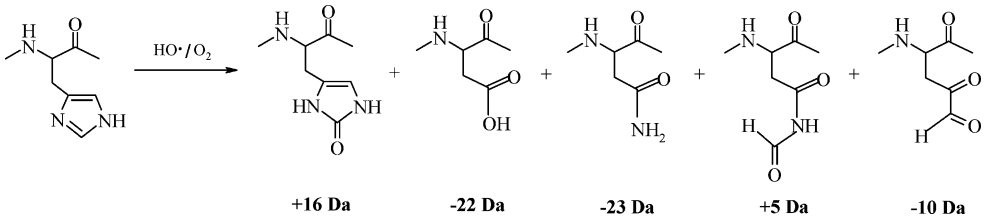

to radical oxidation, leading to very complex products. Some of the primary oxidation products can be seen in an examination of the radiolytic oxidation of the peptide DAHK.[226] The mass spectrum of the peptide irradiated by synchrotron X-rays for 25 ms (Figure 6B) indicates the peak at *m*/*z* 470.2 that belongs to the unmodified peptide. The oxidation of His, as confirmed by tandem mass spectrometry, gives rise to characteristic products with mass shifts of −22 Da at *m*/*z* 448.1, −10 Da at *m*/*z* 460.2, +5 Da at *m*/*z* 475.2, and +16 Da at *m*/*z* 484.2. The −22 Da product results from the conversion of His to aspartic acid, while the +16 Da species corresponds to 2-oxohistidine, consistent with MCO studies of histidine oxidation.[200] We have also identified the −22, −10, +5, and +16 Da oxidation products of His in oxidation of proteins (unpublished data).

The reaction of histidine with hydroxyl radicals is complicated, and all the oxidation products have not been fully characterized.[196,198] The major oxidation products of His residues as proposed in the literature are presented in Scheme 8.[204,226,231] The complexity of histidine oxidation has been demonstrated by metal ion-catalyzed oxidation. Hydroxyl radicals initially attack the imidazole ring of histidine at position C-2, C-4, or C-5 and produce the stabilized allyl-type radicals.[232−235] These radicals can incorporate O_2 to give peroxyl radicals and undergo further reactions, giving rise to a mixture of products that depend on the reaction conditions and the local amino acid sequence.[204,231,236−239] 2-Oxohistidine, asparagines, and aspartic acid have been identified as the major products. Uchida and Kawakishi[231] investigated the damage of histidine within proteins using Cu_2^+/H_2O_2 and *N*-benzoylhistidine as the model compound. Four products including asparagines (−23 Da), aspartic acid (−22 Da), aspartylurea, and formylasparagine were observed, emphasizing the rupture of the imidazole ring. Even more complex reactions were indicated in the case of photooxidation. Tomita et al.[240] demonstrated that histidine was photooxidized to aspartic acid via several intermediate compounds. In addition to the final product, they detected and isolated 17 intermediate products of the reaction.

Lysine. Lysine was reported to be converted to hydroxylysine[241] and α-amino-adipyl-semialdehyde[242,243] by oxidation with MCO or γ-radiolysis.[244] In the presence of oxygen, hydroxyl radicals may abstract hydrogen from and add a hydroxyl group to any carbon of the lysine side chain to give different hydroxylysine products. If hydroxyl attacks the ϵ-carbon, ϵ-hydroxylysine is formed. However, ϵ-hydroxylysine is not stable and becomes 2-amino-adipyl-semialdehyde by loss of an ammonia.[243] In the radiolytic oxidation of peptide DAHK (Figure 6B), tandem mass spectrometry (data not shown) indicated that the lysine residue experienced oxidation, contributing exclusively to the +14 Da product, and provided two-thirds of the +16 Da product.[226] However, radiolysis studies have not identified the 2-amino-adipyl-semialdehyde product of Lys as found in metal-catalyzed oxidation of Lys.[242−245] The hydroxyl and carbonyl groups in the above oxidation products could be located at any carbon except the ϵ-carbon on the side chain of lysine. The reaction of hydroxyl radical with aliphatic amines in aqueous solution is strongly pH dependent.[230,246,247] Under alkaline conditions, the amine group and the α-carbon of the aliphatic amine are the primary targets for hydrogen abstraction by hydroxyl radicals. The reaction of hydroxyl with deprotonated amine is nearly diffusion controlled, and the rate is about 1 or 2 orders of magnitude larger than that

Scheme 9. Decarboxylation of C-Terminal Carboxyl

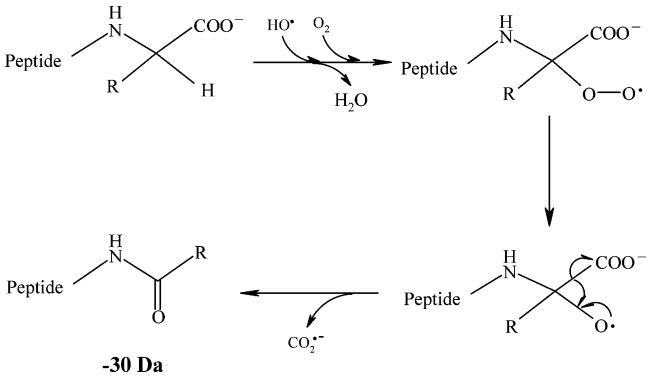

for its protonated counterpart. Under acidic conditions, the amine is protonated, and its strong inductive effect reduces the electron density of the carbon next to it. Thus, the electrophilic hydrogen abstraction by hydroxyl radical seems unfavorable and more likely to take place from carbons further away from the ion.

3.3.3. Oxidation of Acidic Side Chains and the Protein C-Terminus: Decarboxylation

Protein C-Terminus. It has been reported that generation of protein and peptide alkoxyl radicals can give rise to C-terminal decarboxylation.[209] Irradiation of *N*-acetyl amino acids and dipeptides produces hydroperoxides at the α-carbon position of the C-terminal residue. Decomposition of the α-carbon hydroperoxide by incubation of the irradiated samples with Fe(II)-EDTA resulted in C-terminal decarboxylation via a pseudo-Fenton reaction with release of radical $CO_2^{\bullet-}$, which was trapped and detected by EPR spectroscopy. A mechanism of decarboxylation as outlined in Scheme 9 was proposed to explain the release of radical $CO_2^{\bullet-}$, and the α-carbon alkoxyl radical was thought to be the key intermediate in the process. The corresponding amides were proposed to undergo deamidation with release of $^{\bullet}CONH_2$. The proposed oxidation mechanism generates a new carbonyl group at the original α-carbon.[209] In radiolysis studies, decarboxylation products with a −30 Da mass change consistent with this mechanism have been observed.[211] However, the deamidation of a C-terminal amide, which should generate a −29 Da product, has not been seen.

Glutamic Acid. Glu contains an aliphatic side chain with the δ-carbon atom as carboxyl group. The initial hydrogen abstraction by hydroxyl radical is most likely to take place at the β- or γ-carbon atoms. The oxidation produces the typical hydroxylation and carbonyl products, like those for hydrocarbon side chains. In addition, there are two possible outcomes for the γ-carbon-centered radical next to the carboxyl group, as described previously for backbone cleavage. Reaction of oxygen with the carbon-centered radical can lead to decarboxylation with formation of a new aldehyde group at the γ-carbon, resulting in a −30 Da mass shift. The mechanism is similar to that for C-terminal decarboxylation as shown in Scheme 9.[209,211] In the second pathway, the γ-carbon may generate a C-2−C-3 dehydro function, finally leading to cleavage of the protein backbone.[208,210] The characteristic −30 Da decarboxylation product of Glu was also identified in radiolysis of Glu-containing peptides[211] and proteins.[228] Figure 7A shows the ESI-MS spectrum of 20 μM peptide CH_3-EEEPAAR-NH_2 exposed to γ-rays for 6 min. The characteristic −30 Da decarboxylation product from Glu side chains is clearly seen.

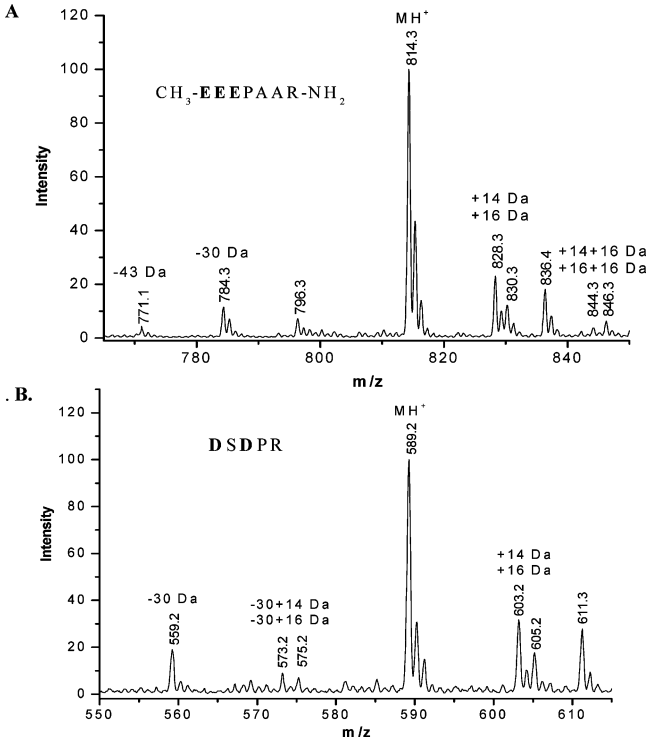

Figure 7. Oxidation of glutamic acid by radiolysis. ESI-MS spectra of (A) 20 μM peptide CH_3-EEEPAAR-NH_2 exposed to ^{137}Cs-source γ-rays for 6 min and **(**B**)** 20 μM peptide DSDPR exposed to ^{137}Cs-source γ-rays for 6 min.

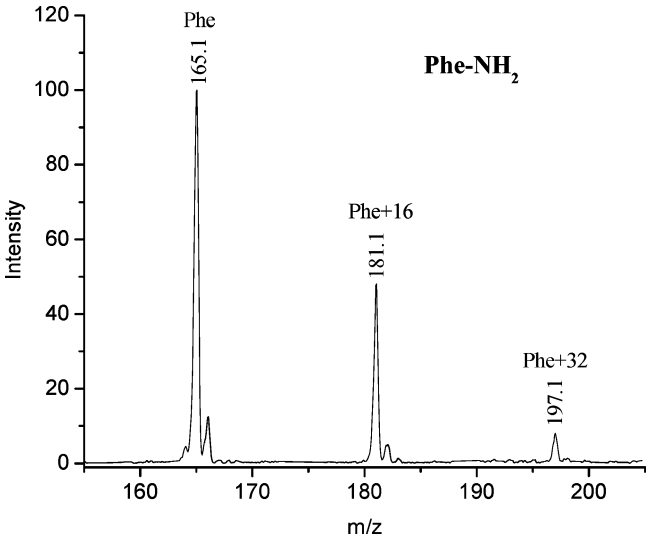

Figure 8. Oxidation of Phe. ESI-MS spectrum of 10 μM Phe-NH_2 exposed to ^{137}Cs-source γ-rays for 8 min.

Aspartic Acid. Oxidation of aspartic acid is similar to that of Glu and may also result in the cleavage of the protein backbone[212] or decarboxylation of a side chain carboxyl group.[211] Oxidation of Asp with a −30 Da mass change is seen for the radiolysis of many Asp-containing peptides, including DSDPR (mass spectrum of 20 μM DSDPP exposed to γ-rays for 6 min is shown in Figure 7B), DRGDS, Ac-DRGDS, ADSDGK, KQAGDV, etc., as well as the aspartic acid derivative *N*-acetylaspartic amide.[211] Therefore, the oxidative decarboxylation leading to a 30 Da mass reduction is characteristic for aspartic acid oxidation. However, Asp is not valuable as a footprinting probe for protein structure, since its reactivity is too low compared to those of other reactive amino acid side chains.[248]

Scheme 10. Oxidation of Phenylalanine

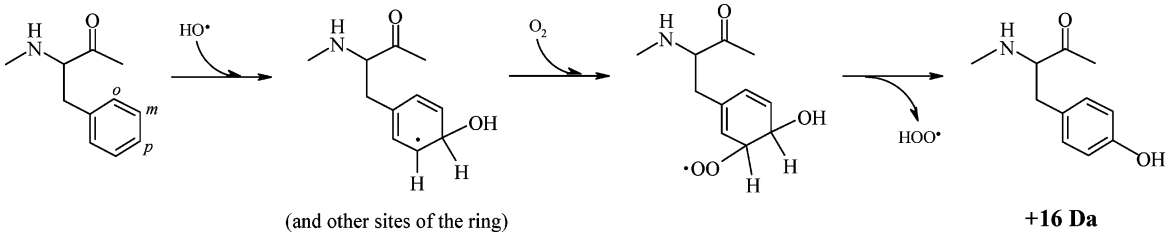

Scheme 11. Oxidation of Tyrosine

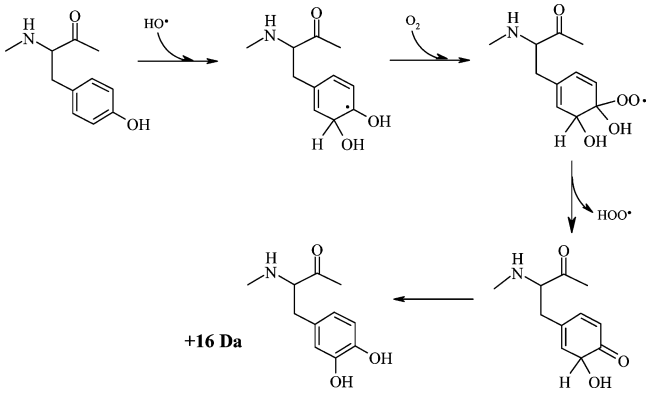

3.3.4. Oxidation of Aromatic Side Chains

Phenylalanine. Radiolytic modification of aromatic amino acid side chains almost invariably results in hydroxyl attack at the aromatic rings by addition, resulting in one or multiple +16 Da mass shifts. Figure 8 shows the mass spectrum of 10 μM Phe-NH_2 exposed to γ-rays for 8 min. The peak at *m*/*z* 165.1 corresponds to the molecular ions of Phe-NH_2. Phe-NH_2 gives rise to an oxidation product at *m*/*z* 181.1 with a +16 Da mass shift and a lower yield product at *m*/*z* 197.1 with a +32 Da mass shift. The oxidation of Phe is illustrated in the Scheme 10. Hydroxyl radical adds rapidly to the aromatic ring of Phe with little positional selectivity to form a hydroxycyclohexadienyl radical, which rapidly reacts with O_2 and subsequently eliminates a HOO• to give rise to a mixture of stereoisomers of tyrosine with the ratio of *o*-/*m*-/*p*-tyrosine being 2:1:1.5 or 2.3:1:2.1 dependent upon experimental conditions.[195,198] Multiple hydroxylations would give rise to dihydroxyphenylalanine (DOPA) or even trihydroxyphenylalanine (TOPA). In the absence of O_2, the overall yield of these tyrosine isomers would be low, and cross-links can be formed.

Tyrosine. Oxidation of Tyr is similar to that of Phe except with much more position selectivity due to the strong directing effect of the hydroxyl substituent. Hydroxyl radical rapidly adds to the sites next to the original hydroxyl substituent at the side chain, followed by addition of an O_2 in the presence of oxygen, as shown in the Scheme 11. The subsequent elimination of peroxyl radical HOO• leads to the final product, 3,4-dihydroxyphenylalanine (DOPA). Multiple hydroxylations would generate trihydroxyphenylalanine (TOPA). In the absence of oxygen, the primary product is still dihydroxyphenylalanine, but with a much low yield, and cross-links can be formed.

Tryptophan. Oxidation of Trp in oxygenated solutions is much more complicated than that of Phe and Tyr and less well characterized.[198,249] Metal-catalyzed oxidation (MCO) of Trp in bovine α-crystallin generated hydroxytryptophan (+16 Da), *N*-formylkynurenine (+32 Da), kynurenine (+4 Da), and 3-hydroxykynurenine (+20 Da).[249,250] Similar oxidation takes place in radiolysis.[198,251] HO• is able to add to both the benzene ring and the pyrrole moiety at the C-2 and C-3 double bond with a relative ratio around 40:60 with preference for the pyrrole moiety (Scheme 12).[252] In the presence of oxygen, the former process leads to the formation of mixed stereoisomers of hydroxytryptophan (+16 Da) (with low yield), while the latter process results in ring opening and gives rise to mixed oxidation products, including 2-hydroxyltryptophan (+16 Da), *N*-formylkynurenine (+32 Da), kynurenine (+4 Da), etc.[249,251] These products may be subjected to further oxidation to give dihydroxytryptophan, hydroxykynurenine, etc. In the radiolysis of Trp-NH_2 and the tripeptide GWG (data not shown), products with +16*n* Da ($n = 1-5$) mass shifts were detected by electrospray mass spectrometry, with +32 Da corresponding to *N*-formylkynurenine and dihydroxytryptophan as the principle products followed by +16 Da and +48 Da products at lower yield. Trivial amounts of +4 Da product were also detected. The results indicate that *N*-formylkynurenine and mono- and

Scheme 12. Oxidation of Tryptophan

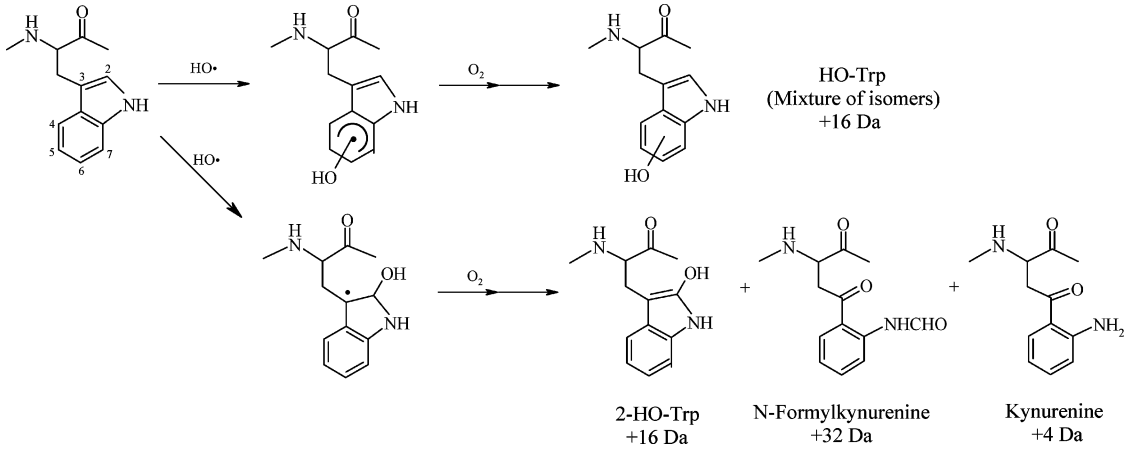

dihydroxytryptophan are the primary radiolytic modification products of tryptophan. That this chemistry can be used to examine structure is seen in a recent report;[253] in this case, a conformational change in the Arp 2/3 protein as a result of binding its WASp coactivator preferentially suppressed the observation of a +16 Da species in favor of the +32 Da oxidation product. Tandem MS confirmed Trp as the site of oxidation, and it was suggested that WASp interacts with the benzene moiety of Trp, suppressing the +16 Da product while the pyrrole moiety is still free to react.

3.3.5. Oxidation of Sulfur-Containing Side Chains

The sulfur-containing amino acid residues, Cys and Met, along with disulfide represent the most reactive side chains of the amino acids.[201] They are valuable structural probes both for their reactivity and for their roles in protein structure and function. Cysteine is important for the catalytic activity of many enzymes[254] and is the second most conserved residue in the primary structure of homologous proteins after Trp.[255] Disulfide bridges are also very important in protein structure, and the classical view that they have been added during evolution for purposes of stability is maturing, as more examples of cleavage of disulfide bonds being important regulatory switches have emerged.[256] Methionine, a hydrophobic residue with a sulfur-containing side chain, generally prefers to be buried in protein hydrophobic cores. It shows minimal conservation on the surface of proteins with the conspicuous exception that it is conserved in known ligand binding sites.[257] Therefore, conservation of Met on the protein surface can imply a prospective site for a macromolecular interface.[257]

Cys and Met are both highly reactive with respect to measured rates of reaction with hydroxyl radicals,[201] and both Met and Cys are easily oxidized in many proteins.[3,31,258−262] The high reactivity of Cys and Met residues requires a full understanding of their oxidation chemistry and careful control of experimental conditions as well sample handling to permit their use as structural probes. Radiolytic oxidation of methionine,[263−269] cysteine,[263,270−279] and cysteine[263,280−286] in peptides and proteins has been the subject of intense study, and the chemistry of sulfur-centered radicals has also been reviewed.[287,288] From these studies it is clear that the oxidation of sulfur-containing amino acids is very complicated and leads to multiple products; in addition, the proposed mechanisms of oxidation are not without some controversy. These studies have been carried out primarily by UV/vis spectroscopy and EPR on the sulfur-centered free radicals or intermediates. Footprinting emphasizes the final oxidation products instead of intermediates, and the intense EPR and UV/vis signals detected in intermediate radicals do not necessarily reflect the levels of relevant products. Recently, mass spectrometry has been used to examine the oxidation products of Cys residues oxidized by hydrogen peroxide.[289,290] In the study, electrospray ionization mass spectroscopy (ESI-MS) and tandem mass spectrometry (MS/MS) were used to investigate the radiolytic modification of sulfur-containing residues and disulfides, emphasizing the detection of final products to improve oxidative footprinting approaches.[309]

Oxidation of Cysteine. The radiolysis chemistry of Cys in aqueous solutions has been subjected to extensive study for decades.[263,270−276,291,292] A number of intermediate radical species have been identified, and their structures and reactivities have been studied using spin-trap EPR, optical, and conductivity measurements in the presence and absence of oxygen.[270,271,274,277,293] Despite this extensive study, the reaction mechanisms for the diverse array of products are not fully understood. Oxidation of free Cys may result in complex products, including sulfonic acid (RSO_3H), sulfinic acid (RSO_2H), disulfide (RSSR′), loss of a sulfhydryl group, and conversion of Cys to dehydroalanine and serine.[294] The oxidation can be clearly demonstrated by radiolysis studies of model compounds as shown in Figure 9.[294] Figure 9A is the negative ESI-MS spectrum of peptide GCG irradiated by γ-rays for 6 min. The peak m/z 234.0 corresponds to the unmodified peptide. A primary oxidation product with mass shift +48 Da is shown at m/z 282, corresponding to oxidation of sulfhydryl in Cys to sulfonic acid. The weak peak at m/z 266.0, with +32 Da mass shift, results from the oxidation of the sulfhydryl in Cys to sulfinic acid. The medium peak at m/z 467.0 is from the disulfide product. The weak peaks at m/z 280.0, 298.0, and 314.0, corresponding to +46, +64, and +80 Da mass shifts, respectively, are due to the further oxidation of disulfide. The peak m/z 200.0, corresponding to −34 Da mass, is possibly the dehydroalanine product due to the loss of H_2S from the side chain. The weak signal at m/z 218.0 is possibly due to the conversion of Cys to Ser by oxidation. The formation of negatively charged sulfonic and sulfinic acid groups in these oxidation products decreases the ionization efficiency in positive electrospray. Similar oxidation products are also found in radiolysis of the peptides FTLCFR-NH_2 and ANPDCKTILKALGPAAT, as shown in Figure 9B and C, respectively. All of these products were confirmed to be due to the oxidation of Cys by tandem mass spectrometry.

The mechanism of Cys oxidation is very complex and is still not completely understood. A variety of mechanisms have been proposed to account for the various products generated subsequent to the formation of the initial radical species as well as the role of oxygen in mediating product formation.[263,270−276,291,292,294] Scheme 13 displays the likely reactions of the primary radical species generated in radiolysis of water with sulfhydryl species and the comprehensive mechanisms of oxidation based on the previous studies. Although some of the reaction intermediates may be open to question, the scheme is a reasonable framework for interpreting the observed oxidation products. The initial step in Cys oxidation is the formation of the thiyl radical species ($RS^{\bullet}$) via hydrogen abstraction from sulfhydryl (RSH) by $HO^{\bullet}$, by $H^{\bullet}$, and possibly by $O_2^{\bullet-}$ and other oxygen reactive species.[270,274,295] $RS^{\bullet}$ undergoes two competitive rapid reactions with molecular oxygen (O_2) or thiolate (RS^-) to generate a thiyl peroxyl radical ($RSOO^{\bullet}$) or a conjugated disulfide radical anion $(RSSR)^{\bullet-}$ dependent on the pH and the oxygen and thiol concentrations.[278,279] $RS^{\bullet}$ reacts rapidly (diffusion controlled) yet reversibly with molecular oxygen (O_2) to generate a thiyl peroxyl radical ($RSOO^{\bullet}$), with rate constants $>10^9$ M^{-1} s^{-1} for the forward and 10^5-10^6 M^{-1} s^{-1} for the reverse reactions,[296] with an equilibrium constant of 10^3-10^4. $RSOO^{\bullet}$ is seen to be the precursor of sulfenic, sulfinic, and sulfonic acid, disulfide, and serine products.[270] Sulfenic acid RSOH and sulfinic acid RSO_2H are both generated from $RSOO^{\bullet}$. Thiyl hydroperoxide (RSOOH) is possibly present as an intermediate in the formation of RSOH, RSO_2H, and disulfide RSSR. Sulfenic acid (RSOH) is typically unstable and highly reactive;[297−299] thus, it is barely observable in these experiments. RSOH can form sulfinic acid (RSO_2H) and sulfonic acid (RSO_3H) through reaction with H_2O_2, $O_2^{\bullet-}$, O_2, or other oxidizing reagents.[283]

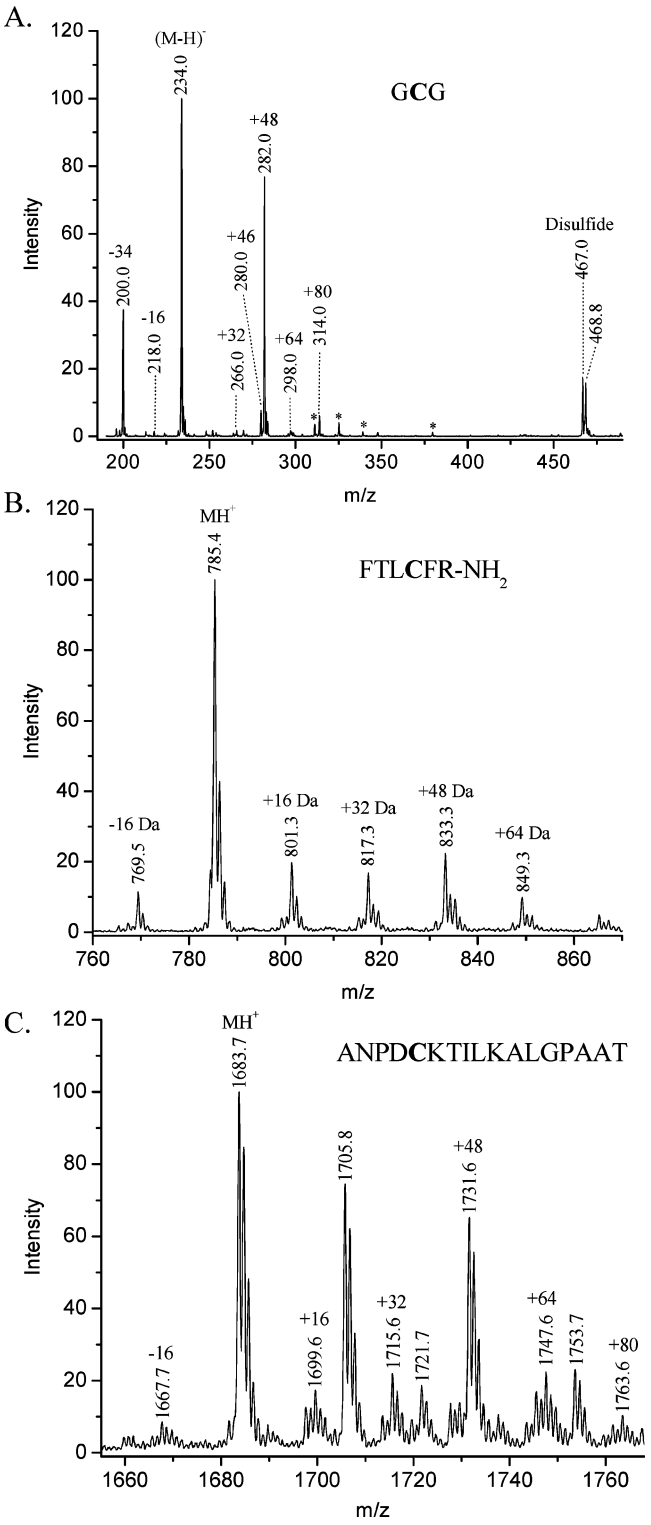

Figure 9. Oxidation of Cys. (A) Negative-ESI-MS spectra of peptide GCG exposed to ^{137}Cs-source γ-rays for 6 min. (B) Positive-ESI-MS spectrum of peptide FTLCFR-NH_2 exposed to synchrotron X-rays for 15 ms. (C) Positive-ESI-MS spectrum of peptide ANPDCKTILKALGPAAT exposed to synchrotron X-rays for 15 ms.

RSOH can also be converted to disulfides by reacting with another thiol group.[274] Sulfinic acid RSO_2H may be generated from RSOO$^\bullet$ via hydrogen abstraction from another thiol group (RSH) or via reaction with hydroperoxyl $HO_2^\bullet$, or it may be generated via isomerization from thiyl hydroperoxide RSOOH or further oxidation from sulfenic acid RSOH by

Scheme 13. Oxidation of Cysteine

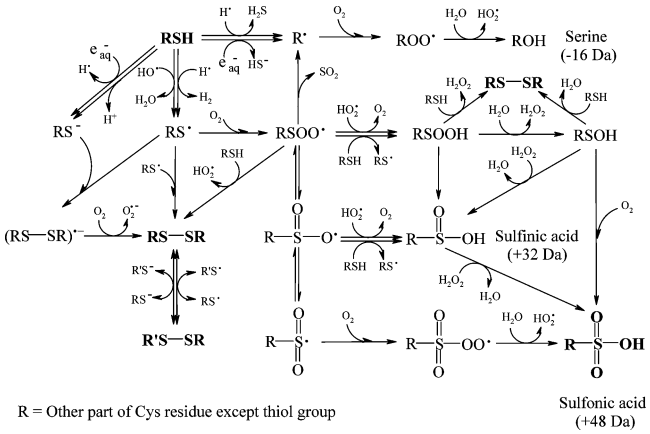

H_2O_2. The sulfonic acid (+48 Da) product presumably dominates in these studies, since it requires the participation of no additional radical species, which are present at very low steady-state concentrations, and only requires rearrangements and further reaction with molecular oxygen or hydrogen peroxide H_2O_2. RSOO$^\bullet$ can easily isomerize to the fully sulfur-centered, thermodynamically favored sulfonyl radical $RSO_2^\bullet$.[271] $RSO_2^\bullet$ may subsequently react with another oxygen molecule and give rise to sulfonyl peroxyl radical,[271] $RSO_2OO^\bullet$. The highly reactive intermediate converts ultimately to sulfonic acid RSO_3H via interacting with a water molecule.[300] Oxygen is necessary for the radiolytic generation of sulfonic acid.[283] The further oxidation of sulfenic and sulfinic acids also leads to sulfonic acid. In the absence of air, sulfinic acid is produced in moderate yield and disulfide is produced in high yield.[285]

Disulfide is one of the primary products for radiolysis of small cysteine-containing peptides under both aerobic and anaerobic conditions.[270,275] There are several avenues to the formation of disulfide. Thiyl radical RS$^\bullet$ can react rapidly with thiolate RS^- to form disulfide radical anion $(RSSR)^{\bullet-}$,[291] which reacts with molecular O_2, giving rise to molecular disulfide RSSR and superoxide radical anion $O_2^{\bullet-}$.[270] The reactions of RS$^\bullet$ with RS^- and O_2 are two competitive reactions dependent upon pH and thiol and O_2 concentrations.[278] Higher pH results in the formation of the disulfide anion by increasing the concentration of thiolate ion; higher thiol concentration and lower O_2 concentration also favor the formation of disulfide and disfavor the formation of oxygen-addition oxidation products. The second approach to generate disulfide is the combination of intermediate RSOOH or RSOH with a parent RSH via loss of a H_2O_2 or water molecule.[292] The third route is the combination of two RS$^\bullet$ radicals in the absence of oxygen,[291] and the probability is greatly reduced in air-saturated solutions because of favored reaction of RS$^\bullet$ with O_2 in higher concentration, around 0.3 mM.[285] The yield of disulfide is particularly high under anaerobic conditions due to a chain reaction which can be inhibited by O_2. If there is more than one free cysteine peptide or cysteine-containing peptide in the solution, mixed disulfide R′SSR can also form via thiol−disulfide exchange, which takes place through displacement reaction of disulfide by RS$^\bullet$ or RS^-.[301] The thiol−disulfide exchange is accelerated at high pH and suppressed at low pH.

The serine product corresponding to a −16 Da mass shift results from the generation of an alanyl radical R$^\bullet$; this carbon-centered radical is likely derived from two separate routes. First, it can be generated directly from the original

thiol through reaction with a solvated electron e_{aq}^- and loss of SH^-[270] or reaction with a hydrogen radical H• and loss of H_2S.[272] Meanwhile, R• can be produced by elimination of neutral SO_2 from thiyl peroxyl radical RSOO•. Similar to all other aliphatic hydrocarbon radicals, the alanyl radical R• reacts with O_2 to give rise to a peroxyl radical ROO•, which leads to the formation of ROH.

The mechanisms leading to the formation of sulfinic and sulfonic acids indicate that both products incorporate oxygen from water or dissolved O_2. Our previous radiolysis studies of cysteine-containing fibronectin peptide (RCDC) in water and ^{18}O-labeled water also indicated the likely prevalence of the cysteine sulfinic and sulfonic acid products and demonstrated that both molecular oxygen and oxygen from water were incorporated in the oxidation products.[25] We have also recently demonstrated that, for proteins, solvent accessible Cys side chains oxidize primarily to the +32 Da cysteine sulfinic and +48 Da sulfonic acids.[302] Disulfide formation is less likely within proteins during radiolysis, because non-disulfide-bound cysteine residues are generally separated in space. However, disulfides can form during proteolysis and storage, because free cysteine residues are sensitive to oxidation from trace amounts of oxygen or H_2O_2 generated during sample irradiation, and mixed disulfides can also be formed by thiol−disulfide exchange. Thus, care needs to be taken in sample handling subsequent to radiolysis exposure.

Oxidation of the Disulfide Bond. Similar to single cysteine residues, the sulfur moiety in the disulfide bond is the principal target of attack, resulting in the formation of thiyl radicals. Consequently, the radiolysis products are analogous to those resulting from the radiolysis of single cysteine residues in the presence of oxygen, with cysteine sulfonic acid $CysSO_3H$ and regenerated disulfides as the primary radiolytic products.[282] The oxidation products are clearly demonstrated by two model peptides subjected to radiolysis oxidation, as shown in their mass spectra in Figure 10:[294] $(GC)_2$ (intermolecular disulfide) and RSSCFGGRIDRIGAC-NH_2 (internal disulfide). Presented in Figure 10A is the negative ESI-MS spectrum of peptide $(GC)_2$ (intermolecular disulfide) exposed to γ-rays for 8 min. The ion at *m*/*z* 353.0 corresponds to the unmodified peptide. Product ions *m*/*z* 208.9, 223.0, 225.0, and 257.0 were analyzed by tandem mass spectrometry. The GC+32 at *m*/*z* 208.9 contains a sulfinic acid group ($-SO_2H$), while GC+46 at *m*/*z* 223.0, GC+48 at *m*/*z* 225.0, and GC+80 at *m*/*z* 257.0 all contain a sulfonic acid group ($-SO_3H$). This indicates the rupture of the disulfide bond and oxidation of Cys to sulfinic and sulfonic acids. The peak at *m*/*z* 257.0 with mass GC+80 is likely the GC-S$-SO_3H$. The cleavage of the disulfide bond and generation of sulfonic acid as the primary product is also demonstrated by the peptide RSSCFGGRIDRIGAC-NH_2, with an internal disulfide, as shown in Figure 10B. The ions at *m*/*z* 1692.6 and 846.9 correspond to the single and double charged oxidation products, with a +98 Da mass shift from the unmodified peptide, resulting from the breakage of the internal disulfide bond and oxidation of both Cys to cysteine sulfonic acid.

The summarized mechanisms of disulfide bond oxidation based on the literature are displayed in Scheme 14.[294] Hydroxyl radical OH•, hydrated electron e_{aq}^-, and hydrogen radical H• are all able to react rapidly with disulfide and generate RS• radicals under anaerobic conditions.[285] Even though Cys and disulfide are the only amino acid residues

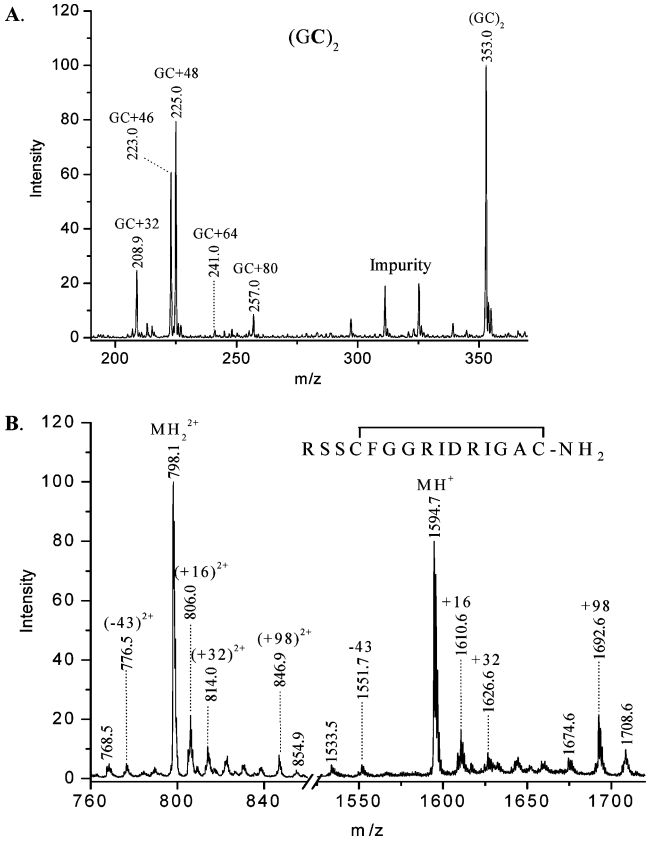

Figure 10. Oxidation of the disulfide bond. (A) Negative-ESI-MS spectrum of peptide $(GC)_2$ (dimer of GC connected by disulfide) exposed to ^{137}Cs-source γ-rays for 8 min. (B) Positive-ESI-MS spectrum of peptide RSSCFGGRIDRIGAC-NH_2 (internal disulfide) exposed to synchrotron X-rays for 20 ms.

Scheme 14. Oxidation of the Disulfide Bond

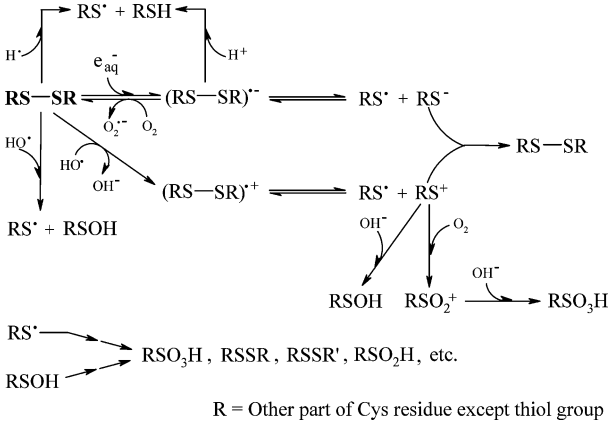

that can compete with O_2 for the solvated electrons according to their reaction rates (Table 1), under air-equilibrated solution conditions and micromolar sample concentrations, e_{aq}^- and H• react primarily with oxygen (which is present at 0.3 mM concentration[285]) to give superoxide or hydroperoxy radicals. Solvated electrons (e_{aq}^-) attack disulfide RSSR by electron attachment (rate constant $\sim 10^{10}$ M^{-1} s^{-1})[303] to give disulfide radical anions $(RSSR)^{\bullet-}$ under anaerobic conditions.[280,293] $(RSSR)^{\bullet-}$ can be identified readily by optical or EPR spectroscopy.[304] It reacts rapidly with protons (rate constant $\sim 10^{10}$ M^{-1} s^{-1}) to give rise to a transient protonated disulfide radical (RSS(H)R)•, which decomposes rapidly into free thiyl radical RS• and thiol components.[305] Hydrogen radical H• may also react with RSSR to produce RS• and

RSH.[276,285] The newly born thiol subsequently reacts with sulfenic acid to produce a new disulfide. $(RSSR)^{\bullet-}$ may also cleave its S−S bond to yield a thiyl radical $RS^{\bullet}$ and a thiolate anion RS^{-} through a reversible reaction.[291] In aerated solutions, these reactions may still occur to some extent, since the reaction rates for reaction of e_{aq}^{-} with thiol and O_2 are similar in magnitude; meanwhile, the $(RSSR)^{\bullet-}$ may react with an O_2 to regenerate RSSR and give rise a superoxide radical $O_2^{\bullet-}$.

Hydroxyl radical $HO^{\bullet}$ attacks disulfide through two likely pathways. $HO^{\bullet}$ may react with RSSR directly and lead to a thiyl radical $RS^{\bullet}$ and sulfenic acid RSOH.[283] $HO^{\bullet}$ may abstract an electron from a disulfide bond, giving rise to a disulfide radical cation $(RSSR)^{\bullet+}$,[291] which is stabilized by electron delocalization. Heterolysis of $(RSSR)^{\bullet+}$ produces a thiyl radical $RS^{\bullet}$ and a sulfenium cation RS^{+};[281] RS^{+} may be neutralized by OH^{-} to form sulfenic acid or may absorb an O_2 to form an sulfonium cation RSO_2^{+}, which combines with an OH^{-} to become sulfonic acid RSO_3H.[282] The thiyl radical $RS^{\bullet}$ and sulfenic acid RSOH produced by the reaction of RSSR with a solvated electron e_{aq}^{-} or a hydroxyl radical $HO^{\bullet}$ are subject to further oxidation, as described in the radiolysis of cysteine, yielding sulfinic acid RSO_2H, sulfonic acid RSO_3H, disulfides, and other products.

Oxidation of Methionine. Met is one of the most reactive amino acid residues subjected to oxidation. Radiolysis of methionine gives rise primarily to methionine sulfoxide (+16 Da mass shift), which can be further oxidized to methionine sulfone (+32 Da mass shift) or another product with a −32 Da mass shift, likely due to aldehyde formation at the γ-carbon. Shown in Figure 11A is the positive ESI-MS spectrum of a simple peptide GMG exposed to γ-rays for 8 min. The primary product is observed at *m*/*z* 280.0 with a +16 Da mass shift from the original peptide at *m*/*z* 264.0, resulting from the oxidation of Met to methionine sulfoxide. Other minor products are present at *m*/*z* 296.0, 250.0, 248.0, 234.0, and 232.0. The +32 Da product corresponds to oxidation of Met to methionine sulfone, while the peaks at *m*/*z* 234.0 (−30 Da) and 250.0 (−30 + 16 Da) are due to the C-terminal decarboxylation from the original peptide and sulfoxide products,[211] respectively. The peak at *m*/*z* 232.0 with a −32 Da mass shift is possibly due to the loss of thioether and formation of an aldehyde group at the Met side chain.[294] The oxidation of Met and the formation of sulfoxide as a primary product and the minor product with a −32 Da shift were also seen in other Met-containing peptides, such as HDMNKVLDL, as shown in Figure 11B.

Radiolytic oxidation of methionine has also been the subject of a long investigation, and a number of intermediate radical species have been identified;[263−269] however, the explicit mechanism is still unclear. A compilation of the conclusions from the literature is presented in Scheme 15. Methionine sulfoxide is the principal oxidation product in most cases and can be further oxidized to methionine sulfone and the −32 Da product under harsh oxidation conditions. The −32 Da product can be generated from radiolysis of methionine as well as methionine sulfoxide-containing peptides,[294] but only in those peptides containing no highly reactive amino acid residues. When another highly reactive amino acid residue such as Trp, Tyr, and Phe is present in the peptide, the −32 Da modification at Met is not observed.[294] Therefore, the −32 Da modification at Met was found in irradiated peptides such as HDMNKVLDL and GSNKGAIIGLM(O) but not in peptides such as LWMRFA-

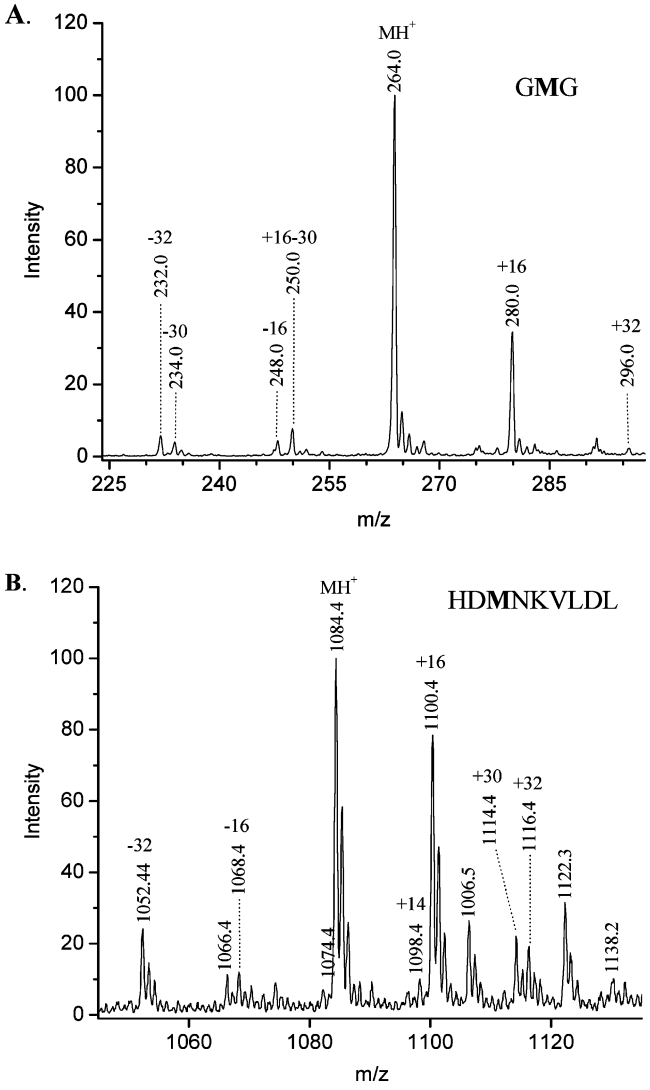

Figure 11. Oxidation of Met. Positive-ESI-MS spectra of (A) GMG exposed to ^{137}Cs-source γ-rays for 8 min and (B) Antiflammin-2 HDMNKVLDL exposed to synchrotron X-rays for 15 ms.

NH_2 and YGGFM(O)R. Radiolytic oxidation of methionine may involve the addition of $HO^{\bullet}$ radical to the sulfur atom and hydrogen abstraction.[264] At low pH (<3.0), methionine behaves like an ordinary aliphatic thioether.[264] At pH > 3.0, the $HO^{\bullet}$-adduct sulfur-centered radical may eliminate a hydroxide anion HO^{-} to give rise to a sulfur-centered radical cation $>S^{\bullet+}$.[263−265,267,306] The process is catalyzed by an electron-rich heteroatom such as O, N, or S on neighboring side chains (Asp, Asn, Glu, Gln, Ser, Thr, Met, etc.) or by adjacent peptide bonds that stabilize the sulfur-centered radical cation via formation of an intramolecular three-electron (S∴N, S∴O, S∴S, etc.) bonded cyclic transient.[263−265,267,306] The S∴N three-electron bonded radicals may convert intramolecularly into the α-carbon-centered radical on the peptide backbone.[269] An intermolecular sulfur−sulfur dimeric radical cation $>(S\therefore S)^{\bullet+}<$ has also been proposed as the reaction intermediate.[301] The sulfur-centered radical cation may also deprotonate from the methyl, $-CH_3$, or methylene, $-CH_2-$, next to the sulfur atom and transform into α-(alkylthio)alkyl radicals in the Met side chain.[265] Methionine can also be oxidized by other oxygen-reactive species such as H_2O_2 via a two-electron mechanism but at much lower rate.[268]

Scheme 15. Oxidation of Methionine

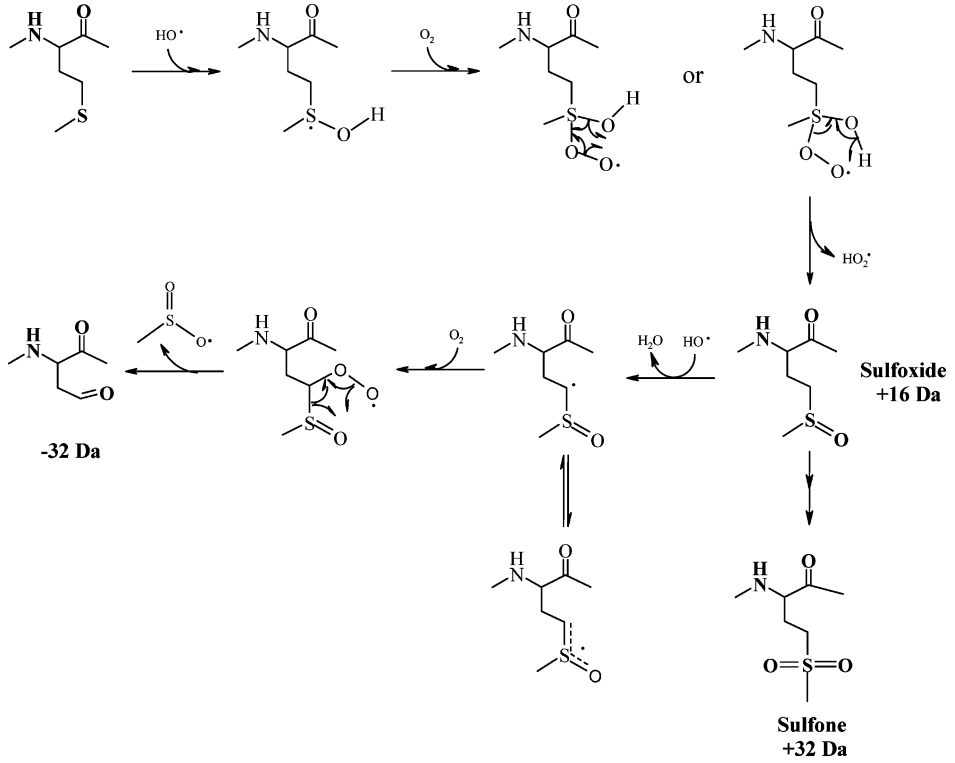

In proteins, the situation is likely different from that of simple peptides. Intermolecular methionine−methionine interactions are generally unlikely, and the protein structure will also restrict conformation fluctuations and formation of the intermediates mentioned above. According to our previous radiolysis studies, the oxygen atom in the methionine sulfoxide originates from both hydroxyl radical and dissolved O_2[25]. Recent studies show consistency with the mechanisms outlined in Scheme 15.[294] The addition of hydroxyl radicals to Met at the sulfur atom initially generates a hydroxysulfuranyl radical,[264] which likely abstracts an O_2 molecule[268] and subsequently loses a hydroperoxyl radical $HO_2^•$, to give rise to methionine sulfoxide (+16 Da mass shift). This radical can rearrange through two different mechanisms, one of which results in the incorporation of oxygen from dissolved O_2 while the other results in incorporation of oxygen from water molecules through the HO• produced by radiolysis. The methionine sulfoxide can be further oxidized to methionine sulfone (+32 Da mass shift) under harsh conditions, possibly by a similar pathway but at a much lower rate. The novel −32 Da product is likely an aldehyde product resulting from the further oxidization of methionine sulfoxide through hydrogen abstraction by HO• radical from the $-CH_2-$ next to the sulfur atom to form a carbon-centered radical, which can be stabilized by electron delocalization to the sulfoxide group. The carbon-centered radical can react with an O_2 molecule to form an aldehyde group with release of a $CH_3S(O)O^•$ radical.

3.3.6. Oxidation of Neutral Aliphatic Side Chains Containing Heteroatoms

The stable products formed from the radiolytic oxidation of Asn, Gln, Ser, and Thr have received little attention. The presence of a heteroatom at the side chain influences the selectivity of radical attack. In radiolysis of Ser and Thr, the products were not well characterized; radiolysis studies observed two products with +16 and −2 Da mass shifts in ESI-MS.[248] It is expected that the hydroxyl group favors hydrogen abstraction by hydrophilic HO• radical from the C−H bond(s) next to it due to stabilization of the incipient radical by electron delocalization.[307] The incipient carbon-centered radical may react with O_2 under aerobic conditions to form a α-hydroxyperoxyl radical, which may readily eliminate a HOO• and convert the orginal hydroxyl to a carbonal group (mass shift −2 Da), or the products may be too unstable and readily undergo further reactions such as loss of H_2O, thus making the product difficult to identify.

The radiolytic oxidation of Gln and Asn side chains has also received minimal attention, possibly due to their low reactivity toward hydroxyl radicals.[248] In the γ-ray irradiated Gln-NH_2,[248] distinct signals with a +16 Da mass shift along with a relatively weaker yet comparable signal with a +14 Da mass shift were found. Gln can be attacked by HO• radical at both side chain methylenes.[307] Asn is expected to be even less reactive than Gln. The oxidation of Gln and Asn has also been reported to cause deamidation.

3.3.7. Secondary Oxidations of Sulfur-Containing Side Chains

Highly reactive amino acid residues are susceptible to further oxidation after radiolytic exposure by those oxidative species generated during the radiolysis of protein solutions. In addition to reactive species with a short half-life, such as hydroxyl radicals (HO•), solvated electrons (e_{aq}^-), and hydrogen radicals (H•),[308] radiolysis of aqueous solutions also gives rise to relatively stable and mild oxidative species, including hydrogen peroxide (H_2O_2) along with peroxides and superoxides, on proteins due to the free radical oxidation of amino acid residues in the presence of oxygen.[309] These mild oxidative species are able to attack highly reactive amino acid side chains, particularly Cys and Met (Scheme 16).[295,310−313] Even though the reactions are relatively slow,

Scheme 16. Oxidation of Sulfur-Containing Residues by Hydrogen Peroxide

Cys oxidation by H_2O_2

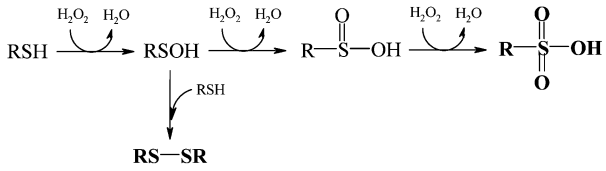

Met oxidation by H_2O_2

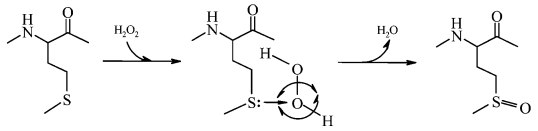

the time period of a few hours to several days between irradiation and sample analysis in typical footprinting experiments would allow these secondary reactions to accumulate and significantly degraded the data precision and accuracy of Met and Cys but not aromatic or other reactive residues.[313] Secondary oxidation of Met with formation of sulfoxide degrades data reproducibility and inflates the perceived solvent accessibility of Met-containing peptides. It can be suppressed by adding trace amounts of catalase or, preferably, a few millimolar Met-NH_2 (or Met-OH) buffer immediately after irradiation; this leads to greatly improved adherence to first-order kinetics and more precise observed oxidation rates. The strategy is shown to suppress secondary oxidation in model peptides and improve data quality in examining the reactivity of peptides within the Arp2/3 protein complex.[313] Cysteine is also subject to secondary oxidation, generating disulfide as the principal product. The disulfides can be reduced before mass spectrometric analysis by reducing agents such as TCEP, while methionine sulfoxide is refractory to reduction by this reagent under typical reducing conditions. The suppression of secondary oxidation significantly improves the precision and accuracy of oxidation data for these sulfur-containing peptides and thus makes this protein footprinting technique more robust.

3.4. Relative Reactivity of Amino Acid Side Chains

Analysis of Side Chain Reactivity. The extent of radiolytic modification of amino acid side chain residues in proteins in aqueous media is determined by two factors: the inherent reactivity relative to its neighbor residues and its steric accessibility. In order to compare the reactivities of different side chains, we need to eliminate the steric effects. Radiolytic oxidation of amino acids has been extensively studied using pulse radiolysis combined with UV/vis and EPR (electron paramagnetic resonance) spectroscopic detection of free radical intermediates.[201] The bimolecular rate constants of reaction of the 20 common amino acids and cysteine with hydroxyl radical and hydrated electron at neutral pH have been examined[198,201] and are listed in Table 1. The range of reactivity is enormous, with free Cys over 1000 times more likely to suffer hydroxyl radical attack as compared to Gly. The table tells us the general susceptibility of an amino acid side chain toward oxidation by hydroxyl radical and hydrated electrons; the amino acids that are most reactive in Table 1 consist of the most familiar footprinting probes. Under typical aerobic conditions, most solvated electrons react with O_2 and thus do not contribute to protein oxidation to any significant degree, since most amino acid residues except Cys react with solvated electrons at a much lower rate compared to O_2.

The potential of an amino acid residue to serve as a footprinting probe under typical aerobic conditions is determined not only by its reactivity but also by the ability to detect stable oxidation products by mass spectroscopy. In addition, footprinting experiments are normally carried out in the micromolar concentration range, unlike those traditional studies that were generally performed at millimolar concentrations of analyte. Fortunately, a detailed comparison of all 20 amino acids and their products has been carried out using radiolysis oxidation and mass spectrometric analysis.[248] The primary oxidation products for amino acid side chains are listed in Table 2.

Table 2. Primary Products and Corresponding Mass Changes for Various Amino Acid Side Chains Subjected to Radiolytic Modification and Detectible by Mass Spectrometry

side chain	side chain modification and mass changes
Cys	sulfonic acid (+48), sulfinic acid (+32), hydroxy (−16)
cystine	sulfonic acid, sulfinic acid
Met	sulfoxide (+16), sulfone (+32), aldehyde (−32)
Trp	hydroxy- (+16, +32, +48, etc.), pyrrol ring-open (+32, etc.)
Tyr	hydroxy- (+16, +32, etc.)
Phe	hydroxy- (+16, +32, etc.)
His	oxo- (+16), ring-open (−22, −10, +5)
Leu[a]	hydroxy- (+16), carbonyl (+14)
Ile[a]	hydroxy- (+16), carbonyl (+14)
Val[a]	hydroxy- (+16), carbonyl (+14)
Pro	hydroxy- (+16), carbonyl (+14)
Arg	deguanidination (−43), hydroxy- (+16), carbonyl (+14)
Lys	hydroxy- (+16), carbonyl (+14)
Glu	decarboxylation (−30), hydroxy- (+16), carbonyl (+14)
Gln	hydroxy- (+16), carbonyl (+14)
Asp	decarboxylation (−30), hydroxy- (+16)
Asn	hydroxy- (+16)
Scr[b]	hydroxy- (+16), carbonyl (−2- or +16-H_2O)
Thr[b]	hydroxy- (+16), carbonyl (−2- or +16-H_2O)
Ala	hydroxy- (+16)

[a] For aliphatic side chains, +14 Da products are normally much less than +16 Da products. [b] For Ser and Thr, only trivial amounts of +16 Da and -2 Da products were found.

To analyze comparative reactivity in the context of mass spectrometry based detection, amino amides of each residue were compared for reactivity and reaction products to ensure the full accessibility of side chains and to avoid complications from the decarboxylation of the carboxyl group.[211] Meanwhile, to avoid the different background quenching due to potential impurities in the chemicals supplied by vendors, an internal standard, Phe-NH_2 or Pro-NH_2, was individually mixed with each experimental amide and a dose response study was carried out for each mixture to obtain the rate constant for the specific amino amide, which could be directly compared to the rate of the internal standard, thus ensuring comparable experimental conditions. Meanwhile, to account for the different ionization efficiencies of different amino amides and their products, another compound was added at an identical amount to each irradiated mixed amide right before mass spectrometric analysis to serve as an external standard for ionization efficiency. The fraction of unmodified compound was calculated using two different

approaches. The first one was referred to as the "self-based" method, in which the fraction of unmodified compound was expressed as the ratio of the signal intensity of the unmodified compound to the sum of the signals of the unmodified compound and the modified products. The second method is referred to as "external-based", in which the relative amount of unmodified compound at a time point of exposure was calculated based on the ratio of the signal intensity of the unmodified compound compared to the intensity of the externally added standard and then the fraction of unmodified compound was calculated based on the ratio of the relative amount of unmodified compound at the specific time point of exposure to that of the unexposed control (zero time exposure of the dose response). The rate constant of radiolytic modification is obtained by nonlinear fitting of the fraction of unmodified compound (calculated by either of the two methods) as a function of exposure time to a first-order kinetics equation as previously described.[31,226] The "external-based" method was used to reduce the errors for those compounds with weak product signals due to generation of multiple products such as (His-NH_2) or low ionization efficiencies (such as the deguanidation product of Arg-NH_2) or compounds with low inherent reactivity. The relative reactivity of an amino amide was presented as the ratio of its rate constant to that of the internal standard, and the reactivity of all amino amides was compared based on the ratios.

Reactivities of Side Chains Compared to a Phenylalanine Standard. The relative reactivities (k_X/k_F) of different amino acid side chains as revealed in Figure 12A are consistent with the rate constants of reaction with hydroxyl radical measured by pulse radiolysis and photospectroscopy as shown in Table 1. Met and Tyr were not evaluated compared to Phe because the 16 Da mass difference between them and Phe makes it difficult to separate Met+16 oxidation products from Phe and Phe+16 oxidation products from Tyr by mass spectrometry. Trp is the most reactive non-sulfur-containing residue and is about 1.6-fold as reactive as Phe in our examination while Table 1 shows it to be 1.9-fold more reactive to initial attack. Our previous studies have shown that disulfide-bonded Cys (cystine) is more resistant to oxidation than free Cys,[294] and the reactivity of cystine is about 85% of that of Phe. The reactivity of His is 69% of that of Phe. The reactivity of aliphatic hydrocarbon side chains normally increases with the number of C−H bonds as well as the side chain length, as revealed by the relative reactivity of 39% for Leu, 38% for Ile, 18% for Val, and 12% for Pro. The reactivities for Arg, Lys, Thr, Gln, and Glu are 26%, 23%, 14%, 6%, and 5% relative to that of Phe, respectively. The data suggest a reactivity order of Trp > Phe > cysteine > His > Leu, Ile > Arg, Lys, Val > Thr, Pro > Glu, Gln.

Reactivity of Side Chains Compared to a Proline Standard. The reactivities of amino acid residues were also investigated using Pro-NH_2 as an internal standard which is less reactive than Phe. The rate constants of 15 amino amides compared with Pro-NH_2 and the ratio of rate constants (k_X/k_p) are shown in Figure 12B. Leu-NH_2 and Ile-NH_2 were not studied with Pro as internal standard, because their molecular weight is 16 Da higher than that of Pro-NH_2 and they cannot be distinguished from the +16 Da oxidation product of Pro-NH_2. The relative reactivity order is the same as that obtained using Phe as an internal standard. Trp is the most reactive side chain except for the sulfur-containing residues. The reactivities of Trp, Tyr, Phe, cystine, and His

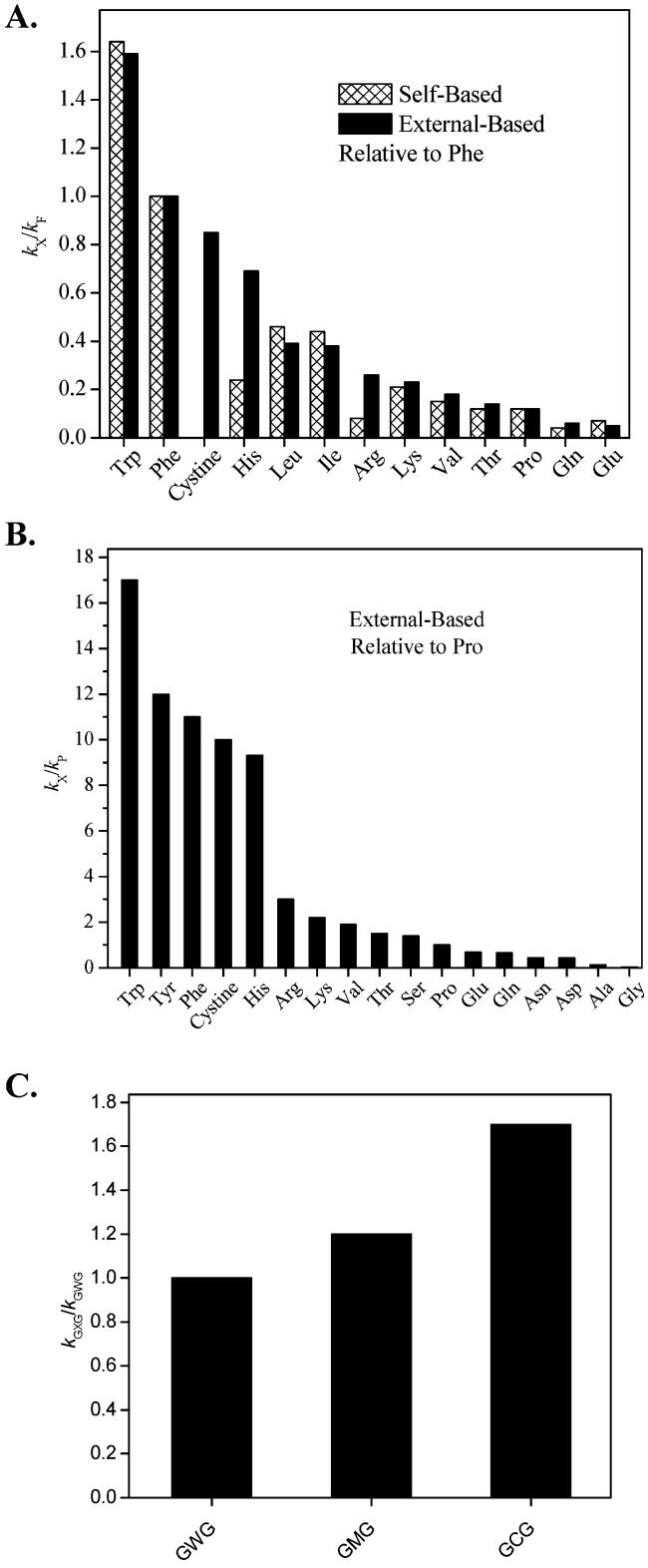

Figure 12. Amino acid side chain reactive relative to (A) Phe, (B) Pro, and (C) Trp.

are about 17-, 12-, 11-, 10-, and 9.3-fold that of Pro. The reactivities of Arg, Lys, and Val are about 3.0-, 2.2-, and 1.9-fold of that of Pro. The hydroxyl-containing side chains, Ser and Thr, also seem to be slightly more susceptible to radiolytic modification than Pro. The reactivity generally decreases for short aliphatic side chains. The reactivities of Gln, Glu, Asn, Asp, and Ala are about 69%, 66%, 44%, 43%, and 14% of that of Pro.

Reactivity of Sulfur-Containing Side Chains. Met and Cys are the two most reactive amino acid residues[294] and are susceptible to significant secondary oxidation reactions from mild oxidizing reagents such as hydrogen peroxide generated during radiolysis.[313] The tripeptides GCG, GMG, and GWG were analyzed to minimize steric effects on the reactivity measurement. The three peptides along with GAG were mixed together and exposed to γ-rays. Because the reactivities of Cys, Met, and Trp are much higher than that of Ala and no oxidation of GAG was found in the irradiated peptide mixture, GAG was used as the internal signal standard for the peptide mixture. The peptide mixture was analyzed right after exposure to minimize secondary reactions. The ratios of the mass spectral signal intensities of the three unmodified peptides to that of GAG were used to represent the relative amounts of GCG, GMG, and GWG, while the fraction of unmodified peptide was calculated as the ratio of the relative amount of irradiated peptide to that of control. The ratios of rate constants compared to that of GWG are shown in Figure 12C. In situations with a minimum of secondary oxidation, the rate constants of GCG and GMG are 1.7- and 1.2-fold of that of GWG, indicating Cys is the most reactive amino acid residue followed by Met, which is 20% more reactive than Trp, the most reactive non-sulfur-containing amino acid residue.

4. Future Prospects

An understanding of the chemistry of hydroxyl radicals has significantly advanced their use in structural mass spectrometry studies. As of now, many groups in the Americas, Asia, and Australia are using hydroxyl radical mediated structural mass spectrometry approaches as a main part of their research programs. As these methods are complementary to deuterium exchange and cross-linking, the American Society for Mass Spectrometry has formed an HD exchange and covalent labeling interest group to promote the approaches and share information on these techniques.

Future advances in the methods will require continued studies to understand the chemistry of oxidation as well as new chromatographic and mass spectrometry methods to detect rare oxidation products that are characteristic of the oxidation mechanisms of particular residues yet may be low abundance ions in the complex oxidation mixture. The aliphatic neutral side chains, such as Gln, Ser, and Thr, are perfect examples, as they appear to be somewhat reactive, but their products have been difficult to detect. Also, the footprinting studies to date have emphasized aerobic conditions that maximize side chain oxidation; anaerobic studies may provide possibilities for enhanced cross-linking, which may provide useful information, especially for protein complexes. In addition, methods based on backbone cleavage are not well developed and can provide unique information on structure if the products can be adequately detected. Overall, the methods have advanced considerably and have seen widespread acceptance in the last 5 years; continued growth over the next 5 years is likely.

5. References

(1) Takamoto, K.; Chance, M. R. *Annu. Rev. Biophys. Biomol. Struct.* **2006**, *35*, 251.
(2) Guan, J. Q.; Chance, M. R. *Trends Biochem. Sci.* **2005**, *30*, 583.
(3) Guan, J. Q.; Almo, S. C.; Chance, M. R. *Acc. Chem. Res.* **2004**, *37*, 221.
(4) Guan, J. Q.; Chance, M. R. In *Encyclopedia of Molecular Cell Biology and Molecular Medicine*, 2nd ed.; Meyers, R. A., Ed.; Wiley-VCH: Weinheim, Germany, 2004.
(5) Takamoto, K.; Chance, M. In *Encyclopedia of Molecular Cell Biology and Molecular Medicine*, 2nd ed.; Myers, R. A., Ed.; Wiley VCH: Weinheim, Germany, 2004.
(6) Brenowitz, M.; Chance, M. R.; Dhavan, G.; Takamoto, K. *Curr. Opin. Struct. Biol.* **2002**, *12*, 648.
(7) Gilbert, W. In *CIBA Foundation Symp. 7: Polymerization in Biological Systems*; Elsevier Publishing Co.: Amsterdam, 1972.
(8) Mirzabekov, A. D.; Kolchinsky, A. M. *Mol. Biol. Rep.* **1974**, *1*, 385.
(9) Mirzabekov, A. D.; Melnikova, A. F. *Mol. Biol. Rep.* **1974**, *1*, 379.
(10) Humayun, Z.; Kleid, D.; Ptashne, M. *Nucleic Acids Res.* **1977**, *4*, 1595.
(11) Galas, D. J.; Schmitz, A. *Nucleic Acids Res.* **1978**, *5*, 3157.
(12) Schmitz, A.; Galas, D. J. *Nucleic Acids Res.* **1979**, *6*, 111.
(13) Jay, D. G. *J. Biol. Chem.* **1984**, *259*, 15572.
(14) Sheshberadaran, H.; Payne, L. G. *Proc. Natl. Acad. Sci. U.S.A.* **1988**, *85*, 1.
(15) Zhong, M.; Lin, L.; Kallenbach, N. R. *Proc. Natl. Acad. Sci. U.S.A.* **1995**, *92*, 2111.
(16) Heyduk, E.; Heyduk, T. *Biochemistry* **1994**, *33*, 9643.
(17) Hanai, R.; Wang, J. C. *Proc. Natl. Acad. Sci. U.S.A.* **1994**, *91*, 11904.
(18) Hachimori, Y.; Horinishi, H.; Kurihara, K.; Shibata, K. *Biochim. Biophys. Acta* **1964**, *93*, 346.
(19) Horinishi, H.; Hachimori, Y.; Kurihara, K.; Shibata, K. *Biochim. Biophys. Acta* **1964**, *86*, 477.
(20) Datwyler, S. A.; Meares, C. F. *Met. Ions Biol. Syst.* **2001**, *38*, 213.
(21) Datwyler, S. A.; Meares, C. F. *Trends Biochem. Sci.* **2000**, *25*, 408.
(22) Guan, J. Q.; Almo, S. C.; Reisler, E.; Chance, M. R. *Biochemistry* **2003**, *42*, 11992.
(23) Schuessler, H.; Schilling, K. *Int. J. Radiat. Biol. Relat. Stud. Phys., Chem. Med.* **1984**, *45*, 267.
(24) Maleknia, S. D.; Ralston, C. Y.; Brenowitz, M. D.; Downard, K. M.; Chance, M. R. *Anal. Biochem.* **2001**, *289*, 103.
(25) Maleknia, S. D.; Brenowitz, M.; Chance, M. R. *Anal. Chem.* **1999**, *71*, 3965.
(26) Guan, J. Q.; Vorobiev, S.; Almo, S. C.; Chance, M. R. *Biochemistry* **2002**, *41*, 5765.
(27) Goldsmith, S. C.; Guan, J. Q.; Almo, S.; Chance, M. *J. Biomol. Struct. Dyn.* **2001**, *19*, 405.
(28) Tullius, T. D.; Dombroski, B. A.; Churchill, M. E.; Kam, L. *Methods Enzymol.* **1987**, *155*, 537.
(29) Katta, V.; Chait, B. T. *J. Am. Chem. Soc.* **1993**, *115*, 6317.
(30) Zhang, Z.; Smith, D. L. *Protein Sci.* **1993**, *2*, 522.
(31) Kiselar, J. G.; Maleknia, S. D.; Sullivan, M.; Downard, K. M.; Chance, M. R. *Int. J. Radiat. Biol.* **2002**, *78*, 101.
(32) Brenowitz, M.; Chance, M. R.; Dhavan, G.; Takamoto, K. *Curr. Opin. Struct. Biol.* **2002**, *12*, 648.
(33) Asmus, K.-D. *Methods Enzymol.* **1984**, *105*, 167.
(34) von Sonntag, C.; Schuchmann, H. P. *Methods Enzymol.* **1994**, *233*, 3.
(35) Simic, M. G. *Methods Enzymol.* **1990**, *186*, 89.
(36) Wardman, P. *Rep. Prog. Phys.* **1978**, *41*, 259.
(37) Klassen, N. V. In *Radiation Chemistry Principles & Applications*; Rodgers, F. a. M. A., Ed.; VCH: Texas, 1987.
(38) Winick, H. In *Synchrotron Radiation Sources*; Winck, A. P. a. H., Ed.; World Scientific: Singapore, 1994.
(39) Bielski, B. H. J.; Cabelli, D. E.; Arudi, R. L.; Ross, A. B. *J. Phys. Chem. Ref. Data* **1985**, *14*, 1041.
(40) Bielski, B. H. J. *Photochem. Photobiol.* **1978**, *28*, 645.
(41) Rogers, F. a. M. A. *Radiation Chemistry Principles & Applications*; VCH: Texas, 1987.
(42) Gupta, S.; Sullivan, M.; Toomey, J.; Kiselar, J.; Chance, M. R. *J. Synchrotron Radiat.* **2007**, *14*, 233.
(43) Sclavi, B.; Woodson, S.; Sullivan, M.; Chance, M.; Brenowitz, M. *Methods Enzymol.* **1998**, *295*, 379.
(44) Ralston, C. Y.; Sclavi, B.; Sullivan, M.; Deras, M. L.; Woodson, S. A.; Chance, M. R.; Brenowitz, M. *Methods Enzymol.* **2000**, *317*, 353.
(45) Volman, D. H.; Chen, J. C. *J. Am. Chem. Soc.* **1959**, *81*, 4141.
(46) Weeks, J. L.; Matheson, M. S. *J. Am. Chem. Soc.* **1956**, *78*, 1273.
(47) Dainton, F. S. *J. Am. Chem. Soc.* **1956**, *78*, 1278.
(48) Elliot, A. J. AECL report 11073, COG-95-167; AECL Research, Chalk River Laboratories: Chalk River, ON, Canada, 1994.
(49) Macgregor, R. B., Jr. *Anal. Biochem.* **1992**, *204*, 324.
(50) Sharp, J. S.; Becker, J. M.; Hettich, R. L. *Anal. Chem.* **2004**, *76*, 672.
(51) Aye, T. T.; Low, T. Y.; Sze, S. K. *Anal. Chem.* **2005**, *77*, 5814.
(52) Hambly, D. M.; Gross, M. L. *J. Am. Soc. Mass. Spectrom.* **2005**, *16*, 2057.
(53) Fenton, H. J. H. *J. Chem. Soc. Proc.* **1894**, *10*, 157.
(54) Berlett, B. S.; Stadtman, E. R. *J. Biol. Chem.* **1997**, *272*, 20313.
(55) Schoneich, C. *Exp. Gerontol.* **1999**, *34*, 19.

(56) Halliwell, B.; Gutteridge, J. M. C. *Methods Enzymol.* **1990**, *186*, 1.
(57) Dean, R.; Simpson, J. A. *Mol. Aspects Med.* **1991**, *12*, 121.
(58) Davies, M. J.; Fu, S.; Wang, H.; Dean, R. T. *Free Radical Biol. Med.* **1999**, *27*, 1151.
(59) Barb, W. G.; Baxendale, J. H.; George, P.; Hargrave, K. R. *Trans. Faraday Soc.* **1951**, *47*, 462.
(60) Barb, W. G.; Baxendale, J. H.; George, P.; Hargrave, K. R. *Trans. Faraday Soc.* **1951**, *47*, 591.
(61) Goldstein, S.; Meyerstein, D.; Czapski, G. *Free Radical Biol. Med.* **1993**, *15*, 435.
(62) Koppenol, W. H. *Free Radical Biol. Med.* **1993**, *15*, 645.
(63) Papavassilios, A. G. *Biochem. J.* **1995**, *305*, 345.
(64) Wardman, P.; Candeias, L. P. *Radiat. Res.* **1996**, *145*, 523.
(65) Liochev, S. I. *Met. Ions Biol. Syst.* **1999**, *36*, 1.
(66) Pierre, J. L.; Fontecave, M. *BioMetals* **1999**, *12*, 195.
(67) Koppenol, W. H. *Redox Rep.* **2001**, *6*, 229.
(68) Liochev, S. I.; Fridovich, I. *Redox Rep.* **2002**, *7*, 55.
(69) Pierre, J. L.; Fontecave, M.; Crichton, R. R. *BioMetals* **2002**, *15*, 341.
(70) Burkitt, M. J. *Prog. React. Kinet. Mech.* **2003**, *28*, 75.
(71) Neyens, E.; Baeyens, J. *J. Hazard. Mater* **2003**, *98*, 33.
(72) Kryatov, S. V.; Rybak-Akimova, E. V.; Schindler, S. *Chem. Rev.* **2005**, *105*, 2175.
(73) Masarwa, A.; Rachmilovich-Calis, S.; Meyerstein, N.; Meyerstein, D. *Coord. Chem. Rev.* **2005**, *249*, 1937.
(74) Pignatello, J. J.; Oliveros, E.; MacKay, A. *Crit. Rev. Environ. Sci. Technol.* **2006**, *36*, 1.
(75) Haber, F.; Weiss, J. *Proc. R. Soc.* **1934**, *147*, 332.
(76) Perez-Benito, J. F. *J. Phys. Chem. A* **2004**, *108*, 4853.
(77) Wells, C. F.; Salam, M. A. *J. Chem. Soc. A* **1968**, 24.
(78) Tullius, T. D.; Dombroski, B. A. *Proc. Natl. Acad. Sci. U.S.A.* **1986**, *83*, 5469.
(79) Pogozelski, W. K.; McNeese, T. J.; Tullius, T. D. *J. Am. Chem. Soc.* **1995**, *117*, 6428.
(80) Balasubramanian, B.; Pogozelski, W. K.; Tullius, T. D. *Proc. Natl. Acad. Sci. U.S.A.* **1998**, *95*, 9738.
(81) Tullius, T. D.; Greenbaum, J. A. *Curr. Opin. Chem. Biol.* **2005**, *9*, 127.
(82) Hampel, K. J.; Burke, J. M. *Methods* **2001**, *23*, 233.
(83) Baron, C. P.; Refsgaard, H. H. F.; Skibsted, L. H.; Andersen, M. L. *Free Radical Res.* **2006**, *40*, 409.
(84) Sawyer, D. T. *Coord. Chem. Rev.* **1997**, *165*, 297.
(85) MacFaul, P. H.; Wayner, D. D. M.; Ingold, K. W. *Acc. Chem. Res.* **1996**, *29*, 409.
(86) Strlic, M.; Kolar, J.; Selih, V. S.; Kocar, D.; Pihlar, B. *Acta Chim. Slov.* **2003**, *50*, 619.
(87) Anipsitakis, G. P.; Dionysiou, D. D. *Environ. Sci. Technol.* **2004**, *38*, 3705.
(88) Simpson, J. A.; Cheeseman, K. H.; Smith, S. E.; Dean, R. T. *Biochem. J.* **1988**, *254*, 519.
(89) Urbanski, N. K.; Beresewicz, A. *Acta Biochim. Pol.* **2000**, *47*, 951.
(90) Bowen, W. S.; Hill, W. E.; Lodmell, J. S. *Methods* **2001**, *25*, 344.
(91) Eguchi, H.; Ikeda, Y.; Koyota, S.; Honke, K.; Suzuki, K.; Gutteridge, J.; Taniguchi, N. *J. Biochem.* **2002**, *131*, 477.
(92) Basak, S.; Nagaraja, V. *Nucleic Acids Res.* **2001**, *29*, e105.
(93) Chakravarty, A. R.; Reddy, P. A. N.; Santra, B. K.; Thomas, A. M. *Proc. Natl. Acad. Sci. U.S.A.* **2001**, *114*, 391.
(94) Kowalik-Jankowska, T.; Ruta, M.; Wisniewska, K.; Lankiewicz, L.; Dyba, M. *J. Inorg. Biochem.* **2004**, *98*, 940.
(95) Archibald, S. F.; Tyree, C. *Arch. Biochem. Biophys.* **1987**, *256*, 638.
(96) Ali, S. F.; Duhart, H. M.; Newport, G. D.; Lipe, G. W.; Slikker, W. *Neurodegeneration* **1995**, *4*, 329.
(97) Moorhouse, C. P.; Halliwell, B.; Grootveld, M.; Gutteridge, J. M. *Biochim. Biophys. Acta* **1985**, *843*, 261.
(98) Shi, X.; Dalal, N. S.; Kasprzak, K. S. *Chem. Res. Toxicol.* **1993**, *6*, 277.
(99) Petit, A.; Mwale, F.; Tkaczyk, C.; Antoniou, J.; Zukor, D. J.; Huk, O. L. *Biomaterials* **2005**, *26*, 4416.
(100) Bridgewater, J. D.; Lim, J.; Vachet, R. W. *Anal. Chem.* **2006**, *78*, 2432.
(101) Torreilles, J.; Guerin, M. *FEBS Lett.* **1990**, *272*, 58.
(102) Shi, X.; Kasprzak, K. S.; Dalal, N. S. *J. Inorg. Biochem.* **1993**, *50*, 211.
(103) Gill, G.; Richter-Rusli, A. A.; Ghosh, M.; Burrows, C. J.; Rokita, S. E. *Chem. Res. Toxicol.* **1997**, *10*, 302.
(104) Chen, C.; Wang, Y.; Huang, W.; Huang, Y. *Toxicol. Appl. Pharmacol.* **2003**, *189*, 153.
(105) Jeowska-Bojczuk, M.; Kaczmarek, P.; Bal, W.; Kasprczak, K. S. *J. Inorg. Biochem.* **2004**, *98*, 1770.
(106) Rana, T. M.; Meares, C. F. *J. Am. Chem. Soc.* **1990**, *112*, 2457.
(107) Rana, T. M.; Meares, C. F. *Proc. Natl. Acad. Sci. U.S.A.* **1991**, *88*, 10578.
(108) Qi, D. F.; Tann, C. M.; Haring, D.; Distefano, M. D. *Chem. Rev.* **2001**, *101*, 3081.
(109) Schmidt, B. D.; Meares, C. F. *Biochemistry* **2002**, *41*, 4186.
(110) Hall, K. B.; Fox, R. O. *Methods* **1999**, *18*, 78.
(111) Trakselis, M. A.; Alley, S. C.; Ishmael, F. T. *Bioconjugate Chem.* **2005**, *16*, 741.
(112) Heilek, G. M.; Noller, H. F. *Science* **1996**, *272*, 1659.
(113) Meares, C. F.; Datwyler, S. A.; Schmidt, B. D.; Owens, J.; Ishihama, A. *Methods Enzymol.* **2003**, *371*, 82.
(114) Lancaster, L.; Kiel, M. C.; Kaji, A.; Noller, H. F. *Cell* **2002**, *111*, 129.
(115) Mukherjee, S.; Sousa, R. *Biol. Proc.* **2003**, *5*, 78.
(116) Joseph, S.; Noller, H. F. *Methods Enzymol.* **2000**, *318*, 175.
(117) Traviglia, S. L.; Datwyler, S. A.; Meares, C. F. *Biochemistry* **1999**, *38*, 4259.
(118) Ermacora, M. R.; Delfino, J. M.; Cuenoud, B.; Schepartz, A.; Fox, R. O. *Proc. Natl. Acad. Sci. U.S.A.* **1992**, *89*, 6383.
(119) Erlanson, D. A.; Chytil, M.; Verdine, G. L. *Chem. Biol.* **1996**, *3*, 981.
(120) Gelasco, A. K.; Crouch, R. K.; Knapp, D. R. *Methods Enzymol.* **2002**, *343*, 162.
(121) Gelasco, A.; Crouch, R. K.; Knapp, D. R. *Biochemistry* **2000**, *39*, 4907.
(122) Bridgewater, J. D.; Lim, J.; Vachet, R. W. *J. Am. Soc. Mass Spectrom.* **2006**, *17*, 1552.
(123) Lim, J.; Vachet, R. W. *Anal. Chem.* **2004**, *76*, 3498.
(124) Lim, J.; Vachet, R. W. *Anal. Chem.* **2003**, *75*, 1164.
(125) Beckman, J. S.; Beckman, T. W.; Chen, J.; Marshall, P. A.; Freeman, B. A. *Proc. Natl. Acad. Sci. U.S.A.* **1990**, *87*, 1620.
(126) Pryor, W. A.; Cueto, R.; Jin, X. *Free Radical Biol. Med.* **1995**, *18*, 75.
(127) Mahoney, L. R. *J. Am. Chem. Soc.* **1970**, *92*, 5262.
(128) Merenyi, G.; Lind, J.; Goldstein, S.; Czapski, G. *Chem. Res. Toxicol.* **1998**, *11*, 712.
(129) Pryor, W. A.; Squadrito, G. L. *Am. J. Physiol. Lung Cell Mol. Physiol.* **1995**, *268*, L699.
(130) Forni, L. G.; Mora-Arellano, V. O.; Packer, J. E.; Willson, R. L. *J. Chem. Soc., Perkin Trans. 2* **1986**, *1*−*6*, 1.
(131) Saha, A.; Goldstein, S.; Cabelli, D.; Czapski, G. *Free Radical Biol. Med.* **1998**, *24*, 653.
(132) Hughes, M. N.; Nicklin, H. G. *J. Chem. Soc. A* **1968**, 450.
(133) Reed, J. W.; Ho, H. H.; Jolly, W. L. *J. Am. Chem. Soc.* **1974**, *96*, 1248.
(134) Beckman, J. S.; Chen, J.; Ischiropoulos, H.; Crow, J. P. *Methods Enzymol.* **1994**, *233*, 229.
(135) Crow, J. P.; Spruell, C.; Chen, J.; Gunn, C.; Ischiropoulos, H.; Tsai, M.; Smith, C. D.; Radi, R.; Koppenol, W. H.; Beckman, J. S. *Free Radical Biol. Med.* **1994**, *16*, 331.
(136) Blough, N. V.; Zsfiriou, O. C. *Inorg. Chem.* **1985**, *24*, 3502.
(137) Saran, M. M. C.; Bors, W. *Free Radical Res. Commun.* **1990**, *10*, 221.
(138) Barat, F.; Hickei, B.; Sutton, J. *Chem. Commun.* **1969**, 125.
(139) Edwards, J. O.; Plumb, R. C. *Prog. Inorg. Chem.* **1994**, *41*, 599.
(140) Nappi, A. J.; Vass, E. *Biochim. Biophys. Acta* **1998**, *1380*, 55.
(141) Logager, T.; Sehested, K. *J. Phys. Chem.* **1993**, *97*, 6664.
(142) Uppu, R. M.; Squadrito, G. L.; Cueto, R.; Pryor, W. A. *Methods Enzymol.* **1996**, *269*, 311.
(143) Hughes, M. N.; Nicklin, H. G. *J. Chem. Soc. A* **1971**, 164.
(144) Leis, J. R.; Pena, M. E.; Rios, A. *J. Chem. Soc., Chem. Commun.* **1993**, 1293.
(145) Uppu, R. M.; Pryor, W. A. *Methods Enzymol.* **1996**, *269*, 322.
(146) Bohle, D. S.; Hansert, B.; Paulson, S. C.; Smith, B. D. *J. Am. Chem. Soc.* **1994**, *116*, 7423.
(147) Koppenol, W. H.; Kissner, R.; Beckman, J. S. *Methods Enzymol.* **1996**, *268*, 296.
(148) King, P. A.; Jamison, E.; Strahs, D.; Anderson, V. E.; Brenowitz, M. *Nucleic Acids Res.* **1993**, *21*, 2473.
(149) Gotte, M.; Marquet, R.; Isel, C.; Anderson, V. E.; Keith, G.; Gross, H. J.; Ehresmann, C.; Ehresmann, B.; Heumann, H. *FEBS Lett.* **1996**, *390*, 226.
(150) van der Vliet, A.; O'Neill, C. A.; Halliwell, B.; Cross, C. E.; Kaur, H. *FEBS Lett.* **1994**, *339*, 89.
(151) Alvarez, B.; Ferrer-Sueta, G.; Freeman, B. A.; Radi, R. *J. Biol. Chem.* **1999**, *274*, 842.
(152) Koppenol, W. H. *Quim. Nova* **1998**, *21*, 326.
(153) Lobachev, V. L.; Rudakov, E. S. *Russ. Chem. Rev.* **2006**, *75*, 375.
(154) Goldstein, S.; Lind, J.; Merenyi, G. *Chem. Rev.* **2005**, *105*, 2457.
(155) Maleknia, S. D.; Chance, M. R.; Downard, K. M. *Rapid Commun. Mass Spectrom.* **1999**, *13*, 2352.
(156) Maleknia, S. D.; Downard, K. *Mass Spectrom. Rev.* **2001**, *20*, 388.
(157) Wong, J. W.; Maleknia, S. D.; Downard, K. M. *Anal. Chem.* **2003**, *75*, 1557.

(158) Maleknia, S. D.; Wong, J. W.; Downard, K. M. *Photochem. Photobiol. Sci.* **2004**, *3*, 741.
(159) Wong, J. W.; Maleknia, S. D.; Downard, K. M. *J. Am. Soc. Mass Spectrom.* **2005**, *16*, 225.
(160) Morand, K.; Talbo, G.; Mann, M. *Rapid Commun. Mass Spectrom.* **1993**, *7*, 738.
(161) Thomas, M. C.; Mitchell, T. W.; Blanksby, S. J. *J. Am. Chem. Soc.* **2006**, *128*, 58.
(162) Wang, W.; Wang, S.; Liu, F.; Zheng, W. *Spectrochim. Acta, Part A* **2006**, *63*, 477.
(163) Locke, B. R.; Sato, M.; Sunka, P.; Hoffmann, M. R.; Chang, J. S. *Ind. Eng. Chem. Res.* **2006**, *45*, 882.
(164) Kirkpatrick, M. J.; Locke, B. R. *Ind. Eng. Chem. Res.* **2005**, *44*, 4243.
(165) Chen, J.; Davidson, J. H. *Plasma Chem. Plasma Process.* **2003**, *23*, 505.
(166) Joshi, A. A.; Locke, B. R.; Arce, P.; Finney, W. C. *J. Hazard. Mater.* **1995**, *41*, 3.
(167) Sun, B.; Sato, M.; Clements, J. S. *J. Electrostat.* **1997**, *39*, 189.
(168) Sunka, P.; Babicky, V.; Clupek, M.; Lukes, P.; Simek, M.; Schmidt, J.; Cernak, M. *Plasma Sources Sci. Technol.* **1999**, *8*, 258.
(169) Hoeben, W. F. L. M.; van Veldhuizen, E. M.; Rutgers, W. R.; Kroesen, G. M. W. *J. Phys. D: Appl. Phys.* **1999**, *32*, L133.
(170) Zhiyi, Z.; Nenghui, W.; Qian, W.; Meifan, L. *Free Radical Biol. Med.* **1993**, *14*, 1.
(171) Zang, L. Y.; Misra, B. R.; Misra, H. P. *Photochem. Photobiol.* **1992**, *56*, 453.
(172) Martin, J. P., Jr.; Burch, P. *Methods Enzymol.* **1990**, *186*, 635.
(173) Ito, A.; Ito, T. *Tanpakushitsu Kakusan Koso* **1988**, *33*, 2795.
(174) Kirkiacharian, B.; Santus, R.; Helene, C. *Ann. Pharm. Fr.* **1969**, *27*, 129.
(175) Azizova, O. A.; Kaiushin, L. P.; Pulatova, M. K. *Biofizika* **1966**, *11*, 970.
(176) Chaulk, S. G.; Pezacki, J. P.; MacMillan, A. M. *Biochemistry* **2000**, *39*, 10448.
(177) Kelly, J. J.; Chernov, B. K.; Tovstanovsky, I.; Mirzabekov, A. D.; Bavykin, S. G. *Anal. Biochem.* **2002**, *311*, 103.
(178) Henn, A.; Halfon, J.; Kela, I.; Orion, I.; Sagi, I. *Nucleic Acids Res.* **2001**, *29*, E122.
(179) Ottinger, L. M.; Tullius, T. D. *J. Am. Chem. Soc.* **2000**, *122*, 5901.
(180) Franchet-Beuzit, J.; Spotheim-Maurizot, M.; Sabattier, R.; Blazy-Baudras, B.; Charlier, M. *Biochemistry* **1993**, *32*, 2104.
(181) Hayes, J. J.; Kam, L.; Tullius, T. D. *Methods Enzymol.* **1990**, *186*, 545.
(182) Greiner, D. P.; Hughes, K. A.; Meares, C. F. *Biochem. Biophys. Res. Commun.* **1996**, *225*, 1006.
(183) Isabelle, V.; Franchet-Beuzit, J.; Sabattier, R.; Spotheim-Maurizot, M.; Charlier, M. I. *Biochimie* **1994**, *76*, 187.
(184) Spotheim-Maurizot, M.; Savoye, C.; Sabattier, R.; Charlier, M. *Bull. Cancer Radiother.* **1996**, *83 Suppl*, 27s.
(185) Spotheim-Maurizot, M.; Charlier, M.; Sabattier, R. *Int. J. Radiat. Biol.* **1990**, *57*, 301.
(186) Spotheim-Maurizot, M.; Franchet, J.; Sabattier, R.; Charlier, M. *Int. J. Radiat. Biol.* **1991**, *59*, 1313.
(187) Makino, K.; Mossoba, M. M.; Riesz, P. *Radiat. Res.* **1983**, *96*, 416.
(188) Riesz, P.; Berdahl, D.; Christman, C. L. *Environ. Health Perspect.* **1985**, *64*, 233.
(189) Gutierrez, M.; Henglein, A.; Fischer, C. H. *Int. J. Radiat. Biol. Relat. Stud. Phys. Chem. Med.* **1986**, *50*, 313.
(190) Henglein, A. *Ultrason. Sonochem.* **1987**, *25*, 6.
(191) Fang, X.; Mark, G.; von Sonntag, C. *Ultrason. Sonochem.* **1996**, *3*, 57.
(192) Price, G. J.; Duck, F. A.; Digby, M.; Holland, W.; Berryman, T. *Ultrason. Sonochem.* **1997**, *4*, 165.
(193) Mark, G.; Tauber, A.; Laupert, R.; Schuchmann, H. P.; Schulz, D.; Mues, A.; von Sonntag, C. *Ultrason. Sonochem.* **1998**, *5*, 41.
(194) Kawai, N.; Iino, M. *Ultrasound Med. Biol.* **2003**, *29*, 609.
(195) Davies, M. J.; Dean, R. T. *Radical-mediated protein oxidation: from chemistry to medicine*; Oxford University Press: Oxford, U.K., 1997.
(196) Hawkins, C. L.; Davies, M. J. *Biochim. Biophys. Acta* **2001**, *1504*, 196.
(197) Hawkins, C. L.; Davies, M. J. *J. Chem. Soc., Perkin Trans.* **1998**, *2*, 2617.
(198) Davies, M. J.; Dean, R. T. *Radical-mediated protein oxidation: from chemistry to medicine*; Oxford University Press: Oxford, 1997.
(199) Garrison, W. M. *Chem. Rev.* **1987**, *87*, 381.
(200) Stadtman, E. R. *Methods Enzymol.* **1995**, *258*, 379.
(201) Buxton, G. V.; Greenstock, C. L.; Helman, W. P.; Ross, A. B. *J. Phys. Chem. Ref. Data* **1988**, *17*, 513.
(202) Easton, C. J. In *Advances in Detailed Reaction Mechanism*; Coxon, J. M., Ed.; JAI Press: Greenwich, CT, 1991.
(203) Easton, C. J. *Chem. Rev.* **1997**, *97*, 53.
(204) Dean, R. T.; Wolff, S. P.; McElligott, M. A. *Free Radical Res. Commun.* **1989**, *7*, 97.
(205) Schuessler, H.; Schilling, K. *Int. J. Radiat. Biol.* **1984**, *45*, 267.
(206) Uchida, K.; Kato, Y.; Kawakishi, S. *Biochem. Biophys. Res. Commun.* **1990**, *169*, 265.
(207) Wolfe, S. P.; Garner, A. G.; Dean, R. T. *Trends Biochem. Sci.* **1986**, *11*, 1.
(208) Garrison, W. M. *Chem. Rev.* **1987**, *87*, 381.
(209) Davies, M. J. *Arch. Biochem. Biophys.* **1996**, *336*, 163.
(210) Sokol, H. A.; Bennett-Corniea, W.; Garrison, W. M. *J. Am. Chem. Soc.* **1965**, *87*, 1391.
(211) Xu, G.; Chance, M. R. *Anal. Chem.* **2004**, *76*, 1213.
(212) Stadtman, E. R.; Levine, R. L. *Amino Acids* **2003**, *25*, 207.
(213) Headlam, H. A.; Mortimer, A.; Easton, C. J.; Davies, M. J. *Chem. Res. Toxicol.* **2000**, *13*, 1087.
(214) Headlam, H. A.; Davies, M. J. *Free Radical Biol. Med.* **2002**, *32*, 1171.
(215) von Sonntag, C. *The chemistry basis of radical biology*; Taylor and Francis: London, 1987.
(216) von Sonntag, C.; Schuchmann, H. P. In *Peroxyl Radicals*; Alfassi, Z. B., Ed.; John Wiley and Sons: Chichester, U.K., 1997.
(217) Fossey, J.; Lefort, D.; Sobra, J. *Free radical in organic chemistry*; Wiley: Chichester, U.K., 1995.
(218) Davies, M. J. *Biochim. Biophys. Acta* **2005**, *1703*, 93.
(219) Russell, G. A. *J. Am. Chem. Soc.* **1957**, *79*, 3871.
(220) Amici, A.; Levine, R. L.; Tsai, L.; Stadtman, E. R. *J. Biol. Chem.* **1989**, *264*, 3341.
(221) Requena, J. R.; Levine, R. L.; Stadtman, E. R. *Amino Acids* **2003**, *25*, 221.
(222) Bogan, A. A.; Thorn, K. S. *J. Mol. Biol.* **1998**, *280*, 1.
(223) Calnan, B. J.; Tidor, B.; Biancalana, S.; Hudson, D.; Frankel, A. D. *Science* **1991**, *252*, 1167.
(224) Ibba, M.; Soll, D. *Nature* **1996**, *381*, 656.
(225) Jones, S.; van Heyningen, P.; Berman, H. M.; Thornton, J. M. *J. Mol. Biol.* **1999**, *287*, 877.
(226) Xu, G.; Takamoto, K.; Chance, M. R. *Anal. Chem.* **2003**, *75*, 6995.
(227) Ayala, A.; Cutler, R. G. *Free Radical Biol. Med.* **1996**, *21*, 65.
(228) Xu, G.; Liu, R.; Zak, O.; Aisen, P.; Chance, M. R. *Mol. Cell. Proteomics* **2005**, *4*, 1959.
(229) Nukuma, B. N.; Goshe, M. B.; Anderson, V. E. *J. Am. Chem. Soc.* **2001**, *123*, 1208.
(230) Mossoba, M. M.; Rosenthal, I.; Riesz, P. *Can. J. Chem.* **1982**, *60*, 1493.
(231) Uchida, K.; Kawakishi, S. *J. Agric. Food Chem.* **1990**, *38*, 660.
(232) Rao, P. S.; Simic, M.; Hayon, E. *J. Phys. Chem.* **1975**, *79*, 1260.
(233) Samuni, A.; Neta, P. *J. Phys. Chem.* **1973**, *77*, 1629.
(234) Tamba, M.; Torreggiani, A. *Int. J. Radiat. Biol.* **1998**, *74*, 333.
(235) Lassmann, G.; Eriksson, L. A.; Himo, F.; Lendzian, F.; Lubitz, W. *J. Phys. Chem. A* **1999**, *103*, 1283.
(236) Stadtman, E. R. *Free Radical Biol. Med.* **1990**, *9*, 315.
(237) Schoneich, C. *J. Pharmacol. Biomed. Anal.* **2000**, *21*, 1093.
(238) Uchida, K.; Kawakishi, S. *FEBS Lett.* **1993**, *332*, 208.
(239) Kopoldova, J.; Hrncir, S. *Z. Naturforsch., C* **1977**, *32*, 482.
(240) Tomita, M.; Irie, M.; Ukita, T. *Biochemistry* **1969**, *8*, 5149.
(241) Trelstad, R. L.; Lawley, K. R.; Holmes, L. B. *Nature* **1981**, *289*, 310.
(242) Diedrich, D. L.; Schenaitman. *Proc. Natl. Acad. Sci. U.S.A.* **1978**, *75*, 3708.
(243) Requena, J. R.; Stadtman, E. R. *Biochem. Biophys. Res. Commun.* **1999**, *264*, 207.
(244) Morin, B.; Bubb, W. A.; Davies, M. J.; Dean, R. T.; Fu, S. *Chem. Res. Toxicol.* **1998**, *11*, 1265.
(245) Requena, J. R.; Chao, C. C.; Levine, R. L.; Stadtman, E. R. *Proc. Natl. Acad. Sci. U.S.A.* **2001**, *98*, 69.
(246) Simiä, M.; Neta, P.; Hayon, E. *Int. J. Radiat. Phys. Chem.* **1971**, *3*, 309.
(247) Neta, P.; Fessenden, R. W. *J. Phys. Chem.* **1971**, *75*, 738.
(248) Xu, G.; Chance, M. R. *Anal. Chem.* **2005**, *77*, 4549.
(249) Finley, E. L.; Dillon, J.; Crouch, R. K.; Schey, K. L. *Protein Sci.* **1998**, *7*, 2391.
(250) Stadtman, E. R. *Methods Enzymol.* **1995**, *258*, 379.
(251) Maskos, Z.; Rush, J. D.; Koppenol, W. H. *Arch. Biochem. Biophys.* **1992**, *296*, 514.
(252) Solar, S. *Radiat. Phys. Chem.* **1985**, *26*, 103.
(253) Kiselar, J. G.; Mahaffy, R.; Pollard, T. D.; Almo, S. C.; Chance, M. R. *Proc. Natl. Acad. Sci. U.S.A.* **2007**, *104*, 1552.
(254) Claiborne, A.; Mallett, T. C.; Yeh, J. I.; Luba, J.; Parsonage, D. *Adv. Protein Chem.* **2001**, *58*, 215.
(255) van Vlijmen, H. W.; Gupta, A.; Narasimhan, L. S.; Singh, J. *J. Mol. Biol.* **2004**, *335*, 1083.
(256) Hogg, P. J. *Trends Biochem. Sci.* **2003**, *28*, 210.
(257) Ma, B.; Elkayam, T.; Wolfson, H.; Nussinov, R. *Proc. Natl. Acad. Sci. U.S.A.* **2003**, *100*, 5772.
(258) Kiselar, J. G.; Janmey, P. A.; Almo, S. C.; Chance, M. R. *Mol. Cell. Proteomics* **2003**, *2*, 1120.

(259) Kiselar, J. G.; Janmey, P. A.; Almo, S. C.; Chance, M. R. *Proc. Natl. Acad. Sci. U.S.A.* **2003**, *100*, 3942.
(260) Guan, J. Q.; Almo, S. C.; Reisler, E.; Chance, M. R. *Biochemistry* **2003**, *42*, 11992.
(261) Liu, R.; Guan, J. Q.; Zak, O.; Aisen, P.; Chance, M. R. *Biochemistry* **2003**, *42*, 12447.
(262) Gupta, S.; Mangel, W. F.; McGrath, W. J.; Perek, J. L.; Lee, D. W.; Takamoto, K.; Chance, M. R. *Mol. Cell. Proteomics* **2004**, *3*, 950.
(263) Prutz, W. A.; Butler, J.; Land, E. J.; Swallow, A. J. *Int. J. Radiat. Biol.* **1989**, *55*, 539.
(264) Hiller, K.; Masloch, B.; Goebl, M.; Asmus, K. *J. Am. Chem. Soc.* **1981**, *103*, 2734.
(265) Schoneich, C.; Pogocki, D.; Hug, G. L.; Bobrowski, K. *J. Am. Chem. Soc.* **2003**, *125*, 13700.
(266) Vogt, W. *Free Radical Biol. Med.* **1995**, *18*, 93.
(267) Bobrowski, K.; Holcman, J. *Int. J. Radiat. Biol. Relat. Stud. Phys. Chem. Med.* **1987**, *52*, 139.
(268) Miller, B. L.; Williams, T. D.; Schöneich, C. *J. Am. Chem. Soc.* **1996**, *118*, 11014.
(269) Lu, C.; Yao, S.; Lin, N. *Biochim. Biophys. Acta* **2001**, *1525*, 89.
(270) Lal, M. *Radiat. Phys. Chem.* **1994**, *43*, 595.
(271) Sevilla, M. D.; Becker, D.; Yan, M. *Int. J. Radiat. Biol.* **1990**, *57*, 65.
(272) Hoffman, M. Z.; Hayon, E. *J. Phys. Chem.* **1973**, *77*, 990.
(273) Al-Thannon, A.; Peterson, R. M.; Trumbore, C. N. *J. Phys. Chem.* **1968**, *72*, 2395.
(274) Al-Thannon, A. A.; Barton, J. P.; Packer, J. E.; Sims, R. J.; Trumbore, C. N.; Winchester, R. V. *Int. J. Radiat. Phys. Chem.* **1974**, *6*, 233.
(275) Dewey, D. L.; Beecher, J. *Nature* **1965**, *206*, 1369.
(276) Markakis, P.; Tappel, A. L. *J. Am. Chem. Soc.* **1960**, *82*, 1613.
(277) Becker, D.; Swarts, S.; Champagne, M.; Sevilla, M. D. *Int. J. Radiat. Biol. Relat. Stud. Phys. Chem. Med.* **1988**, *53*, 767.
(278) Wardman, P.; von Sonntag, C. *Methods Enzymol.* **1995**, *251*, 31.
(279) Schoneich, C. *Methods Enzymol.* **1995**, *251*, 45.
(280) Purdie, J. W. *Can. J. Chem.* **1971**, *49*, 725.
(281) Owen, T. C.; Wilbraham, A. C. *J. Am. Chem. Soc.* **1969**, *91*, 3365.
(282) Owen, T. C.; Rodriguez, M.; Johnson, B. G.; Roach, J. A. *J. Am. Chem. Soc.* **1968**, *90*, 196.
(283) Purdie, J. W. *J. Am. Chem. Soc.* **1967**, *89*, 226.
(284) Fang, X.; Wu, J.; Wei, G.; Schuchmann, H. P.; von Sonntag, C. *Int. J. Radiat. Biol.* **1995**, *68*, 459.
(285) Purdie, J. W. *Radiat. Res.* **1971**, *48*, 474.
(286) Bonifacic, M.; Asmus, K. D. *Int. J. Radiat. Biol. Relat. Stud. Phys. Chem. Med.* **1984**, *46*, 35.
(287) Chatgilialoglu, C.; Asmus, K.-D. *Sulfur-Centered Reactive Intermediates in Chemistry and Biology*; Plenum Press: New York, 1990.
(288) Alfassi, Z. B. *S-Centered Radicals*; Alfassi, Z. B., Ed.; John Wiley & Sons: New York, 1999.
(289) Willett, W. S.; Copley, S. D. *Chem. Biol.* **1996**, *3*, 851.
(290) Deutsch, J. C.; Santhosh-Kumar, C. R.; Kolhouse, J. F. *J. Chromatogr., A* **1999**, *862*, 161.
(291) Armstrong, D. A. In *Sulfur-centered Reactive Intermediates in Chemistry and Biology*; Asmus, C. C. a. K. D., Ed.; Plenum Press: New York, 1990.
(292) Owen, T. C.; Brown, M. T. *J. Org. Chem.* **1969**, *34*, 1161.
(293) Asmus, K. D. *Methods Enzymol.* **1990**, *186*, 168.
(294) Xu, G.; Chance, M. R. *Anal. Chem.* **2005**, *77*, 2437.
(295) Winterbourn, C. C.; Metodiewa, D. *Free Radical Biol. Med.* **1999**, *27*, 322.
(296) Asmus, K. D. *S-Centered Radicals*; Alfassi, Z. B., Ed.; John Wiley & Sons: New York, 1999.
(297) Allison, W. S. *Acc. Chem. Res.* **1976**, *9*, 293.
(298) Carballal, S.; Radi, R.; Kirk, M. C.; Barnes, S.; Freeman, B. A.; Alvarez, B. *Biochemistry* **2003**, *42*, 9906.
(299) Davis, F. A.; Billmers, R. L. *J. Am. Chem. Soc.* **1981**, *103*, 7016.
(300) Zhang, X.; Zhang, N.; Schuchmann, H. P.; von Sonntag, C. *J. Phys. Chem.* **1994**, *98*, 6541.
(301) Asmus, K.-D. In *S-Centered Radicals*; Alfassi, Z. B., Ed.; John Wiley & Sons: New York, 1999.
(302) Gupta, S.; Mangel, W. F.; McGrath, W. J.; Perek, J. L.; Lee, D. W.; Takamoto, K.; Chance, M. R. *Mol. Cell. Proteomics* **2004**, *3*, 950.
(303) Braams, R. *Radiat. Res.* **1966**, *27*, 319.
(304) Gilbert, B. C. In *Sulfur-Centered Reactive Intermediates in Chemistry and Biology*; Asmus, C. C. a. K. D., Ed.; Plenum Press: New York, 1990.
(305) Hoffman, M. Z.; Hayon, E. *J. Am. Chem. Soc.* **1972**, *94*, 7950.
(306) Hong, J.; Schoneich, C. *Free Radical Biol. Med.* **2001**, *31*, 1432.
(307) Rustgi, S.; Joshi, A.; Moss, H.; Riesz, P. *Int. J. Radiat. Biol. Relat. Stud. Phys. Chem. Med.* **1977**, *31*, 415.
(308) Von Sonntag, C.; Schuchmann, H. P. *Methods Enzymol.* **1994**, *233*, 3.
(309) Xu, G.; Chance, M. R. *Anal. Chem.* **2005**, *77*, 2437.
(310) Neumann, N. P. *Methods Enzymol.* **1972**, *25*, 393.
(311) Caldwell, K. A.; Tappel, A. L. *Biochemistry* **1964**, *20*, 1643.
(312) Benrahmoune, M.; Therond, P.; Abedinzadeh, Z. *Free Radical Biol. Med.* **2000**, *29*, 775.
(313) Xu, G.; Kiselar, J.; He, Q.; Chance, M. R. *Anal. Chem.* **2005**, *77*, 3029.

CR0682047